An *ex vivo* investigation of the potential drug permeation enhancing effects of selected pepper extracts

AS van Niekerk

orcid.org/ 0000-0002-5797-7053

Dissertation submitted in fulfilment of the requirements for the degree Master of Science in Pharmaceutics at the North West University

Supervisor: Prof. JH Hamman

Co-supervisor: Dr. JD Steyn

Co-supervisor: Dr. L Badenhorst

Graduation: May 2019

Student number: 24282340

Declaration by candidate

“I hereby declare that the dissertation submitted in partial fulfilment of the requirements for the degree Magister Scientiae in Pharmaceutics at the Potchefstroom Campus of the North-West University, is my own original work and has not previously been submitted to any other institution of higher education. I further declare that all sources cited or quoted are indicated and acknowledged by means of a comprehensive list of references”

Miss AS van Niekerk

24282340

Acknowledgements

~What is the difference between an obstacle and an opportunity? Our attitude toward it. Every opportunity has a difficulty, and every difficulty has an opportunity~ J.Sidlow Baxter.

This dissertation is presented to you not only on my own accord. It would not have been possible without the assistance of various contributors. I would like to acknowledge the following individuals:

- Firstly, my Heavenly Father. Without you precious talents that you granted on me, gracious love, guidance and protection none of this would have been possible.
- To my parents, Elna and Hennie van Niekerk. Thank you for your continuous love, guidance, encouragement and believing in me. Without you support over all these years, this would have been an impossible task to finish.
- To my brother, Cornèl van Niekerk. Thank you for your support and being my partner in crime.
- Murray-Hancke Oberholster, closer to a real sister I could not get. Thank you for every little thing you do for me, I do not deserve a friend like you, you cared for me and put up with my mixed emotions at times, but still you kept on encouraging me.
- Lauren Cilliers, your friendship, support and help through these two years meant more to me than you will ever believe. I will always remember and appreciate you.
- My fellow students, especially Corneli Jacobzs, Alex Laux, Carmen Annandale, Anja Haasbroek and Sarika du Plessis, thank you that you were always willing to lend a helping hand, give advice and contributed to a positive working environment.
- Prof. Sias Hamman, my study leader. I would like to thank you for the opportunity that you gave me to do my masters degree and guiding me with so much compassion and dedication. The respect and admiration that I have for your superb academic ability as a leader in pharmaceutical research is indescribable. It was a privilege to work under your supervision and guidance.
- Dr. Dewald Steyn and Dr. Liezl Badenhorst, thank you for your support and being always willing to help during these two years. I appreciate it.
- Prof. Jan du Preez, thank you for your assistance with the HPLC characterisation of my samples.
- Prof. Suria Ellis, for assisting me with my statistical analysis.
- I want to acknowledge the following financial support: The North West University funding me with a masters and institutional bursary as well as the National Research Foundation for my grant-holder linked bursary (grant nr 98939) from my supervisor, Prof Sias (JH) Hamman.

Abstract

Although the oral route is the most preferred and convenient route of drug administration when considering the patient, certain drugs (e.g. protein and peptide drugs) are mostly administrated by means of injections. This invasive route of administration causes poor patient compliance due to drawbacks such as pain, discomfort, possibility of infections and lipohypertrophy. Hurdles related to oral administration of protein and peptide drugs include pre-systemic enzymatic degradation as well as poor penetration of the intestinal mucosa, leading to ineffective absorption in the intestinal tissue. Poor membrane permeation can be overcome by the simultaneous administration of the drug molecule with an absorption enhancer. Previous studies have proven that absorption enhancers of natural origin, e.g. *Aloe vera* leaf materials, bile salts, naringin, turmeric and peppermint oil can improve the absorption of drug molecules as shown in different intestinal epithelial transport models.

During this study, pepper extract compounds (i.e. piperine and capsaicin) were investigated as potential intestinal drug absorption enhancers. *Ex vivo* transport studies were conducted across excised pig jejunum tissue mounted in a Sweetana-Grass diffusion apparatus. The effect of the selected pepper extract compounds on rhodamine-123 (RH-123, 5 µM) and fluorescein isothiocyanate (FITC)-dextran (FD-4, 100 µg/ml) was investigated. Bi-directional transport studies were conducted on RH-123, a known P-glycoprotein (P-gp) efflux transporter substrate, to determine if piperine and capsaicin have the ability to inhibit P-gp efflux. Transport studies in the absorptive direction were conducted on FD-4, a macromolecular model drug, to determine if piperine and capsaicin have the ability to open tight junctions and thereby cause enhanced paracellular transport. The transport studies were conducted over a time period of 2 h, while taking 200 µL samples every 20 min from the acceptor chamber. These samples were then analysed by means of a validated fluorescence analytical method on the Spectramax Paradigm® plate reader. The trans-epithelial electrical resistance (TEER) of the mounted excised pig intestinal tissue was measured every 20 min to determine membrane integrity and also as an indication of tight junction modulation. For each model compound, a transport study was conducted without any absorption enhancing agent, which served as the control groups. The permeability coefficient (P_{app}) values of the transport experiments were calculated from the transport curves.

Piperine and capsaicin improved the absorption of RH-123 in a concentration dependant manner in the apical-to-basolateral (AP-BL) direction across the intestinal tissue when compared with the control group. The P_{app} values of RH-123 in the AP-BL direction increased from 1.54×10^{-7} cm/s (RH-123 alone) to 1.65×10^{-7} cm/s, 1.56×10^{-7} cm/s and 2.859×10^{-7} cm/s in the presence of piperine in 50 µM, 100 µM and 200 µM, respectively. Furthermore, the P_{app} values increased from 1.54×10^{-7} cm/s (RH-123 alone) to 4.09×10^{-7} cm/s, 6.11×10^{-7} cm/s and 8.15×10^{-7} cm/s in the

presence of capsaicin in 50 µM, 100 µM and 200 µM, respectively. In accordance with this enhanced absorptive transport result, RH-123 transport was decreased in the basolateral-to-apical (BL-AP) direction in a concentration dependant manner when compared with the control group. The P_{app} value of RH-123 in the BL-AP direction decreased from 5.28×10^{-7} cm/s (RH-123 alone) to 4.17×10^{-7} cm/s, 2.71×10^{-7} cm/s and 2.49×10^{-7} cm/s in the presence of piperine in 50 µM, 100 µM and 200 µM, respectively. Furthermore, the P_{app} value decreased from 5.28×10^{-7} cm/s (RH-123 alone) to 4.2×10^{-7} cm/s, 2.44×10^{-7} cm/s and 2.68×10^{-7} cm/s in the presence of capsaicin in 50 µM, 100 µM and 200 µM, respectively. These results indicated that piperine and capsaicin have the ability to inhibit P-gp efflux and thereby enhance the absorptive transport of efflux transporter substrates. During the transport studies with FD-4 in the presence of piperine, the absorption of FD-4 increased as the piperine concentration increased, while the TEER values decreased. The P_{app} values of FD-4 increased from 1.76×10^{-7}cm/s (FD-4 alone) to 3.6×10^{-7} cm/s, 4.06×10^{-7}cm/s and 4.39×10^{-7}cm/s in the presence of piperine in 50 µM, 100 µM and 200 µM, respectively. These results indicate that piperine has the ability to open tight junctions and thereby improve paracellular transport across the excised intestinal tissue. During transport studies with FD-4 in the presence of capsaicin, the absorption of FD-4 did not increase and the TEER values remained stable. Capsaicin therefore did not show the ability to modulate tight junctions to allow enhanced paracellular transport across the intestinal tissues.

Although very promising drug absorption enhancing results were obtained for piperine and capsaicin with the *ex vivo* transport studies, *in vivo* studies are necessary to determine if these absorption enhancers have the ability to improve drug absorption in a clinically significant way.

Key words: absoption enhancement, capsaicin, *ex* vivo, fluorescein isothiocyanate, oral route P-glycoprotein, piperine, Rhodamine 123

Table of contents

Declaration by candidate i

Acknowledgements ii

Abstract iii

List of tables xiv

List of figures xvi

List of Abbreviations xix

Chapter 1: Introduction 1

1.1 Drug absorption challenges in the gastro-intestinal tract 1

1.1.1 Physico-chemical characteristics of peptide and protein drugs 1

1.1.2 Barriers affecting oral absorption of peptide and protein drugs 1

1.1.2.1 Physical barriers 1

1.1.2.2 Biochemical barriers 2

1.2 Oral drug delivery enhancement strategies 2

1.3 Bioavailability modulators of natural origin 9

1.3.1 Piperine 10

1.3.2 Capsaicin 10

1.4 *In vitro* models to evaluate drug permeability 11

1.4.1 Cell cultures 11

1.4.2 *Ex vivo* models 12

1.5 Research problem 12

1.6 Aim and objectives 13

1.6.1 Aim 13

1.6.2 Objectives 13

1.7 Ethics 13

1.8 Dissertation layout 14

Chapter 2: Oral delivery of therapeutic protein and peptide drugs 15

2.1 Introduction 15

2.2 Transport mechanisms of drug absorption after oral administration 16

2.2.1 Transcellular transport 16

2.2.2 Paracellular transport 17

2.2.3 Carrier-mediated transport 17

2.2.4 Efflux transporters 18

2.2.5 Receptor-mediated transport 18

2.2.5.1 Endocytosis 18

2.3 Experimental models used to predict drug absorption 19

2.3.1 *In vivo* models 19

2.3.1.1 Loc-I-Gut™ 20

2.3.1.2 Pharmacokinetic study in human volunteers 20

2.3.2 *In vitro* models 20

2.3.2.1 Cell cultures 20

2.3.2.1.1 Caco-2 cell monolayers 21

2.3.2.1.2 MDCK cell monolayers 21

2.3.2.2 Artificial membranes 21

2.3.3 *In situ* models 22

2.3.4 *Ex vivo* models 22

2.3.4.1 Everted gut sacs 22

2.3.4.2 Diffusion chambers 23

2.3.5 *In silico* models 23

2.4 Challenges associated with oral delivery of protein and peptide drugs 24

2.4.1 Physical barriers 25

2.4.1.1 Tight junctions 25

2.4.1.2 Mucus and unstirred water layer 25

2.4.1.3 The intestinal epithelial cell membrane 26

2.4.1.4 Efflux transporters 26

2.4.2 Biochemical barriers 26

2.5 Oral drug delivery enhancement strategies for peptide and protein drugs 27

2.5.1 Chemical approaches 27

2.5.1.1 Pro-drug strategies 27

2.5.1.2 Structural changes (derivatization of proteins) 28

2.5.1.3 Peptidomimetics 28

2.5.1.4 Targeting of endogenous cell carrier systems 29

2.5.1.5 Cell-penetrating peptides 29

2.5.2 Biochemical approaches 30

2.5.2.1 Enzyme inhibitors 30

2.5.3 Formulation approaches 30

2.5.3.1 Site-specific delivery systems 30

2.5.3.2 Physically forced transport 31

2.5.3.3 Formulation of drug carrier vehicles (particulate delivery systems) 31

2.5.3.4 Absorption enhancers 32

2.5.3.5 Absorption enhancers of plant origin 33

2.5.3.5.1 Piperine 33

2.5.3.5.1.1 Botany of *Piper nigrum* (Black pepper) 33

2.5.3.5.1.2 Chemistry of piperine 34

2.5.3.5.1.3 Medicinal properties of piperine 35

2.5.3.5.1.3.1 Antimicrobial activity 35

2.5.3.5.1.3.2 Anti-oxidant activity 35

2.5.3.5.1.3.3 Anti-cancer activity 35

2.5.3.5.1.3.4 Anti-inflammatory and analgesic activity 36

2.5.3.5.1.3.5 Hepatoprotective activity 36

2.5.3.5.1.3.6 Anti-diarrhoea activity 36

2.5.3.5.1.3.7 Digestive activity 37

2.5.3.5.1.3.8 Anti-depressant activity 37

2.5.3.5.1.3.9 Immuno-modulatory activity 37

2.5.3.5.1.3.10 Anticonvulsant activity 37

2.5.3.5.1.3.11 Absorption enhancement characteristics 38

2.5.3.5.2 Capsaicin 38

2.5.3.5.2.1 Botany of *Capsicum* species 39

2.5.3.5.2.2 Chemistry of capsaicin 39

2.5.3.5.2.3 Medicinal properties of Capsaicin 40

2.5.3.5.2.3.1 Cardiovascular benefits of capsaicin 40

2.5.3.5.2.3.2 Protective effect on erythrocyte integrity 40

2.5.3.5.2.3.3 Anti-oxidant effect of capsaicin 41

2.5.3.5.2.3.4 Antinociceptive effects of capsaicin 41

2.5.3.5.2.3.5 Chemopreventive activity of capsaicin 41

2.5.3.5.2.3.6 Anti-diabetic potential 42

2.5.3.5.2.3.7 Thermogenic and weight reducing influence of capsaicin 42

2.5.3.5.2.3.8 Anti-ulcer activity of capsaicin 42

2.5.3.5.2.3.9 Anti-inflammatory effect of capsaicin 42

2.5.3.5.2.3.10 Absorption enhancement characteristics 42

2.6 Summary 43

Chapter 3: Materials and Methods 44

3.1 Introduction 44

3.2 Materials 44

3.3 Fluoroscence spectroscopic analytical method validation for Rhodamine 123 (RH-123), FITC-dextran (FD-4) and Lucifer Yellow (LY) 45

3.3.1 Linearity 45

3.3.2 Accuracy 46

3.3.3 Limit of detection (LOD) and limit of quantification (LOQ) 46

3.3.4 Precision 47

3.3.4.1 Intra-day precision 47

3.3.4.2 Inter-day precision 47

3.3.5 Specificity 48

3.4 Characterisation of pepper raw materials by making use of a HPLC method 48

3.5 *Ex vivo* transport studies 50

3.5.1 Preparation of buffer solution for the transport studies 50

3.5.2 Preparation of experimental solutions for the transport studies 50

3.5.2.1 Preparation of FITC-dextran solutions 50

3.5.2.2 Preparation of experimental solutions of Rhodamine-123 50

3.5.3 Collection and preparation of pig intestinal tissue for *ex* vivo transport studies 51

3.5.4 Transport studies using the Sweetana-Grass diffusion chamber technique 54

3.6 Assessment of intestinal tissue integrity 55

3.7 Analysis of the transport samples 55

3.8 Data processing and statistical analysis 56

3.8.1 Percentage transport (% transport) 56

3.8.2 Apparent permeability coefficient (P_{app}) 56

3.8.3 Efflux ratio (ER) 56

3.8.4 Statistical analysis of results 57

Chapter 4: Results and discussion 58

4.1 Introduction 58

4.2 Fluorescence spectrometry analytical method validation for Rhodamine 123 (RH-123), FITC-dextran (FD-4) and Lucifer Yellow (LY) 59

4.2.1 Method validation results for Rhodamine 123 (RH-123) 59

4.2.1.1 Linearity 59

4.2.1.2 Accuracy 60

4.2.1.3 Limit of detection (LOD) and limit of quantification (LOQ) 61

4.2.1.4 Precision 61

4.2.1.4.1 Intra-day precision 61

4.2.1.4.2 Inter-day precision 62

4.2.1.5 Specificity 62

4.2.2 Method validation results: FITC-dextran (FD-4) 62

4.2.2.1 Linearity 62

4.2.2.2 Accuracy 63

4.2.2.3 Limit of detection (LOD) and limit of quantification (LOQ) 64

4.2.2.4 Precision 65

4.2.2.4.1 Intra-day precision 65

4.2.2.4.2 Inter-day precision 65

4.2.2.5 Specificity 65

4.2.3 Method validation results: Lucifer Yellow 66

4.2.3.1 Linearity 66

4.2.3.2 Accuracy 67

4.2.3.3 Limit of detection and limit of quantification 68

4.2.3.4 Precision 68

4.2.2.3.1 Intra-day precision 68

4.2.2.3.2 Inter-day precision 69

4.2.4 Summary of validation results 69

4.3 Characterisation of pepper raw materials by making use of a HPLC method 69

4.3.1 Characterisation of piperine 69

4.3.1.1 Linearity of the Pharmacopoeia reference standard piperine CRS (Chemical Reference standard) 69

4.3.1.2. Determining the purity of the piperine raw material used in the transport studies 70

4.3.2 Characterisation of capsaicin 70

4.3.2.1 Linearity of the Pharmacopoeia reference standard capsaicin 70

4.3.2.2 Determining the purity of the capsaicin raw material used in the transport studies 71

4.4 *Ex vivo* transport studies 71

4.4.1 Bi-directional transport studies with Rhodamine 123 71

4.4.1.1 Bi-directional transport studies in the presence of piperine 72

4.4.1.2 Bi-directional transport studies in the presence of capsaicin 74

4.4.1.3 Evaluation of efflux ratios 76

4.4.1.4 Comparison and evaluation of TEER 77

4.4.2. Transport studies with FITC-dextran (FD-4) 78

4.4.2.1 Transport studies in the presence of piperine 78

4.4.2.2 Transport studies in the presence of capsaicin 80

4.4.2.3 Comparison and evaluation of TEER 81

4.5 Assessment of intestinal tissue integrity 82

4.6 Conclusions 83

Chapter 5: Final conclusions and future recommendations 84

5.1 Final conclusions 84

5.2 Future recommendations 85

Addendum A: Ethics Approval 86

Addendum B: *Ex vivo* transport data of Rhodamine 123, Lucifer yellow and FITC-dextran (FD-4) across excides pig jejunum tissue and apparent permeability coefficient (P_{app}) values 86

Addendum B: *Ex vivo* transport data of Rhodamine 123, Lucifer yellow and FITC-dextran (FD-4) across excised pig jejunum tissue and apparent permeability coefficient (P_{app}) values 87

Addendum C: Efflux ratios of Rhodamine 123 99

Addendum D: Trans-Epithelial electrical resistance (TEER) measurements 101

Addendum E: Statistical Analysis 113

References 115

List of tables

Table 1.1: Oral drug delivery enhancement strategies for peptide and protein molecules 3

Table 2.1: Summary of *in vivo* studies where the co-administration of piperine showed effects on drug pharmacokinetics 38

Table 3.1: Summary of the chromatographic conditions for the piperine determination 49

Table 3.2: Summary of the chromatographic conditions for the capsaicin determination 49

Table 4.1: Fluorescence values of Rhodamine-123 recorded over a specific concentration range, slope and correlation coefficient (R^2) value 59

Table 4.2: Results obtained during determination of accuracy of the fluorometric analytical method for Rhodamine-123 60

Table 4.3: Average blank fluorescence detection values together with the standard deviation, limit of detection (LOD) and limit of quantification (LOQ) values for the fluorometric analytical method for Rhodamine-123 61

Table 4.4: Data obtained for intra-day precision of the fluorometric analytical method for Rhodamine-123 61

Table 4.5: Data obtained for inter-day precision of the fluorometric analytical method for Rhodamine-123 62

Table 4.6: Percentage recovery (% Recovery) of Rhodamine-123 in the presence of different pepper extracts 62

Table 4.7: Fluorescence values of FITC-dextran recorded over a specific concentration range, slope and correlation coefficient (R^2) value 63

Table 4.8: Results obtained during determination of accuracy of the fluorometric analytical method for FITC-dextran 64

Table 4.9: Average blank fluorescence detection values with the standard deviation, limit of detection (LOD) and limit of quantification (LOQ) values for the fluorometric analytical method for FITC-dextran 64

Table 4.10: Data obtained for intra-day precision of the flurometric analytical method for FITC-dextran 65

Table 4.11: Data obtained for inter-day precision of the fluorometric analytical method for FITC-dextran 65

Table 4.12: Percentage Recovery (% Recovery) of FITC-dextran in the presence of different pepper extracts 66

Table 4.13: Fluorescence values of Lucifer Yellow recorded over a specific concentration range, slope and correlation coefficient (R^2) value 66

Table 4.14: Results obtained during determination of accuracy of the fluorometric analytical method for Lucifer Yellow 67

Table 4.15: Average blank fluorescence detection values together with the standard deviation, Limit of detection (LOD) and Limit of quantification (LOQ) values for the fluorometric analytical method for Lucifer Yellow 68

Table 4.16: Data obtained for intra-day precision of the fluorometric analytical method for Lucifer Yellow 68

Table 4.17: Data obtained for inter-day precision of the fluorometric analytical method for Lucifer Yellow 69

Table 4.18: Percentage purity of the piperine raw material 70

Table 4.19: Percentage purity of the Sigma Standard for capsaicin 71

Table 4.20: Summary of the P_{app} values and efflux ratio (ER) values for the selected pepper extracts at selected concentrations 76

Table 4.21: Percentage trans-epithelial electrical resistance (TEER) across excised tissue exposed to each of the selected pepper extracts at 120 min after administration (T_{120}) during the Rhodamine-123 transport studies 77

Table 4.22: Average percentage trans-epithelial electrical resistance (TEER) for excised tissue exposed to each of the selected pepper extracts over a two-hour period in the presence of FITC-dextran (FD-4) (all the values are expressed as average percentage change from the initial T_0 to the T_{120} value) 81

Table 4.23: The permeability coefficient values for Lucifer Yellow and Lucifer Yellow + 4% ethanol across excised pig intestinal jejunum tissue 82

List of figures

Figure 2.1: Illustration of the absorption mechanisms across the gastro-intestinal tract epithelium: A) passive paracellular transport, B) carrier mediated transport, C) passive transcellular transport, D) receptor mediated transport and E) efflux transport. (Adapted from Anilkumar et al. (2011:437); Sugano et al. (2010:598-599), produced by making use of Servier Medical Art, (Servier-Medical-Art, 2018)).....16

Figure 2.2: Flow-chart illustrating the experimental models that can be used to predict drug absorption 19

Figure 2.3: Schematic illustration of the different barriers encountered after the oral administration of peptide and protein drugs (Adapted from Jhanwar and Gupta (2014:444); Roger et al. (2010:288); produced using Servier Medical Art, (Servier-Medical-Art, 2018)).....24

Figure 2.4: A) Geographical distribution of *Piper nigrum*; B) Photograps of *Piper nigrum* and the pepper fruits in all three the stages (Adapted from KEW-Science KEW-Science:Plants-of-the-world-online (2018)) 34

Figure 2.5*:* Chemical structure of piperine (Adapted from Gorgani et al*. (2017a:125).* 34

Figure 2.6: A) Geographical distribution of *Capsicum anuum* (KEW-Science:Plants-of-the-world-online, 2017). B) Image showing the plant, flower and fruits of *Capsicum anuum* (Adapted from (Wikipedia, 2018).....39

Figure 2.7: Chemical structure of capsaicin showing the different parts with distinctive characteristics: A) Aromatic ring, B) Amide bond, C) Hydrophobic side chain. (Adapted from (Reyes-Escogido et al., 2011:1254).....40

Figure 3.1: Photographic images showing A) excised pig intestinal jejunum tissue mounted on a glass tube, B) removal of the serosal layer from the excised pig jejunum tissue.....52

Figure 3.2: Photographic image illustrating a Peyer's patch in the excised jejunal intestinal tissue 52

Figure 3.3: Photographic images of A) the jejunum being cut along the mesenteric border, B) the jejunum being washed from the glass tube with Krebs Ringer bicarbonate buffer and C) the jejunum tissue sheet being transferred onto heavy duty filter paper 53

Figure 3.4: Photographic images illustrating A) and B) the cutting into smaller sections of the excised jejunal tissue sheet, C) and D) the mounting of the segments onto the pins of the diffusion half-cells, E) the removal of the heavy duty filter paper, F), G) and (H) the assembling of two half-cells into a single diffusion chamber. 53

Figure 3.5: Photographic image showing a complete assembly of the Sweetana-Grass diffusion chamber apparatus with six chambers loaded into the heating block and the connected carbogen supply 54

Figure 3.6: Photographic image illustrating the setup for trans-epithelial electrical resistance measurement in the Sweetana-Grass diffusion chamber apparatus 54

Figure 4.1: Linear regression curve of Rhodamine-123 with the straight line equation and correlation coefficient (R^2) value 60

Figure 4.2: Linear regression curve of FITC-dextran (FD-4) with the straight line equation and correlation coefficient (R^2) value 63

Figure 4.3: Linear regression curve of Lucifer Yellow with the straight line equation and correlation coefficient (R^2) value 67

Figure 4.4: Linear regression curve of the Pharmacopoeia reference standard piperine illustrating the straight line equation as well as the correlation coefficient (R^2) value obtained with high performance liquid chromatography 70

Figure 4.5: Linear regression curve of the Pharmacopoeia reference standard Capsaicin Chemical Reference Standard (CRS) illustrating the straight line equation as well as the correlation coefficient (R^2) value 71

Figure 4.6: Apical-to-basolateral transport of Rhodamine-123 in the presence of different concentrations of piperine across excised pig jejunum tissue plotted as a function of time 72

Figure 4.7: Basolateral-to-apical transport of Rhodamine-123 in the presence of different - concentrations of piperine across excised pig jejunum tissue plotted as a function of time 73

Figure 4.8: Average P_{app} values for bi-directional transport of Rhodamine-123 in the presence of different concentrations of piperine across excised pig jejunum tissue (*statistically significant difference, $p \leq 5$) 74

Figure 4.9: Apical-to-basolateral transport of Rhodamine-123 in the presence of different concentrations of capsaicin across excised pig jejunum tissue plotted as a function of time 74

Figure 4.10: Basolateral-to-apical transport of Rhodamine-123 in the presence of different concentrations of capsaicin across excised pig jejunum tissue plotted as a function of time 75

Figure 4.11: P_{app} values for bi-directional transport of Rhodamine-123 in the presence of different concentrations of capsaicin across excised pig jejunum tissue (*statistically significant difference, $p \leq 0.05$) 76

Figure 4.12: Transport of FITC-dextran in the presence of different concentrations of piperine across excised pig jejunum tissue plotted as a function of time 79

Figure 4.13: P_{app} values for transport of FITC-dextran in the presence of different concentrations of piperine across excised pig jejunum tissue 79

Figure 4.14: Transport of FITC-dextran in the presence of different concentrations of Capsaicin across excised pig jejunum tissue plotted as a function of time 80

Figure 4.15: Average P_{app} values for transport of FITC-dextran in the presence of different concentrations of capsaicin across excised pig jejunum tissue 80

Figure 4.16: Average percentage TEER reduction plotted as a function of concentration over a two-hour period (Error bars represent the standard deviation) 81

Figure 4.17: Apical to basolateral transport of Lucifer Yellow and Lucifer Yellow + 4% ethanol across excised pig intestinal jejunum tissue plotted as a function of time 82

List of Abbreviations

ABC	Adenosine triphosphate binding cassette
AP	Activator protein
AP	Apical
AP-BL	Apical-to-basolateral
ATP	Adenosine triphosphate
Ave	Average
BL	Basolateral
BL-AP	Basolateral-to-apical
Caco-2	Colonic adenocarcinoma cells
CGRP	Calcitonin gene-related peptide
CODES	Colon drug delivery system
COX-2	Cyclo-oxygenase 2
CPP	Cell penetrating peptide
CRS	Chemical reference standard
CYP	Cytochrome P450
Da	Dalton (g/mol)
DNA	Deoxyribonucleic acid
ER	Efflux ratio
FD-4	Fluorescein isotiocyanate dextran (4000 Da)
FDA	Food and Drug Administration
FITC	Fluorescein isothiocyanate
HER2	Human epidermal growth factor receptor 2

HPLC	High performance liquid chromatography
INF/IFN	Interferon
i-NOX	Nitric oxide synthases
KRB	Krebs-Ringer bicarbonate
LOD	Limit of detection
LOQ	Limit of quantification
LY	Lucifer Yellow
MDCK	Madin-Darby canine kidney cells
MRP2	Multidrug resistance associated protein 2
NF	Nuclear factor
O/W	Oil-in-water
PAMPA	Parallel artificial membrane permeability assay
P_{app}	Apparent permeability
PEG	Polyethylene glycol
PG	Prostaglandin
P-gp	P-glycoprotein
R^2	Correlation coefficient
RH-123	Rhodamine 123
RNA	Ribonucleic acid
RSD	Relative standard deviation
S	Slope
S/O/W	Solid-in-oil-in water
SD	Standard deviation

SLC	Solute carrier
Tat	Transactivator of transcriptation
TEER	Trans-epithelial electrical resistance
TNF	Tumour necrosis factor
TRPV	Transient receptor potential vanilloid
ZO	Zonula occludens
ZOT	Zonula occludens toxin

Chapter 1: Introduction

1.1 Drug absorption challenges in the gastro-intestinal tract

The oral route is one of the most acceptable routes of drug administration, and is associated with a high degree of patient compliance. However, the gastro-intestinal tract possesses barriers that make it difficult for certain drugs (e.g. hydrophilic and large molecules) to be absorbed intact into the systemic blood circulation (Hamman *et al.*, 2005:165). The gastro-intestinal tract is designed for the digestion and uptake of nutrients, fluids and electrolytes, but concurrently it has to protect the human body against invasion of pathogens, antigens and toxins (Moroz *et al.*, 2016:109). To accomplish this protective task, specific barrier mechanisms exist that can be divided into physical and biochemical components. The physical barrier mainly consists of the epithelial cell lining, which includes the cell membranes and the tight junctions between adjacent epithelial cells. The mucosal layer can also play a role in preventing molecules from reaching the epithelial surface of the gastro-intestinal tract. The luminal enzymes and active efflux transporters form part of the biochemical barrier (Hamman *et al.*, 2005:166; Pawar *et al.*, 2014:169).

1.1.1 Physico-chemical characteristics of peptide and protein drugs

Peptide and protein drugs are grouped in Class III of the Biopharmaceutics Classification System (BCS) due to the fact that they are highly soluble in an aqueous environment, but exhibit poor membrane permeability. The hydrophilic nature and high molecular weight of peptide and protein drugs contribute to their poor membrane permeability. However, it is important to note that peptide and protein molecules with cationic and anionic functional groups may face pH-dependent solubility challenges. Due to the variability in the pH of the gastro-intestinal tract, the pH of the environment can range from below to above the isoelectric point of the peptide or protein drug as it moves along the gastro-intestinal tract. The solubility of insulin, for example, is higher in an environment where the pH is below the isoelectric point than where it is equal to the isoelectric point (Maher *et al.*, 2016:278).

1.1.2 Barriers affecting oral absorption of peptide and protein drugs

As mentioned before, the barriers that can affect the absorption of peptide and protein drugs in the gastro-intestinal tract can be divided into two categories namely, physical barriers and biochemical barriers.

1.1.2.1 Physical barriers

For a drug to reach the systemic circulation after oral intake, it has to pass through the epithelial barrier of the intestinal mucosa (Tatiraju *et al.*, 2013b:55). Transcellular passive diffusion of drugs across biological membranes depends on their size, lipophilicity and charge. Peptide and protein molecules are generally very large and hydrophilic molecules that render it challenging to be

transported across the lipid bilayer of the apical membrane of the intestinal epithelium (Choonara *et al.*, 2014:1270). Efflux pumps like P-glycoprotein (P-gp) can cause a decrease in the bioavailability of drugs. These efflux pumps actively transport the drug molecules from within the epithelial cells back into the lumen of the gastro-intestinal tract (Hamman *et al.*, 2005:167-168; Tatiraju *et al.*, 2013b:56).

The paracellular pathway of xenobiotic uptake is restricted by the presence of tight junctions between the adjacent enterocytes. These inter-cellular structures restrict the paracellular uptake of drugs to molecular weights of smaller than 100-200 Dalton. The paracellular route is therefore naturally only applicable to the transport of small hydrophilic molecules (Antunes *et al.*, 2013:5; Choonara *et al.*, 2014:1271). However, a lot of attention has been given to improve the paracellular transport of hydrophilic drugs. This task has been accomplished by using intestinal permeation enhancers that can modulate tight junction proteins, for example, chitosan. These intestinal permeation enhancers have special features of transiently opening the tight junctions between the epithelial cells leading to the absorption of hydrophilic macromolecules (Lin *et al.*, 2007:1).

The unstirred aqueous diffusion layer that exists on the surface of the intestinal epithelium can impede macromolecules like protein and peptides from reaching the epithelial membrane in order to be absorbed (Jhanwar & Somdatt, 2014:444; Pawar *et al.*, 2014:171). This aqueous unstirred diffusion layer consists of water, mucus and glycocalyx. The main physical barrier in the unstirred water layer that leads to difficulty of absorption is the mucus component. Glycoproteins in mucus have high molecular weights that increases the viscosity and could also possibly interact with the molecules that have to be absorbed *via* electrostatic/ionic, Van der Waals, hydrophobic and hydrogen bond interactions (Hamman *et al.*, 2005:167; Maher *et al.*, 2016:279; Yun *et al.*, 2013:825).

1.1.2.2 Biochemical barriers

Proteolytic enzymes are present in the lumen of the gastro-intestinal tract, the brush border membrane and in the cytosol of the small intestinal enterocytes that can cause the breakdown of peptide and protein molecules (Pawar *et al.* (2014:171). This contributes largely to the poor bioavailability of these types of drugs after oral administration. Peptides are specifically sensitive to the enzyme pepsin, which causes degradation by breaking down hydrogen bonds, disulfide bridges and electrostatic bonds (Maher *et al.*, 2016:279).

1.2 Oral drug delivery enhancement strategies

There have been various approaches and strategies that were used in previous studies to overcome the barriers against oral peptide and protein drug delivery. Table 1.1 gives a summary of some of the approaches and strategies that were used in previous studies.

Table 1.1: Oral drug delivery enhancement strategies for peptide and protein molecules

CHEMICAL APPROACHES				
Name	**Example**	**Mechanism of action**	**Drawbacks**	**Reference**
Pro-drug strategies	Phenyl propionic acid	Pharmacologically inactive chemicals to mask the unwanted drug properties like low bioavailability and chemical instability. After enzymatic transformation the pro-drug will be transformed into an active drug compound.	Structural complexity, stability of proteins and limitations in the methodology.	(Choonara *et al.*, 2014:1274; Muheem *et al.*, 2016:419-420)
Structural changes (Derivatization of proteins)	Polyethylene glycol	Protects against enzymatic degradation. Protects molecules from recognition by the immune system.	Non-specific PEGylation	(Muheem *et al.*, 2016:419)
Peptidomimetics	Pseudo-peptides, semi-peptides and peptoids	Mimics the biological activity of peptides.	Difficult to yield potent lead compounds.	(Sawyer, 2007:617)
Endogenous cell carrier system	Vit. B12, Transferrin, invasins, viral haemoagglutinin, toxins and lectin	Receptor-mediated endocytosis	Only small drugs can be transported	(Muheem *et al.*, 2016:420-421)
Cell-penetrating peptides	Oligoarginine, penetratin, transactivator of transcription peptide, chimeric peptides	Initiate endocytosis, formation of channels within the cell membrane at high concentration and direct translocation.	Toxic	(Maher *et al.*, 2016:303; Muheem *et al.*, 2016:421)
BIOCHEMICAL APPROACHES				
Name	**Example**	**Mechanism of action**	**Drawback**	**Reference**
Enzyme inhibitors	Aprotinin, Soybean trypsin inhibitors, camostat mesilate, chromostatin, carboxymethyl cellulose, serpin	Prevent enzyme degradation in the stomach and small intestine.	Protease inhibitors can influence the absorption of other proteins that can lead to severe toxicity during chronic drug therapy.	(Iyer *et al.*, 2010:181; Park *et al.*, 2011:281)
FORMULATION APPROACHES				
Name	**Example**	**Mechanism of action**	**Drawback**	**Reference**

Site specific delivery systems (primary approaches)	pH sensitive polymer coated drug delivery system	Drug is in the core of the formulation containing an absorption enhancer, coated with a pH sensitive polymer. The first coating is an acid soluble polymer coating while the second coating is an enteric coating.	The location and environment where the coating will start to dissolve is uncertain.	(Singh *et al.*, 2018:15)
	Time dependent drug delivery system	Drug is being released in the colon after a specific time interval.	Gastric emptying time and transit time may vary.	(Amidon *et al.*, 2015:735)
	Microbially triggered system	Drug is being released from the dosage form when the polysaccharides are degraded by colonic microflora bacteria.		(Singh *et al.*, 2018:16)
	Polysaccharide-based delivery systems (e.g. cellulose acetate, pectin, chitosan, chondroitin sulphate, galactomannan, amylose, xanthan gum and guar gum)	The drug is set in a matrix core composed of biodegradable polymers.		(Amidon *et al.*, 2015:736; Singh *et al.*, 2018:16)
	Pressure controlled drug-delivery system	Drug release occurs after disintegration of the water insoluble capsule due to pressure in the colon. Drugs are in a liquid form.		(Challa *et al.*, 2011:178)

Site specific drug delivery (Newly developed approaches)	Pulsatile colon targeted drug delivery	**Palsincap system:** Enteric coated unit that is made up by a non-disintegrating half capsule, filled with drug content, sealed at the open end with a hydrogel plug and covered with a watersoluble cap. **Port system:** Capsule body is formed from a semipermeable membrane. The capsule body is filled with an insoluble plug consisting of osmotically active agents and the drug formulation. After contact with the dissolution fluid the semipermeable membrane permits fluid flow into the capsule and this leads to the development of pressure leading to the release of the drug due to expelling of the plug.		(Rangari & Puranik, 2015:182; Ratnaparkhi *et al.*, 2013:38)
	Combination of pH dependent and microbially triggered colon drug delivery system (CODES)	System is made up by a traditional tablet which contains lactulose, coated with an acid-soluble material (Eudragit E) and over-coated with an enteric substance (Eudragit L). Coating protects drug while in the stomach and in the small intestine. Bacteria in the colon enzymatically degrades the lactulose into an organic acid leading to drug release		(Challa *et al.*, 2011:178)

Site specific drug delivery (Newly developed approaches)	Osmotic controlled drug delivery systems	The system is regulated by osmotic pressure. The hard gelatine capsule dissolves due to the pH of the small intestine and allows the entering of water into the unit, leading to forcing out of the drug.		(Amidon *et al.*, 2015:738)
Site specific drug delivery (Newly developed approaches)	Multi-particulate systems	Can include pellets, micro-particles, granules and nano-particles. Sub-units can be compressed into tablet, filled into a sachet or be encapsulated.	Method of manufacturing involves organic solvents, heat and agitation, which may be harmful to protein and peptide drugs.	(Singh *et al.*, 2018:18) (Reddy *et al.*, 2013:51) (Rangari & Puranik, 2015:183)
	Azo hydrogel	Peptide capsules are coated with polymers cross-linked with azo-aromatic groups protecting the drug against digestion in the stomach and small intestine. In the colon the azo bond is reduced and the drug is being released.		(Challa *et al.*, 2011:176; Ratnaparkhi *et al.*, 2013:35)
	Probiotic approach	At body temperature, the probiotic strain is activated and the digestion of the carrier takes place. The drug is then released.		(Singh *et al.*, 2018:19)

	Ora-lyn™	Small particles from an aqueous spray into the oral cavity. This allows the rapid absorption of insulin.	Bioavailability is low. Repeated administration.	(Cefalu, 2004:214; Lassmann-Vague & Raccah, 2006:515)
Site specific drug delivery (Oral transmucosal route)	Gas driven delivery system by means of carbon dioxide forced transport.	Deliver the protein to the surface of the small intestine.		(Muheem *et al.*, 2016:421)
Forced transport	Emulsions: Solid-in-oil-in-water (S/O/W), Oil-in-water (O/W), Enteric coated.	Improve intestinal uptake of peptide and protein molecules.	The stability of these emulsions in long-term storage could be problematic.	(Maher *et al.*, 2016:298; Muheem *et al.*, 2016:420)
Formulation vehicles	Liposomes: Double liposomes, Fusogenic liposomes, Archaeosome, Cross-linked liposomes.	Helps to control the release of drug molecules. Protects against breakdown due to bile salts and lipases.	Ionic/hydrophobic interactions with the liposomal components and the inflexibleness of the bilayer that was formed effects the efficiency of the peptides.	(Niu *et al.*, 2016:346)
	Microspheres: Endragril-S100, pH-sensitive poly methacrylic acid-g-ethylene glycol.	Deliver the protein to a specific site in the gastro-intestinal tract.	Particle aggregation can take place.	(Muheem *et al.*, 2016:420; Park *et al.*, 2011:281)
	Nanoparticles: Poly methyl methacrylate, chitosan, polystyrene, poly lactic-co-glycolic acid polyethylene glycol.	Increased absorption through intestinal epithelium. Increase in membrane permeability.		(Muheem *et al.*, 2016:420)
	Surfactants: sodium lauryl sulphate (Ionic), polysorbate (non-ionic), Tween 80 (non-ionic)	Increase absorption of protein and peptide molecules that cross the epithelium through the transcellular pathway.	Unwanted molecules reach the systemic circulation.	(Choonara *et al.*, 2014:1273)

Absorption enhancers	Bile salts: sodium glycholate, sodium deoxycholate, taurodeoxycholate, taurocholate	Increase in drug absorption by decreasing the density of mucus, forming of mixed micelles and disruption in phospholipid acyl chain.	Non selective for peptides and proteins. Unwanted molecules reach the gastro-intestinal tract.	(Choonara *et al.*, 2014:1273; Maher *et al.*, 2016:295; Muheem *et al.*, 2016:418,420)
	Fatty acids: Sodium caprate, acyl carnites, oleic acid, lauric acid, acyl choline, caprylic acid	Increase the levels of intracellular calcium through the activation of phospholipase C in the plasma membrane resulting in an increase in paracellular permeation.	Causes cell damage in *in vitro* everted sac models, like oedema and the length of the villi decrease.	(Anilkumar *et al.*, 2011:440; Choonara *et al.*, 2014:1273; Sharma *et al.*, 2005:890)
Absorption enhancers	Chitosan and derivatives: N-trimethyl chitosan chloride	Reduction of the integrity of the tight junctions and paracellular transport is increased.	Unwanted molecules reach the systemic circulation.	(Anilkumar *et al.*, 2011:440-441; Choonara *et al.*, 2014:1273) (Muheem *et al.*, 2016:420)
Absorption enhancers of plant origin	Piperine	Stimulates micelle formation, stimulate active transport. Increase thermogenic action on the epithelial cells, P-gp and enzyme inhibition.		(Majeed & Prakash, 2007:77-78)
	Aloe vera	Open tight junctions between epithelial cells, promotes paracellular transport.		(Chen *et al.*, 2009b:588)
	Capsaicin	Inhibits P-gp related efflux. Reversible opening of tight junctions.	The burning sensation is problematic in the development of permeability enhancers.	(Han *et al.*, 2006:1728) (Kanda *et al.*, 2018:1-3)
	Quercetin	Inhibit CYP3A4 and P-gp efflux pumps.		(Tatiraju *et al.*, 2013a:57)
	Naringin	Inhibits CYP3A4 and P-gp efflux pumps.		(Dudhatra *et al.*, 2012:23)

	Genistein	Inhibits the efflux function of P-gp, BCRP and MRP2.		(Ajazuddin *et al.*, 2014:6)
	Curcumin	Inhibits CYP3A4 and P-gp efflux pumps.		(Dudhatra *et al.*, 2012:18)
	Turmeric	Inhibits CYP3A4 and P-gp efflux pumps.		(Tatiraju *et al.*, 2013a:57)
	Carum carvi	P-gp efflux pump inhibitor.		(Kumar-Sarangi *et al.*, 2018:16)
	Peppermint oil	Mechanism unknown, but the most probable mechanism is the inhibition of CYP3A4.		(Kumar-Sarangi *et al.*, 2018:16)
	Sinomenium acutum	Inhibition of P-gp efflux pumps.		(Tatiraju *et al.*, 2013a:59)
	Caraway	P-gp efflux pump inhibitor		(Tatiraju *et al.*, 2013a:58)

1.3 Bioavailability modulators of natural origin

Evidence exists that combinations of herbs were used to treat diseases in patients by ancient civilizations in order to find a 'panacea' or perfect mixture. Reference to herbal mixtures can be found in the ancient Egyptian medicinal book *Papyrus Ebers*, the *Materia Medica* by Dioscoridus and the 12th century manuscript *Antidotarium Nicolai*. These treatments were mainly based on the positive outcomes observed when herbal products were combined (Che *et al.*, 2013:5126; Gertsch, 2011:1088). With the combination of several plant extracts (or multi-extract combinations), a multi-target synergistic effect could be achieved. Even single crude extracts contain a mixture of phytochemicals. This means that several pharmacological targets could be reached at the same time (Wagner & Ulrich-Merzenich, 2009:98). This is only one of the mechanisms through which combinations of herbs or drugs can elicit synergistic effects (Wagner, 2011:35).

The combination of drugs with natural bioenhancers received growing interest in the improvement of bioavailability of poorly absorbable drugs (Ajazuddin *et al.*, 2014:2). The two major mechanisms by which natural bioenhancers can change the pharmacokinetics of drugs are by modulation of metabolizing enzymes and/or membrane permeation (e.g. through opening of tight junctions, inhibition of efflux transporters by causing changes in the membrane properties). There are two major transporter systems that are involved in herb-drug interactions namely ATP-binding cassette (ABC) and solute carrier (SLC) transporters. ABC transporters consist of three well

known transporters namely, P-gp, multi-drug resistance associated proteins (MRP) and breast cancer resistance protein (BCRP) as well as various other transporters. These ABC transporters are responsible for efflux of molecules and are mainly located on the apical side of epithelial cells, causing a first line barrier to absorption of drug substrates. The inhibition of efflux transporters may improve the bioavailability of certain co-administered drugs. Solute carrier transporters consist of organic cation transporters, organic anion transporters and organic anion-transporting polypeptides. These transporters are responsible for the uptake of substances into the cells. The inhibition or potentiation of active uptake transporters may have an effect on the bioavailability of certain drugs (Wu *et al.*, 2016:237). Several active plant constituents are known to influence the activity of transporters. In the following sections piperine and capsaicin is being discussed.

1.3.1 Piperine

Piperine is the major alkaloid component of black pepper (*Piper nigrum*) and long pepper (*Piper longum*) *(*Khajuria *et al.,* 2002:224*).* Piperine can be considered as one of the world's first bioavailability enhancers and its use could be dated back to the 7th century BC (Ajazuddin *et al.*, 2014:1). Piperine is also known for biological activities such as anti-inflammatory, anti-pyretic, anti-fungal, anti-diarrheal and anti-cancer effects. It has also shown analgesic effects, lowering of hypertension, anti-depressant effect as well as anti-oxidative effects (Ahmad *et al.*, 2012:1947-1950).

Piperine has shown the ability to increase the bioavailability of curcumin, the active principle in *Curcuma longa* (turmeric) (Tatiraju *et al.*, 2013b:57). Gastro-intestinal tract and liver enzymes are the main cause of the rapid metabolism of curcumin. Due to the ability of piperine to inhibit hepatic and intestinal glucuronidation, the bioavailibility of curcumin could be increased by 200% with the co-administration of piperine (Jhanwar & Somdatt, 2014:448). The possible mechanisms by which piperine enhances drug bioavailability is by inhibiting cytochrome P450 (CYP) enzymes and by inhibiting efflux transporters (Di *et al.*, 2015:144). Another mechanism of drug absorption enhancement by piperine could possibly be by increasing thermogenesis (Majeed & Prakash, 2007:74).

1.3.2 Capsaicin

Capsaicin, a vanillyl amide alkaloid, is known as the main active ingredient in *capsicum* fruits. Capsaicin is responsible for the pungent flavour of pepper fruits. Except for the use of pepper fruits as a flavouring in food, capsaicin has a wide range of biological activities and clinical uses in the body. The uses of capsaicin include cardiovascular benefits, protective effect on erythrocyte integrity, anti-oxidant effects, anti-nociceptive activity, chemopreventive effects, anti-diabetic potential, thermogenic and weight reducing influences, anti-ulcer activity, anti-

inflammatory effect and absorption enhancement characteristics (Hayman & Kam, 2008:340-342; Srinivasan, 2016:1489-1495).

The possible mechanism by which capsaicin helps to enhance drug bioavailability is by inhibiting CYP and P-gp (Zhang *et al.*, 2016:339). Another mechanism by which absorption of drug molecules can be enhanced with the co-administration of capsaicin is by the opening of tight junctions (Kanda *et al.*, 2018:3).

1.4 *In vitro* models to evaluate drug permeability

There are a number of models that can be used to predict the intestinal absorption of drug molecules namely *in vivo, in vitro, ex vivo, in situ* and *in silico* models:

- *In vivo* models include whole animals and healthy human subjects where oral bioavailability, distribution, clearance and formation of drug metabolites can be determined directly by means of blood sampling and analysis (Zhang *et al.*, 2012:550).
- *In vitro* models include cultured cell monolayers. Some of the cell culture models that are frequently used are the human colonic adenocarcinoma cells (Caco-2) and Madin-Darby canine kidney (MDCK) cell lines (Antunes *et al.*, 2013:15)
- *In silico* models are computerised and mathematical models that play an important role in drug research and development and are used to address issues regarding drug absorption and bioavailability (Antunes *et al.*, 2013:6).
- *In situ* models include the perfusion of intestinal segments of rodents with drug solutions to determine drug absorption (Antunes *et al.*, 2013:11)
- In *ex vivo* models, excised animal tissues are mounted in Ussing-type chambers to determine the rate, extent and mechanism of drug permeation across mucosal membranes (Antunes *et al.*, 2013:13).

In vitro models are in general less labour and cost intensive and the ethical related aspects are less than those for *in vivo* studies. Some of the drawbacks of *in vitro* studies include the absence of gastric emptying rate, gastro-intestinal transit rate and changes in gastro-intestinal pH cannot be incorporated into the study. *In vitro* models are still considered to be good screening tools to select compounds with acceptable drug-like properties during the drug discovery process (Antunes *et al.*, 2013:7). These studies cannot replace *in vivo* studies, but the controlled environment of these studies contribute to generate important information regarding the pharmacokinetics of drug molecules (Griffin & O'Driscoll, 2007:34).

1.4.1 Cell cultures

The Caco-2 cell line is one of the most frequently used cell lines for *in vitro* permeation studies. Although the Caco-2 cell line originated from human colorectal carcinoma, the cells of the Caco-

2 line have structural and functional similarities to mature enterocytes (Fearn & Hirst, 2006:172). These cells contain apical microvilli, tight junctions between cells, as well as small amounts of intestinal enzymes such as hydrolases, transferases, aminopeptidase-N and certain CYP isoenzymes (Ölander *et al.*, 2016:822-824). Studies on Caco-2 cell monolayers can help with the early identification of the permeability of a drug across the gastro-intestinal tract epithelium before *in vivo* studies are done (Fearn & Hirst, 2006:175). The disadvantage of this cell line is that it takes 21 days to grow into confluent monolayers and CYP enzymes are expressed to a relatively low extent (Ölander *et al.*, 2016:824).

1.4.2 *Ex vivo* models

Ex vivo models used for transport studies refer to excised animal tissues that are mounted in a diffusion apparatus such as Ussing-type chambers (Antunes *et al.*, 2013:15). Animals used for *ex vivo* experiments with respect to the prediction of human intestinal absorption include pigs, dogs, monkeys and rats (Antunes *et al.*, 2013:14). The gastro-intestinal tract of pigs has particular physiological, anatomical and biochemical similarities when compared to that of humans. This makes it an appropriate *ex vivo* model to evaluate drug absorption (Sjögren *et al.*, 2014:109). The body weight to small intestine length ratio of a pig is similar to that of humans. A study using excised pig intestinal tissue in the Sweetana-Grass diffusion apparatus can help with the identification of absorption mechanisms of drug molecules (Luo *et al.*, 2013:211). This is considered to be a cost-effective method to do drug transport studies, because it is less labour intensive and the tissue could be collected as a byproduct from the local abattoir where animals are slaughtered for meat production purposes (Antunes *et al.*, 2013:7; Nunes *et al.*, 2015a:208).

1.5 Research problem

It is challenging to deliver macromolecules into the systemic circulation *via* the oral route of administration due to enzymatic breakdown in the gastro-intestinal tract, as well as poor membrane permeability due to the size and hydrophilic nature of these molecules. Most peptide and protein drugs have to be administered by means of the parenteral route, but several drawbacks are associated with this route of administration such as pain, discomfort, possibility of infections and poor patient compliance. It is well known that several plant materials and extracts have the ability to enhance the bioavailability of co-administered drugs/herbs (Ajazuddin *et al.*, 2014:2). It has been shown that piperine can enhance the membrane permeation of molecules most likely by changing the lipid dynamics of the epithelial cell membranes (Khajuria *et al*., 2002:224), by reducing metabolism (Di *et al.*, 2015:144) and by inhibition of P-gp related efflux (Bhardwaj *et al*., 2002:645). However, the effect of piperine on the permeation of peptide and protein drugs (or macromolecular compounds) has not been investigated yet. Furthermore, capsaicin, the active compound in pepper fruits, have certain characteristics that could help to possibly enhance the absorption of macromolecules. This includes the inhibition of CYP, P-gp

and the reversible opening of tight junctions (Kanda *et al.*, 2018:3; Zhang *et al.*, 2016:339). However, the effect of capsaicin on the permeation of peptide and protein drugs (macromolecular compounds) has not been investigated yet on in *ex vivo* model.

1.6 Aim and objectives

1.6.1 Aim

The main aim of this study was to investigate P-gp related inhibitory effects and macromolecular drug absorption enhancement effects of capsaicin and piperine across excised pig intestinal tissue.

1.6.2 Objectives

The specific objectives of the study were to:

- Validate fluorometric analytical methods for two selected model compounds Rhodamine 123 (P-gp substrate) and fluorescein isothiocyanate (FITC)-dextran (macromolecular), as well as for Lucifer Yellow (a membrane exclusion marker molecule to test membrane integrity) on the Spectramax Paradigm® fluorimeter in terms of linearity, accuracy, limit of detection, limit of quantification, repeatability and selectivity.
- Conduct bi-directional *ex vivo* permeation studies on Rhodamine 123 in the presence and absence (control groups) of the selected pepper extract compounds at different concentrations.
- Conduct *ex vivo* permeation studies in the apical-to-basolateral direction on FITC-dextran (4000 Da) in the presence and absence (control group) of selected pepper extract compounds at different concentrations.
- Chemically characterise the purity of the pepper raw materials (capsaicin raw material and piperine raw material) by means of high performance liquid chromatography (HPLC) analysis with respect to piperine and capsaicin reference standards.
- Process and interpret the permeation data in terms of P_{app} (apparent permeability coefficient), ER (efflux ratio) values and calculating the percentage trans-epithelial electrical resistance (%TEER) of the transport studies.

1.7 Ethics

Intestinal tissue was collected at the abattoir (Potchefstroom, South Africa) from pigs that were already slaughtered for meat production purposes and not for research purposes. Ethical consideration was required for the control regarding the site of tissue collection and the correct disposal procedures after the completion of transport studies. Ethical approval was obtained from

the Animal Ethics Committee (AnimCare) of the North West University (NWU-00025-15-A5) for use of excised pig intestinal tissues from Potchefstroom abattoir for drug permeation studies.

Waste was removed according to approved SOP's (Biological waste management as well as Chemical, toxic and pharmaceutical substance waste management).

1.8 Dissertation layout

In this dissertation, Chapter 1 gives a brief background, describes the rationale of the study and states the research problem and gives the aim and objectives of this study. A literature review is given in Chapter 2, where the mechanisms of drug absorption are described as well as different absorption enhancement strategies to improve the oral uptake of protein and peptide drug molecules. The absorption enhancement effects of capsaicin and piperine and different methods available for determining drug permeation are also described in Chapter 2. Chapter 3 describes the methods and materials used to execute the experiments in order to collect data during the study. In Chapter 4, the results obtained from the experiments are reported, including explanations of P_{app} and efflux ratio values and changes in % trans-epithelial electrical resistance. Statistically analysed data and discussions of relevant results are also included in Chapter 4. The final conclusions and future recommendations are presented in Chapter 5.

Chapter 2: Oral delivery of therapeutic protein and peptide drugs

2.1 Introduction

The oral route is considered to be the most preferred route of drug administration due to numerous advantages associated with patient compliance and production of oral drug products. Advantages regarding the patient include a painless method of drug administration, which increases patient compliance specifically for chronic diseases. The manufacturing of oral dosage forms is more cost-effective when compared to sterile dosage forms and it is not necessary to train patients on how to correctly administer oral drug products (Ahmad *et al.*, 2014:1; Maher & Brayden, 2012:113). The formulation of oral dosage forms, especially for protein and peptide drugs, is a complex process due to numerous variables that need to be taken into consideration. This is especially important in terms of the bioavailability of drugs that are administered by means of the oral route. The fraction of a drug that is absorbed intact and able to avoid first pass hepatic, as well as intestinal metabolism, is known as the bioavailability of the administered drug. Limited absorption is caused by various factors including physiological barriers as well as the physicochemical properties of the drug molecules (Gaucher *et al.*, 2010:147).

Some protein and peptide molecules are attractive drug candidates due to their high selectivity towards a specific receptor site, effectiveness, potent physiological action and low toxicity (Woitiski *et al.*, 2008:223). However, there are various hurdles that need to be taken into consideration in the development of oral drug delivery systems for these bio-macromolecules, such as the hostile environment in the gastrointestinal tract and poor absorption or permeability of these drug molecules across biological membranes (Hassani *et al.*, 2015:12).

The gastro-intestinal tract is designed to break down large molecules and deactivate pathogens (Moroz *et al.*, 2016:109). The pH in the stomach is acidic (between 1-2.5), which leads to the protonation as well as unfolding of proteins, to form a distinctive sequence on the molecule for recognition by protein-degrading enzymes. Pepsin in the stomach as well as chymotrypsin, amino- and carboxypeptidases, RNases and DNases in the small intestine split proteins and peptides into smaller fragments, while in the large intestine further degradation takes place due to enzymatic fermentation processes (Fuhrmann & Leroux, 2014:1099-1100). Another barrier against oral absorption of drug molecules is the possibility that a drug molecule could be a substrate for active apical efflux transporters. Drug absorption will be limited due to the fact that these transporters pump substrates back into the intestinal lumen (Fearn & Hirst, 2006:169). The first-pass effect contributes to a limited amount of active drug molecules that reaches the systemic circulation (Fearn & Hirst, 2006:170; Hassani *et al.*, 2015:13).

Unfavourable physico-chemical properties of macromolecules can be seen as a major hurdle regarding their uptake after oral administration. Protein and peptide drug molecules usually have

a very large molecular weight and are hydrophilic (Khafagy & Morishita, 2012:532). Most protein and peptide drug molecules do not comply to the Lipinski rule of five and therefore bioavailability after oral administration is problematic (Maher *et al.*, 2016:284).

2.2 Transport mechanisms of drug absorption after oral administration

There are mainly two well-defined pathways for the absorption of molecules across the intestinal epithelial membrane namely, transcellular and paracellular pathways. Furthermore, mechanisms of drug absorption *via* these pathways include passive diffusion, receptor-mediated transport, carrier-mediated transport as well as active efflux (Anilkumar *et al.*, 2011:437; Pawar *et al.*, 2014:170). The extent of absorption through each pathway depends on the physico-chemical properties of the drug molecules such as molecular weight, hydrophobicity, structural orientation, ionization constants, pH and pKa related solubility (Pawar *et al.*, 2014:170). Figure 2.1 illustrates the different absorption mechanisms across the gastrointestinal tract.

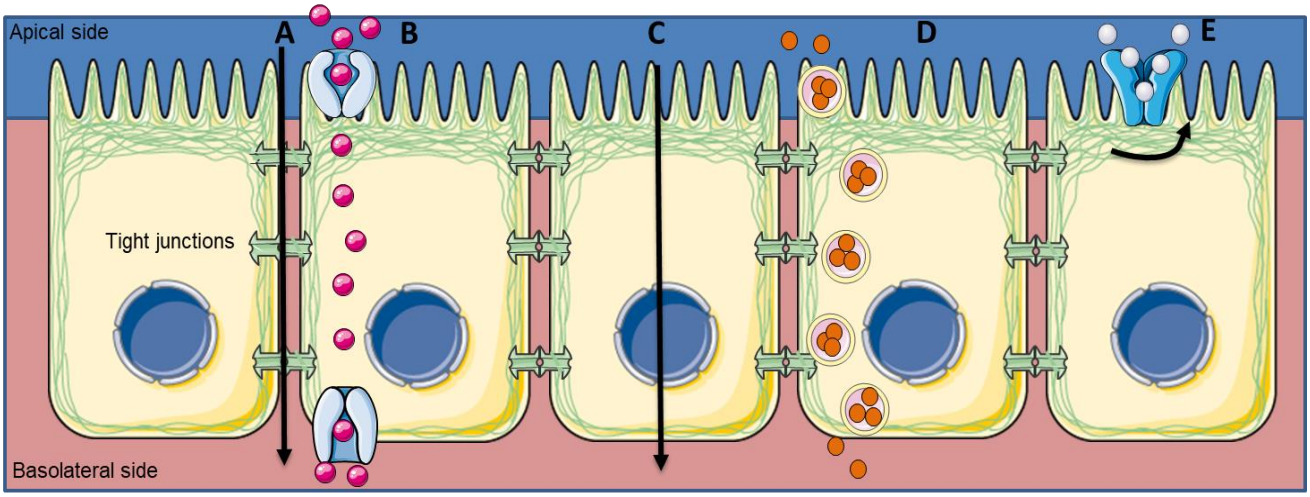

Figure 2.1: Illustration of the absorption mechanisms across the gastro-intestinal tract epithelium: A) passive paracellular transport, B) carrier-mediated transport, C) passive transcellular transport, D) receptor-mediated transport and E) efflux transport. (Adapted from Anilkumar et al. (2011:437); Sugano et al. (2010:598-599), produced by making use of Servier Medical Art, (Servier-Medical-Art, 2018)).

2.2.1 Transcellular transport

Passive transcellular transport is a process where diffusion takes place across cells as seen in Figure 2.1. The cell membranes consist of a phospholipid bilayer that contains membrane proteins. The membrane structure of the intestinal enterocytes differs on the apical and basolateral sides. The apical side of the cell has a lower permeability than the basolateral side of the cell (Anilkumar *et al.*, 2011:437). For a molecule to be absorbed by intestinal cells, it has to pass through the mucus layer first to reach the enterocyte's surface (Roger *et al.*, 2010:294). The process of transcellular transport can be divided into the following three main steps and is driven by a concentration gradient:

- An uptake process at the apical side of the cell that is initiated by an endocytic process.
- Transport through the cell.
- Release at the basolateral side of the cell.

2.2.2 Paracellular transport

Paracellular transport of drugs occurs through the intercellular spaces between the cells in a passive manner by making use of diffusion as seen in Figure 2.1 (Muheem *et al.*, 2016:416; Roger *et al.*, 2010:291). Tight junctions, specifically the zonula occludens protein are the major rate-limiting barrier affecting the absorption of molecules through the paracellular pathway (Renukuntla *et al.*, 2013:77; Yun *et al.*, 2013:823).

Epithelial cells are kept in formation by means of tight junctions thereby forming a continuous layer. Despite the tight arrangements of the tight junctions, there are gaps named aquaporins between two adjacent cells forming a channel that connects the luminal space to the areas beneath the basolateral membrane. Aquaporins are the main supply of water into the cell, due to their uninhibited aqueous exchange ability. Claudins, occlaudins and junction adhesion molecules are protein-related structures and form the functional components of aquaporins (Pawar *et al.*, 2014:170). Drugs with a small to moderate molecular weight can permeate through these water-filled aquaporins. The average pore diameter of these gaps in a human small intestine is 8-13 Å, which will limit drugs to undergo paracellular permeation with a diameter smaller than 8 Å (Anilkumar *et al.*, 2011:438).

2.2.3 Carrier-mediated transport

Carrier-mediated transport can be divided into facilitated and active transport processes that are saturable (Sugano *et al.*, 2010:610). If adenosine triphosphate (ATP) is directly or indirectly required for the transport process, it is known as active transport and there is no need for a concentration gradient of the permeant. For the primary active transport process to take place, an ATP-binding cassette (ABC) transporter superfamily must bind and hydrolyse ATP. Solute carrier (SLC) transporters are powered by an ion gradient that is formed by an ATP-dependent primary transporter, for example sodium/potassium ATPase. Facilitated transport is when the transport process is not energy driven, but a concentration gradient as well as a transporter protein is required for the process to take place (Sugano *et al.*, 2010:598).

Carrier-mediated transport makes use of certain proteins known as shuttle transporters to shuttle specific molecules through a membrane. These transporters are expressed on the apical side as well as the basolateral side of the membrane, facilitating the movement of nutrients and other endogenous substances (Pawar *et al.*, 2014:170).

2.2.4 Efflux transporters

Efflux transport is a first line defence mechanism, preventing the absorption of toxins and unfamiliar substances into the bloodstream (Takano *et al.*, 2006:138). P-glycoprotein (P-gp), multidrug resistance-associated protein 2 (MRP 2) and breast cancer resistance protein (BCRP) are efflux transporters belonging to the ATP binding cassette transporter family, situated at the apical membrane of the small intestine, leading to limited bioavailability of orally administered drugs that are substrates for these transporters (König *et al.*, 2013:945). The apical membrane of the intestine is rich in these transporters thereby limiting the absorption of certain clinically important drugs. These efflux transporters make use of ATP as a source of energy to pump substrates against a concentration gradient (Estudante *et al.*, 2013:1341).

2.2.5 Receptor-mediated transport

Protein drug molecules transported by means of receptor-mediated transport either act as a receptor specific ligand for surface-attached receptors or as a receptor for surface ligands (Yun *et al.*, 2013:824). An example of a receptor-mediated transport process is when an exogenous ligand binds to a specific membrane receptor. This binding is followed by membrane invagination until an internal vesicle (receptosome) forms inside the cell. Membrane proteins, lipids and extracellular solutes are also surrounded during this process (Swaan, 1998:827).

2.2.5.1 Endocytosis

There are four mechanisms of action for the endocytosis process namely, clathrin-mediated endocytosis, caveolae, macropinocytosis and phagocytosis. For clathrin-mediated endocytosis and caveolin-dependend endocytosis to take place, a macromolecule has to bind to a specific receptor and after the receptor binding process internalization will take place. Neither in clarthrin-mediated endocytosis nor in caveolin-dependend endocytosis will the endocytotic vesicle be larger than 150 nm in size (Lundquist & Artursson, 2016:263). Macropinosomes and phagosomes involves the formation of large membranous cavities reaching a diameter of several microns (Bohdanowicz & Grinstein, 2013:84). Phagocytosis is restricted mainly to the M-cells and transports larger particles of 0.5 µm in size, as well as pathogens. Macropinocytosis is a transport mechanism where fluid filled vesicles are transported across a membrane. The vesicle can be between 0.2- 5 µm in size (Bohdanowicz & Grinstein, 2013:84-94; Lundquist & Artursson, 2016:263; Pawar *et al.*, 2014:171).

2.3 Experimental models used to predict drug absorption

One of the major goals in the design, optimization and selection of drugs designed for oral delivery is the prediction of their human intestinal absorption. Various models are currently used to evaluate the absorption of drugs in the different phases of drug discovery and development. These models include *in vivo, in vitro, in situ, ex vivo* and *in silico* models (Antunes *et al.*, 2013:4). In Figure 2.2, the different models for drug absorption prediction are listed.

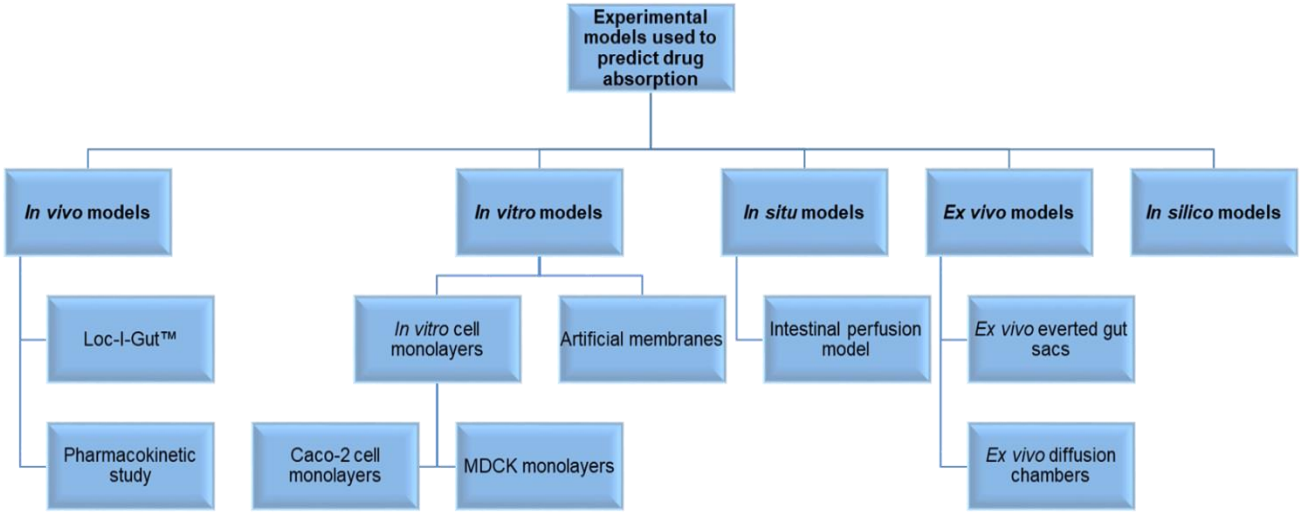

Figure 2.2: Flow-chart illustrating the experimental models that can be used to predict drug absorption (compiled from Billat et al., 2017:766; Antunes et al., 2013:7; Holmstock et al., 2012:1474; Balimane et al., 2000:305)

2.3.1 *In vivo* models

In vivo models are good methods to measure drug absorption due to the fact that all the physiological parameters are intact (Billat *et al.*, 2017:766). While *in vitro* models focus only on one specific process for example the absorption of certain drug molecules, the multi-factorial results of *in vivo* models include the effects on permeability, distribution and excretion. Pharmacokinetic parameters, as well as the toxicology endpoint can be determined. Animal models as *in vivo* models are necessary to measure drug exposures and also for determining potential toxicities (Zhang *et al.*, 2012:555). *In vivo* models involve highly resource intensive processes (Balimane *et al.*, 2000:309). There is a large difference between some animal models and humans regarding metabolism, drug transport, the absorption surface area and the flora present in the gastrointestinal tract. This means that some animal models are not appropriate in predicting drug pharmacokinetics in humans (Billat *et al.*, 2017:767).

2.3.1.1 Loc-I-Gut™

This method is based on a jejunal perfusion system consisting of a multi-channel tube and two inflatable balloons named the Loc-I-Gut™ system. This is a method that could be used as a golden reference standard to compare drug absorption obtained from other models because it is the most realistic and representative method that was developed to date. A 5.3 mm in diameter polyvinyl chloride tube is being placed orally into the small intestine. This tube consists out of six channels and two latex balloons 10 cm apart from each other. The latex balloons are being used to isolate a specific area in the intestine. The wide channels at the sides is used to full the balloons with air and supply the intestine with fluid and air. The channels in the middle is used to administrate the marker molecule and drainage. The drawbacks regarding this method include costs (it is expensive) and ethical issues related to human volunteers (Billat *et al.*, 2017:767).

2.3.1.2 Pharmacokinetic study in human volunteers

A pharmacokinetic study is done by administering a specific drug orally to healthy volunteers. Blood samples are withdrawn at different time intervals after the drug was taken. Gastric emptying, gastro-intestinal and liver metabolism, the difference in the expression of transporters as well as the elimination period may lead to extremely large intra-individual and inter-individual variability in this results. The only manner to overcome these variations is by making use of a large number of individuals (Billat *et al.*, 2017:767).

2.3.2 *In vitro* models

In vitro models that are used to predict drug absorption are less labour intensive, less costly and the ethical considerations are fewer than that of *in vivo* studies (Balimane *et al.*, 2000:305). A universal drawback of *in vitro* models is that physiological factors such as gastric empting rate, gastrointestinal transit rate and gastrointestinal pH cannot be taken into consideration when results are being interpreted (Antunes *et al.*, 2013:7).

2.3.2.1 Cell cultures

A variety of cell lines are grown on semi-porous filters to form monolayers that have similar barrier properties in a morphological and functional manner than that of the intestinal epithelium. These monolayers are placed into a diffusion apparatus consisting of apical (AP) and basolateral (BL) chambers. The AP side represents the lumen (mucosa) of the intestine, while the BL side represents the blood (serosal) side. Drugs may be placed in the AP or BL chamber. When drugs are placed in the BL chamber efflux is measured, while when drugs are placed in the AP chamber absorptive transport is measured. The apparent permeability coefficient (P_{app}) is calculated from the rate of drug accumulation in the receiver chamber, taking the cell monolayer area and chamber volumes into consideration (Volpe, 2010:674).

2.3.2.1.1 Caco-2 cell monolayers

The human epithelial colorectal adenocarcinoma cell line (Caco-2), represents the primary epithelial cell type in the gastro-intestinal tract. The Caco-2 monolayers are ready within 15-25 days after seeding for permeation studies. An appropriate transepithelial electrical resistance (TEER) value of the cell monolayer when the experiment is performed is between 260-450 Ω/cm^2. This gives an indication of the integrity of the cell monolayer (Gamboa & Leong, 2013:803). Caco-2 cells originated from the colon, but express a majority of morphological as well as functional characteristics that are present in the small intestinal absorptive cells. These cell monolayers contain transporters, tight junctions between cells as well as expressing a significant amount of P-gp transporters. Other advantages of Caco-2 cells are that it is a well characterized model, the cells are of human origin and high-throughput screening can be done. Disadvantages of making use of Caco-2 monolayers are that there is an under-expression of CYP 3A enzyme as well as absence of mucus. These monolayers are impermeable for the transport of hydrophilic molecules transported by means of paracellular transport. This is due to the much tighter junctions between cells than those observed in humans and animals. Small molecules will diffuse much easier through these cells due to their ability to reach microvilli easier as a result of the absence of mucus (Antunes *et al.*, 2013:10; Gamboa & Leong, 2013:803; Holmstock *et al.*, 2012:1473).

2.3.2.1.2 MDCK cell monolayers

Madin-Darby canine kidney (MDCK) cells differentiate quickly and can be used to perform transport studies after three days from the time it was seeded (Putnam *et al.*, 2002:27). These cells have a lower TEER value than that of Caco-2 cell monolayers and this value is much closer to that of *in vivo* small intestinal tissue. These cells contain tight junctions and a brush border similar to Caco-2 cells, but the P-gp expression level is lower than that of Caco-2 cells. M-cells as well as a mucus layer are not present in these cells (Billat *et al.*, 2017:768).

2.3.2.2 Artificial membranes

Parallel artificial membrane permeability assay (PAMPA) is a popular method used to predict transcellular passive diffusion across biological membranes during the drug development process. This method is used to measure passive absorption of a compound from a donor compartment to an acceptor compartment separated by a lipophilic artificial membrane (Petit *et al.*, 2016:425). Advantages of this *in vitro* model include rapid identification of the permeation potential of biologically active compounds; cost-effectiveness, stable and structural adaptable for a specific purpose. A disadvantage of this method is that only transcellular transport can be measured (Yu *et al.*, 2015:1-2).

2.3.3 *In situ* models

By making use of an *in situ* model to predict drug absorption, a segment of the intestine of an anesthetized animal is cannulated and perfused with a pre-determined concentration of a certain drug. For the duration of the experiment, the animal is kept sedated and its body temperature is controlled by making use of an overhead lamp as well as a heating pad. During the perfusion process of the intestinal segment, drugs will be absorbed to a certain extent based on its physico-chemical and biopharmaceutical properties, causing a decrease in concentration of the perfusion liquid containing the compound. By comparing the drug concentration in the donor solution to that obtained on the other side of the cannulated segment of the intestine, the amount of drug that was absorbed by means of transcellular or paracellular transport may be calculated (Stappaerts *et al.*, 2015:666). *In situ* models offer a better prediction of human absorption when comparing it with a cell-based model due to the following advantages: a fully intact intestinal mucosa with nerve supply and blood flow, sink conditions are present and all the enzymes present in the gastro-intestinal tract are expressed as well as the transporters (Holmstock *et al.*, 2012:1474). The major disadvantage of this model is that a large number of animals is required to obtain statistically significant absorption data (Antunes *et al.*, 2013:15).

2.3.4 *Ex vivo* models

Ex vivo models have certain characteristics that distinguish them from *in vitro* models. Realistic paracellular transport can take place across the small intestinal epithelial used in *ex vivo* models, a mucus layer is present and transport proteins are fully expressed. Shortfalls in this model are the lack of blood supply and the absence of a nerve system. Regardless the shortfalls, this is an easy and widely use model in the development of potential new drugs (Luo *et al.*, 2013:209).

2.3.4.1 Everted gut sacs

An euthanized animal's intestine is removed, flushed with a buffer and cut into small segments, making it possible to evaluate permeability in different sections of the intestine. A 2-4 cm sac is connected to the one end of a glass tube, filled with an oxygenated buffer solution and connected at the other end. This setup is then placed in a container filled with the drug solution dissolved in an oxygenated buffer solution. At specific time periods, the drug concentration in the sac is then measured and the P_{app} values are normalized by taking the surface area of the sac into consideration (Volpe, 2010:673). Advantages of making use of this model are that active and passive transport mechanisms can be studied and efflux transporters can also be evaluated due to the expression of P-gp. A mucus layer is present, it is a relatively fast and cost-effective technique to study drug absorption and absorption mechanisms. Disadvantages include a lack of blood and nerve supply leading to the rapid loss of viability, and by everting the intestine, morphological damage is possible (Balimane *et al.*, 2000:305; Le Ferrec *et al.*, 2001:661).

2.3.4.2 Diffusion chambers

Grass and Sweetana improved the Ussing chamber technique to study drug transport instead of transepithelial ion transport. For this method, a specific section of the small intestine is removed from a euthanized animal and opened to form a flat sheet of epithelial tissue, which is cut into sections of approximately 2-3 cm and mounted between two chambers. These chambers are then filled with Krebs-Ringer Bicarbonate buffer (KRB) and gassed with a mixture of O_2:CO_2 (95:5), which helps to improve the viability of the tissue. The continuous gas supply cause fluid circulation, which reduces the effect that the unstirred water layer may have on transport. P_{app} is defined as the rate of drug accumulation in the receiver chamber, normalized by taking the surface area available for absorption into consideration (Bohets *et al.*, 2001:372; Volpe, 2010:673). Advantages of this model is the fact that the architecture of the gastro-intestinal tract is sustained and closely mimics an *in vivo* situation, leading to the evaluation of all the absorption processes in one assay. Furthermore, transepithelial drug transport can be evaluated in combination with intestinal metabolism, absorption from different parts of the intestine can be studied and the amount of drug needed to perform an *ex vivo* study is relatively small when comparing it to *in vivo* studies, while the collected analytical samples are clean and could be directly used for analysis. Other advantages of this model include the fact that an apical mucus layer is present and P-gp substrate efflux could be measured (Antunes *et al.*, 2013:13). Disadvantages of this specific model are that there is a lack in blood and nerve supply, tissue viability decreases rapidly during the experimental process, morphology and functionality of the transport proteins can change during the surgery and mounting process of the tissue and the possibility exists that the serosal layer was not completely removed. It has a low-throughput, the setup time takes relatively long and a large amount of animal tissue is required (Antunes *et al.*, 2013:13; Balimane *et al.*, 2000:305-306).

2.3.5 *In silico* models

In silico models are computer programs that make use of the relationship of drug characteristics, formulation factors and human physiology when predicting drug absorption from the gastro-intestinal tract (Sjögren *et al.*, 2016:1764). *In silico* models are divided into two classes. The first class focuses on the interactions of a certain drug and its receptors, transporters and the direct environment of drug absorption. The second class focuses on the integration of the different physiological compartments and the pharmacokinetics *via* complex modelling. Advantages associated with the use of *in silico* models is that no living material and less consumables are required. The disadvantages of these models are that specialized computational resources are required and it is difficult to predict the absorption of drugs that are involved in a combination of complex interactions during the absorption process (Billat *et al.*, 2017:770; Sjögren *et al.*, 2016:1764).

2.4 Challenges associated with oral delivery of protein and peptide drugs

The primary function of the gastro-intestinal tract is to digest food and break it up into nutrients that can be absorbed, and simultaneously protect the body from the invasion of toxins and pathogens including peptides, viruses and bacteria (Lundquist & Artursson, 2016:257). Due to this protective function, the oral route of administration is challenging for peptide and protein drugs, due to barriers such as enzymes (e.g. proteases), the epithelial physical barrier, efflux pumps, mucus layer, tight junctions and the harsh gastrointestinal milieu as seen in Figure 2.3 (Bruno *et al.*, 2013:1444; Lundquist & Artursson, 2016:257). The barriers to protein and peptide delivery can be divided into different sections including physical and biochemical barriers as discussed below.

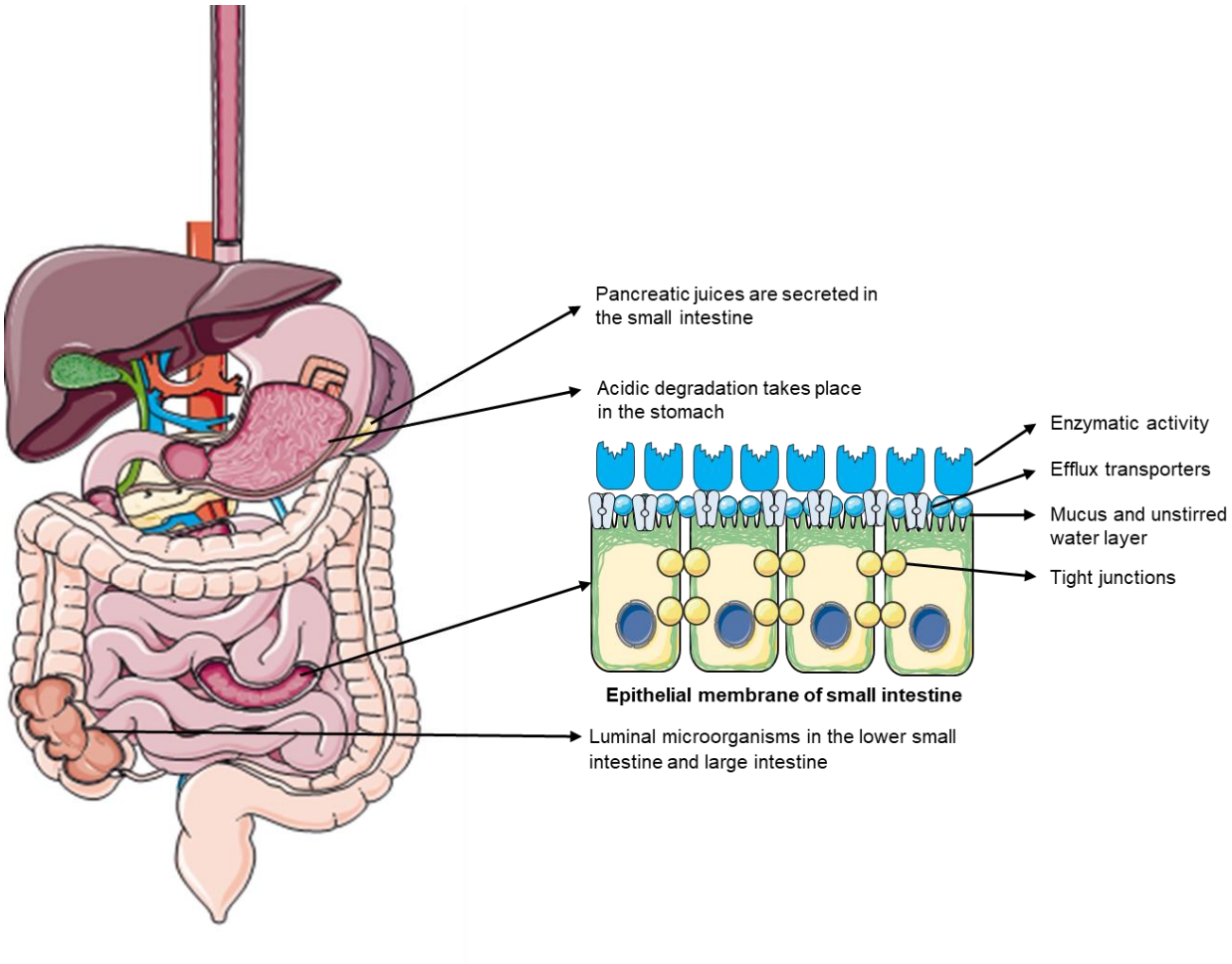

Figure 2.3: Schematic illustration of the different barriers encountered after the oral administration of peptide and protein drugs (Adapted from Jhanwar and Gupta (2014:444); Roger et al. (2010:288); produced using Servier Medical Art, (Servier-Medical-Art, 2018))

2.4.1 Physical barriers

2.4.1.1 Tight junctions

Tight junctions form a major barrier for drug delivery due to the inability of molecules, greater than 2 nm, to pass through the epithelial membrane by means of paracellular transport (Gamboa & Leong, 2013:801). Tight junctions are formed by a group of transmembrane and cytosolic proteins. These proteins include occludins, claudins and zona occludens-1 (Roger *et al.*, 2010:291). Tight junctions form a barrier in the intestine to protect the organism against the invasion of pathogens and foreign molecules through intercellular spaces. The extracellular part of a tight junction is formed by claudins and occludins. In the epithelial cells, claudins are linked to peripheral scaffolding proteins named zona occludens-1 protein. These scaffolding proteins are then linked to the cytoskeleton by means of linker proteins referred to as actin and microtubules (Artursson & Knight, 2015:716). The tight junction barrier can be overcome by making use of absorption enhancers that modulate the proteins in these junctions to cause larger pore sizes through which molecules can diffuse (Muheem *et al.*, 2016:415-416; Woitiski *et al.*, 2008:225).

2.4.1.2 Mucus and unstirred water layer

The mucus barrier acts as the first physical barrier when absorption of molecules has to take place from the gastrointestinal tract lumen. This mucus barrier forms a hydrogel layer on the apical side of the epithelial tissue and is composed of large glycoproteins, mainly originating from the mucin family that is secreted by the goblet cells and the seromucous glands of the lamina propria (Griffiths *et al.*, 2015:218). The function of this hydrogel layer is to protect the intestine from mechanical damage, the invasion of pathogens by binding the pathogens before it can reach the epithelial barrier and to lubricate the passage. Hydrophobic interactions take place between proteins and peptide drug molecules leading to immobilization of the molecules in the outer loosely adherent mucus layer, preventing it from reaching the epithelial surface and causing clearance of these molecules with the faeces from the body (Lundquist & Artursson, 2016:259-260).

An unstirred water layer is formed near the epithelial surface of the gastro-intestinal tract due to limited flow of the fluids close to the epithelial cells' surface. Absorption of small molecules and ions is slowed due to the absence of convective mixing forces in the unstirred water layer. If a molecule has the ability to penetrate through the mucus barrier, the unstirred water layer may act as an absorption enhancer by allowing the molecule prolonged exposure time to the epithelial surface (Bruno *et al.*, 2013:1444). On the other hand, the unstirred water layer can also act as a barrier towards the absorption of nanoparticles and large molecules due to the reduction of their diffusion through this layer (Lopes *et al.*, 2014:631).

2.4.1.3 The intestinal epithelial cell membrane

The epithelial membrane barrier constitutes one of the largest challenges when considering the absorption of protein and peptide drugs. The intestinal epithelium is composed of a single layer of columnar epithelial cells that include enterocytes, goblet cells, endocrine cells and Paneth cells, supported by the *lamina propria* and a muscularis mucosa (Bruno *et al.*, 2013:1444; Hamman *et al.*, 2005:167). The size of protein and peptide molecules plays an important role in their passive diffusion across membranes, but the chemical composition and morphology of these molecules also contributes to the obstruction. The carboxylic acid and amino groups that are present in amino acids and peptides causes ionization of the molecules and leads to the formation of zwitterionic molecules with hydrophilic characteristics. This makes the absorption of these molecules by means of transcellular transport difficult or impossible unless the charge is neutralized by means of ion pairing (Gamboa & Leong, 2013:801; Woitiski *et al.*, 2008:225).

2.4.1.4 Efflux transporters

Originally, efflux transporters were only associated with cancer cells causing multi-drug resistance (Gaucher *et al.*, 2010:152). However, it was shown that ABC transporters, in particular P-glycoprotein (P-gp) and Breast Cancer Resistance Protein (BCRP), have an effect on drug absorption and distribution due to their ability to recognize and actively pump a large collection of drug molecules back into the lumen of the gastro-intestinal tract (Tanaka *et al.* (2016:432). The main function of efflux transporters is to protect organisms against the invasion of certain toxins (Nakanishi & Tamai, 2015:753). P-gp, the most widely studied efflux transporter, is an energy-dependent efflux transporter that is especially expressed on the apical side of epithelial cells, is located in a wide range of tissues, including the intestinal tract, liver, blood-brain barrier, kidney and placenta (Hamman *et al.*, 2005:168; Ji *et al.*, 2016:459-460; Nakanishi & Tamai, 2015:757).

2.4.2 Biochemical barriers

The harsh acidic environment of the stomach can be seen as a major barrier for protein and peptide drug absorption. In addition, the luminal pH values rise to 7.5 in the proximal end of the ileum, drops to 6.4 in the ceacum and rises again to pH of 7.0 in the colon. These major variations in pH causes pH-induced oxidation and deamination of protein drug molecules (Gamboa & Leong, 2013:801; Gedawy *et al.*, 2018:201).

Proteins make up a large part of the human diet and therefore powerful measures are in place to hydrolyze them due to the fact that only amino acids and oligopeptides can be absorbed efficiently from within the small intestine (Carsten *et al.*, 2015:2617). Digestion of protein molecules starts within the stomach where hydrochloric acid and pepsin are present. Bile salts, amylase, trypsin and lipase are present in the duodenum of the small intestine. Furthermore, pancreatic juices are also present in the small intestine and are composed of pancreatin, α-chymotrypsin, trypsin,

lipase, peptidase and maltase. The pre-systemic degradation of protein molecules is also possible in enterocytes by means of aminopeptidases, cytosolic proteases and CYP enzymes (Ahmad *et al.*, 2014:2; Gamboa & Leong, 2013:801; Gedawy *et al.*, 2018:201).

Luminal microorganisms in the lower small intestine as well as in the large intestine limit the absorption of protein and peptide drug molecules due to their ability to cause metabolic reactions for example deglucoronidation, reduction of double bonds, ester and amide hydrolysis, decarboxylation and dihydroxylation (Woitiski *et al.*, 2008:225).

2.5 Oral drug delivery enhancement strategies for peptide and protein drugs

Numerous approaches have been used over decades to improve the absorption of protein and peptide drug molecules after oral administration. The main aim of these approaches is to increase the absorption of these molecules across the intestinal membrane, protecting it against the harsh environment of the gastro-intestinal tract and enzymatic degradation (Hassani *et al.*, 2015:13). These enhancement strategies are mainly divided into chemical, biochemical and formulation approaches.

2.5.1 Chemical approaches

Oral bioavailability enhancement of drugs can be achieved by changing their physico-chemical nature by chemical strategies, aiming to improve membrane permeability and protection against degradation at the site of absorption. Examples of chemical approaches to improve drug bioavailability include pro-drug formulation, sequence modifications of amino acids thereby reducing immunogenicity and proteolytic cleavage, the binding of peptide drugs to natural or synthetic polymers, and structural changes to improve recognition by transporters or receptor-mediated endocytosis (Hamman *et al.*, 2005:168; Renukuntla *et al.*, 2013:87).

2.5.1.1 Pro-drug strategies

Pro-drugs are chemicals with little or no pharmacological activity that have the ability to transform into therapeutically active metabolites due to enzymatic or non-enzymatic transformation just before crossing barriers. The goal of making use of the pro-drug strategy is to improve solubility, stability, targetability and permeability of molecules (Testa, 2009:338). Challenges when making use of pro-drugs for the oral absorption of protein and peptide drugs include the lack of methodology for synthesis, poor stability of proteins and the complexity of the structure (Renukuntla *et al.*, 2013:88). Regardless of these challenges, studies have shown promising results with chemical modifications for several peptide and protein drugs. One of these examples is where a phenylpropionic acid-based cyclic pro-drug of (Lue^5)-enkephaline is formed by making use of bioreversible cyclization. The phenylpropionic acid-based cyclic pro-drug of (Lue^5)-enkephaline showed an improvement in permeation of approximately 1680 fold, when compared

to (Lue^5)-enkephaline alone, tested in a Caco-2 cell model (Muheem *et al.*, 2016:419; Renukuntla *et al.*, 2013:88). In a recent study done by Vadlapudi *et al.* (2012:315), a lipid raft was conjugated with a parent drug molecule to influence the lipophilicity of the drug. On the other terminal of the lipid raft, a targeting moiety, recognised by a specific transporter or receptor in the cell membrane, was attached to facilitate active targeting. The results of this study have shown that the combination of a lipid moiety with a targeting moiety have a synergistic effect towards cellular uptake of drug molecules. The study concluded that the novel pro-drug design may help in the absorption of hydrophilic therapeutics such as genes, DNA, RNA, proteins and peptides as well as oligonucleotides (Vadlapudi *et al.*, 2012:315).

2.5.1.2 Structural changes (derivatization of proteins)

The structural characteristics of protein and peptide molecules that control their specificity for a certain receptor are mostly responsible for the unwanted physicochemical properties that prevent intestinal absorption. Structural modifications are a potential method for the optimization of the biopharmaceutical properties of drugs, provided that there is no adverse impact on the pharmacological effect of the drug (Hamman *et al.*, 2005:169).

PEGylation is a form of structural modification of a drug molecule where polyethylene glycol (PEG) is covalently attached to the therapeutic drug molecule. Polyethylene glycol, a FDA approved product, has certain favorable properties that makes it safe to use in human oral, intravenous and dermal applications and include the non-toxicity, non-immunogenic, non-antigenic and amphiphilic properties of the molecule (Li *et al.*, 2013:422). Polyethylene glycoldrug conjugates have the following advantages: decrease in the degradation of proteolytic enzymes, reduced immunologic response and an increase in size, reducing renal filtration of the drug molecules (Roberts *et al.*, 2012:117). Overthe past few years, numerous PEGylated protein, oligonucleotides and anti-body fragments have been approved by the FDA and are currently available on the market. Some examples of these products include Adagen®, PEG-adenosine deaminase, used in the treatment of severe combined immunodeficiency disease and Pegasys®, PEG-interferon-α2a, used in the treatment of Hepatitis C (Pasut & Veronese, 2012:462).

2.5.1.3 Peptidomimetics

A peptidomimetic is a compound that has the ability to mimic a natural peptide or protein and can bind to a specific receptor and thereby produce the same biological effect, but is not completely peptidic in nature. Peptidomimetics are designed to overcome certain obstacles linked to natural peptides. These include the improvement in the stability against proteolysis, poor bioavailability, receptor selectivity and potency (Vagner *et al.*, 2008:292).

Peptoids, a type of peptidomimetic, is used in the development of antimicrobial peptides to potentially replace ordinary antibiotics, which may assist in overcoming resistance against

bacteria. Peptoids are well suited to mimic antimicrobial peptides, because they are easy to synthesize by means of the solid phase technique. It is also a relatively cost-effective process (Chongsiriwatana *et al.*, 2008:2794).

An example of a biodegradable pseudo-peptide polymer is poly (L-lysine iso-phthalamide). This pseudo-peptide is made up by a hydrophobic backbone and pendant carboxyl groups without any hydrophobic side-chains (Chen *et al.*, 2009a:1955). Pseudo-peptides are prepared by making a change in the peptide bond of the original peptide while maintaining the biological properties of the peptide to improve properties such as degradation, elimination, bioavailability and selectivity (Vlieghe *et al.*, 2010:44).

2.5.1.4 Targeting of endogenous cell carrier systems

The binding of protein and peptide molecules to transport carrier molecules, recognized by endogenous cellular transport systems that are present in the gastro-intestinal tract, is a possibility for more effective delivery of protein and peptide drug molecules after oral administration. The transport mechanism by which these protein and peptide molecules are transported include membrane transporters and receptor-mediated endocytosis processes (Morishita & Peppas, 2006:907). P-glycoprotein, an efflux transporter present in the gastro-intestinal tract, may contribute to the limited bioavailability of peptide and protein drugs after oral administration. By co-administering or binding a protein or peptide drug molecule to a P-gp inhibitor the bioavailability of these macromolecules may be improved (Muheem *et al.*, 2016:421). Examples of receptor detectable ligands are lectins, toxins, transferrin, epidermal growth factor, immunoglobulins, viral hemagglutinins, invasion and vitamins like riboflavin, biotin and vitamin B_{12} (Hamman *et al.*, 2005:170; Morishita & Peppas, 2006:907).

2.5.1.5 Cell-penetrating peptides

Cell-penetrating peptides transport their cargo into the cytoplasm by perturbation through the lipid bilayer of the cell membrane or by a transport mechanism named endocytosis. In a study where insulin was linked to a cell penetrating peptide (insulin-CPP hybrids), intestinal absorption of insulin increased when compared to normal insulin tested in the Caco-2 cell model (Renukuntla *et al.*, 2013:89).

Human immunodeficiency virus 1 transactivator of transcriptation (HIV-1 Tat), oligoarginine and penetratin are forms of cell-penetrating peptides and are considered useful tools for the intracellular delivery of macromolecules. These cell-penetrating proteins have the ability to enhance absorption of biodrugs through intestinal epithelial membranes. The low permeability of protein and peptide drug molecules through the intestinal epithelial membrane can be seen as the major barrier for oral delivery of these drug molecules, which can possibly be overcome by making use of cell-penetrating peptides (Khafagy & Morishita, 2012:531).

2.5.2 Biochemical approaches

2.5.2.1 Enzyme inhibitors

Increased intestinal absorption of protein and peptide molecules can be facilitated by the co-administration of enzyme inhibitors, targeting the enzymatic barrier by preventing the degradation of proteins and peptide drug molecules before they reach the systemic circulation (Choonara *et al.*, 2014:1273). Examples of enzyme inhibitors include aprotinin (inhibiting trypsin and chymotrypsin), amastatin, bestatin, boroleucine and purmycin (inhibiting aminopeptidase), soybean trypsin inhibitor (inhibition of pancreatic endopeptidase), FK448 (chymotrypsin inhibitor) and chicken and duck ovomucoids (inhibiting trypsin) (Choonara *et al.*, 2014:1273; Park *et al.*, 2011:281; Renukuntla *et al.*, 2013:80).

Enzyme inhibitor administration could be problematic due to non-specific interaction with certain dietary proteins that would normally be degraded, damage in the intestinal mucosa and feedback-regulated protease secretion after chronic use. Prolonged use of enzyme inhibitors could induce severe toxic effects (Choonara *et al.*, 2014:1273; Renukuntla *et al.*, 2013:80).

2.5.3 Formulation approaches

2.5.3.1 Site-specific delivery systems

The absorption of molecules from the gastro-intestinal tract is not uniform throughout the entire length. Site-specific absorption from the gastro-intestinal tract takes place due to variations in the structure and thickness of the mucus layer, pH, area for absorption and enzymatic activity (Choonara *et al.*, 2014:1275; Hamman *et al.*, 2005:174).

The colon is seen as an attractive site for protein and peptide drug delivery due to the avoidance of enzymatic activity, absorption into the lymphatic system is maximized and hepatic extraction is bypassed (Owens *et al.*, 2003:888). Other advantages of colonic drug delivery are the prolonged transit and the responsiveness to agents that can enhance the absorption of drugs that are usually poorly absorbed (Singh *et al.*, 2018:12). Colon-targeted oral drug delivery systems unfortunately also have many limitations. Multiple manufacturing steps are required. Different degrees of acidity or basidties are precent, fluid volumes and transit times are present during the movement to this site after oral intake. Low bioavailability of drug molecules is usually attributed to non-specific binding to dietary residue, faecal matter, mucus and intestinal secretion. Microflora, present in the colon can cause metabolic degradation of drugs. The solubility of drugs in the colon is a large concern, due to the small volume of fluid present in the colon, neutral pH and the high viscosity (Amidon *et al.*, 2015:732; Rangari & Puranik, 2015:171-173; Singh *et al.*, 2018:12).

For colon-specific drug delivery the following formulation approaches are used namely, pH sensitive polymer-coated drug delivery systems, time dependent drug delivery systems, microbial

triggered systems, pro-drug approaches, polysaccharide-based delivery systems, pressure controlled drug delivery systems, pulsatile colon targeted drug systems, combination of pH dependent and microbially triggered colon drug delivery systems, osmotic controlled drug delivery systems, multi-particulate systems, azo-hydrogel and pro-biotic approaches (Singh *et al.*, 2018:14-19).

Another promising site-specific route for oral peptide and protein drug delivery is the transmucosal route of the oral cavity (Madhav *et al.*, 2009:3). The buccal and sublingual routes of administration are the most commonly used. This is due to the overall higher permeability when compared to the other mucosa of the oral cavity (Patel *et al.*, 2011:109). The attractive features of the mucosa of the mouth for the administration of peptide and protein drugs is the ease of accessibility, direct access to systemic circulation through the internal jugular vein, bypassing of the first-pass metabolism in the liver, small amount of enzymatic activity, painless drug administration and the drug absorption to the blood is predictable (Khafagy *et al.*, 2007:1526-1527). Aminopeptidase, one of the enzymes present in the oral cavity, can be problematic in the absorption of peptide drug. Therefore, peptide drugs should be administered in combination with enzyme inhibitors and absorption enhancers (Lassmann-Vague & Raccah, 2006:515; Patel *et al.*, 2011:109).

2.5.3.2 Physically forced transport

A gas powered drug delivery system was designed that acted by means of carbon-dioxide forced transport of protein and peptide drugs. This mechanism was combined with mucoadhesive polymers such as polyethylene oxide and trimethyl chitosan. Carbon-dioxide bubbles (produced by the citric acid and sodium bicarbonate present in the enteric coated tablet) are used to apply polyethylene oxide and trimethyl chitosan to the mucous membrane of the small intestine without losing its ability to open tight junctions and micoadhesiveness. An enteric coating is then used to release the content of the gas powered drug delivery system in the proximal part of the small intestine where CO_2 gas mediates the binding of polyethylene oxide (micoadhesive) onto the mucosa of the small intestine. After the attachment of polyethylene oxide to the mucous membrane of the small intestine, trimethyl chitosan also binds, modulating the opening of tight junctions and mediating the absorption of insulin via the paracellular pathway. This method was tested *ex vivo* in sheep intestines and the results showed a 7-fold improvement in the absorption of insulin (Sadeghi *et al.*, 2009:11-12).

2.5.3.3 Formulation of drug carrier vehicles (particulate delivery systems)

The aim of particulate drug delivery systems is to protect the drug against enzymatic degradation and to improve the transfer of the drug molecules across epithelial membranes. Formulation vehicles used in the protection against enzymatic degradation and improvement of absorption include emulsions, liposomes, microspheres and nanoparticles. A Solid-in-oil-in-water (S/O/W)

emulsion for the delivery of insulin was developed. Lipophilic surfactant-coated insulin was used in the development of the emulsion. This formulation helped to enhance the permeation of insulin through the intestinal mucosa while avoiding enzymatic degradation (Morishita & Peppas, 2006:907; Park *et al.*, 2011:282).

2.5.3.4 Absorption enhancers

Drug absorption enhancers can be used to improve the poor oral absorption of protein and peptide drugs from the gastro-intestinal tract (Pawar *et al.*, 2014:173). Examples of absorption enhancers include surfactants, bile salts, calcium ion-chelating agents, fatty acids like palmitic acid, chitosan and its derivatives, zonula occludens toxin (ZOT) and polycarbophyl-cysteine conjugate (Anilkumar *et al.*, 2011:439-441; Wong *et al.*, 2016:1100). Absorption enhancers make use of different mechanisms to increase drug permeability. Firstly, they can open epithelial tight junctions reversibly, increasing paracellular transport. Secondly, absorption enhancers can disturb the mucosal surface mildly by adjusting membrane fluidity to improve transcellular permeation. Thirdly, they can interrupt the mucus layer on the epithelial bilayer by decreasing mucus viscosity. Lastly, non-covalent complexes can be formed (Di, 2015:136-137; Moroz *et al.*, 2016:117).

Sodium caprate, a medium chain length fatty acid, enhances oral bioavailability by the activation of phospholipase C, inducing contraction of calmodulin-dependant actin-myosin filaments. Calmodulin-dependant actin-myosin filament contraction leads to the dissociation of plaque protein ZO-1 and transmembrane protein occludin from the tight junctions. This mechanism leads to absorption enhancement through the paracellular pathway (Pillay *et al.*, 2012:267). Sodium caprate was actively evaluated in advanced clinical trials to enhance peptide drug delivery. In 2011, phase III clinical trials were completed on the enhancement of insulin combining it with alkylated polyethylene glycol-peptide conjugate in a tablet form. However, this study was unsuccessful in proving sufficient insulin delivery. In another study done by Merrion Pharma (Ireland) and Novo-Nordisk (Denmark) in 2010, insulin and GLP-1 analogues were combined and formulated in a matrix tablet with sodium caprate as an absorption enhancer (Brayden & Mrsny, 2011:1569).

Ideal properties of an absorption enhancer include non-hazardous to the gastro-intestinal epithelium, pharmacological and chemically inertness, be reversible in their action, non-irritating and non-allergenic (Anilkumar *et al.*, 2011:444; Wong *et al.*, 2016:1100). Some of the biggest concerns of using absorption enhancers is permanent damage to the epithelial cells of the intestine and toxic metabolites or contaminants that may be transported through the epithelium and thereby reaching the systemic circulation (Pawar *et al.*, 2014:174; Pillay *et al.*, 2012:267).

2.5.3.5 Absorption enhancers of plant origin

Absorption enhancers from natural origin are confronted with a number of challenges. When herbal bioenhancers are investigated in laboratory-based studies, only a small quantity is required, but when used in commercial products, large scale production would be required. Furthermore, before clinical application of absorption enhancers, they have to be approved by an appropriate regulatory authority (Javed *et al.*, 2016:160; Kesarwani & Gupta, 2013:255).

There are numerous absorption enhancers off plant origin that are studied by scientists around the world. In the sections below, the two plant extracts namely piperine and capsaicin are discussed in detail.

2.5.3.5.1 Piperine

Black pepper (*Piper nigrum* L., family Piperaceae) is one of the most widely used spices in the world and contains the active molecule piperine. Piperine is the pungent alkaloid found in plants (Singh *et al*., 2014:2084). White and black pepper originate from the same species, where white pepper is produced from ripe, dried, naked seeds, while black pepper is prepared by briefly cooking and drying the unripe fruits of the plant (Meghwal & Goswami, 2013:1121). Besides the culinary applications, black pepper is also used for its medicinal actions, as a preservative and in the perfume industry (Singh *et al.*, 2014:2084). Black pepper was used as a natural remedy in ancient Chinese and Indian medicines for the treatment of pain, chills, rheumatism, flu and muscular pains (Gorgani *et al.*, 2017b:2199).

2.5.3.5.1.1 Botany of *Piper nigrum* (Black pepper)

Black pepper originated from and is cultivated in Indonesia, Brazil and India's tropical regions. *Piper nigrum* acquired its generalized name, black pepper, as a result of the colour of the peppercorn fruits from the plant. *Piper nigrum* is known as the "King of Spices". This is due to the fact that it is used in the international trading market (Srivastava & Singh, 2017:224).

Piper nigrum is an perennial woody vine that can reach up to 4 meters in height with branched smooth, woody and round stems (Barceloux, 2009:381). These plants grow easily in the shade and require the support of trees, trellises or poles. When the vines of these plants touch the ground, roots may form from within the leaf nodes. The leaves are heart-shaped and can reach 5-10 cm in length and 3-6 cm in width, with 5-7 definite palmate veins. The small white flowers produce globular drupes, which are 3-4 mm in diameter when unripe and approximately 5 mm in diameter with a dark red colour when fully mature. These plants bear pepper fruit from the fourth year until the seventh year (Damanhouri & Ahmad, 2014:1-2). Figure 2.4 illustrates the geographical distribution, plant and fruits of *Piper nigrum.*

Figure 2.4: A) Geographical distribution of *Piper nigrum*; B) Photographs of *Piper nigrum* and the pepper fruits in all three the stages (Adapted from KEW-Science KEW-Science:Plants-of-the-world-online (2018))

2.5.3.5.1.2 Chemistry of piperine

Piperine (piperoylpiperidine) is known as the alkaloid that appears in *Piper nigrum*. Hans Christian Ørsted isolated piperine for the first time in 1819. The chemical structure of piperine was identified much later, with the chemical formula of $C_{17}H_{19}NO_3$ and a molecular weight of 285.34 g/mol (Gorgani *et al.*, 2017a:124; Singh *et al.*, 2014:2087). The molecule of piperine contains typical features of an alkaloid namely a nitrogen-containing heterocyclic ring with oxygen atoms. Although the C=O bond in the molecular structure adds some polarity to the molecule, the conjugated bridge and the benzene ring makes this molecule non-polar or hydrophobic (Patil *et al.*, 2016:3645). Figure 2.5 illustrates the chemical structure of piperine.

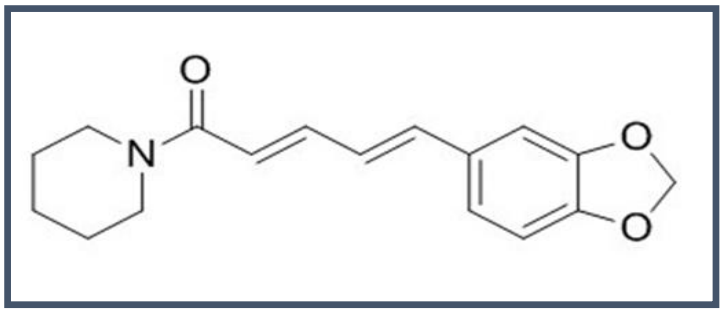

Figure 2.5*:* Chemical structure of piperine (Adapted from *Gorgani et al. (2017a:125).*

2.5.3.5.1.3 Medicinal properties of piperine

2.5.3.5.1.3.1 Antimicrobial activity

During a study by Khan and Siddiqui in 2007, the antimicrobial potential of aqueous solutions, containing an extract prepared from the fruits of these plant species, of *Piper nigrum, Coriandum sativum, Pimpinella anisum and Laurus nobilis* were evaluated against different bacteria isolated from the oral cavity of 200 individual volunteers. *Piper nigrum* showed the strongest antimicrobial activity when compared to aqueous solutions of *Laurus nobilis* and *Pimpinella anisum* at a concentration of 10 µl/disc (Khan & Siddiqui, 2007:111-113). A study that was done by Karsha and Lakshmi reported the antimicrobial activity of an extract from *Piper nigrum* and focused on the mechanism of action of this plant extract. They discovered the inhibitory effects that *Piper nigrum* have on the growth of gram positive bacteria for example, *Staphylococcus aureus, Bacillus cereus* and *Streptococcus faecalis. Piper nigrum* also had a positive inhibitory effects on gram negative bacteria, for example *Pseudomonas aeruginosa*, *Salmonella typhi* and *Escherichia coli* (Karsha & Lakshmi, 2010:214-215).

2.5.3.5.1.3.2 Anti-oxidant activity

Free radicals in the body are produced due to exposure to environmental pollutants and radiation, the injury of tissue, infections and auto-immune processes. Free radicals cause damage and could be reduced by increasing the antioxidant levels in the tissues. Piperine has anti-oxidant effects in the body leading to the reduction of thiobarbituric acid-reactive substances and high-fat-diet-induced oxidative stress in cells. Piperine also helps with the maintainance of superoxide dismutase, catalase, glutathione peroxidase and glutathione-S-transferase (Gorgani *et al.*, 2017a:125). Piperine is administrated as a co-adjuvant for treating and slowing the ageing processes and diseases and conditions relating to the aging process. These diseases include atherosclerosis, hypertension, tumours, obesity, diabetes, overweight, hypertriglyceridemia, skin aging, cellulite, alopecia, osteoporosis, cerebral ageing (Alzheimer's, Parkinson and dementia), memory loss, depression, stress, menopausal syndrome and benign prostate hypertrophy (Chopra *et al.*, 2016:82).

2.5.3.5.1.3.3 Anti-cancer activity

During a study that was done by Umadevi *et al.* (2013:5466) a series of piperine analogs were synthesized by making use of condensation of piperic acid in combination with different amino acids and substituted aniline. The different synthesized piperine analogs were tested for their anticancer activity against human cancer cell lines. These cell lines included MCF-7, a breast cancer cell line, and Hela cervix cell line. These analogues of piperine showed significant activity against both of these human cancer cell lines.

HER2, a type of breast cancer that tests positive for a protein called human epidermal growth factor receptor 2, gene expression at the transcriptional level is inhibited by piperine, therefore piperine can be considered as a potential agent to aid in prevention and treatment of human breast cancer where HER2 overexpression is present. Piperine shows an inhibition in cell growth on human prostate cancer cells by blocking the cell cycle and autophagy (Wang *et al.*, 2014:13).

2.5.3.5.1.3.4 Anti-inflammatory and analgesic activity

The anti-analgesic and anti-arthritic effect of piperine was evaluated on carrageen, an induced acute paw model of pain and arthritis in rats. A dose dependant (10-100 µg/ml) reduction of the synthesis of prostaglandin E2 (PGE2) was found in groups that were treated with piperine. A significant inhibition of PGE2 was observed even at a low dose of 10 µg/ml. Inhibition of the expression of interleukin 6 (IL 6) and matrix metallo-proteinase 13 also took place. Piperine inhibited the migration of activator protein 1 (AP-1) into the nucleus of IL-1β treated synoviocytes, while no effect was observed in the migration of nuclear factor κβ (NF-κβ). Furthermore, arthritic and pain symptoms were reduced significantly in rats after the treatment with piperine (Damanhouri & Ahmad, 2014:3-4). Inhibition of INF-1 leads to the inhibition of lipopolysaccharide-induced endotoxin shock, making piperine a useful gastrointestinal anti-inflammatory agent (Gorgani *et al.*, 2017a:126).

2.5.3.5.1.3.5 Hepatoprotective activity

The effect of piperine and metformin alone and in combination was tested on gentamicin-induced hepatotoxicity. Piperine alone in a dose of 50 mg/kg and 100 mg/kg and metformin alone at a dose of 100 mg/kg or piperine/metformin combination therapy at a dose of 50 mg/kg piperine and 50 mg/kg metformin were beneficial in the treatment of gentamicin-induced hepatotoxicity (Chopra *et al.*, 2016:84).

During a study that was done on mice with D-galactosamine-induced liver toxicity, piperine was given in different concentrations. Piperine inhibited the increase in serum levels of glutamic-pyruvic transaminase as well as glutamic-oxaloacetic transaminase. This inhibitory effect is possibly due to the reduced sensitivity of hepatocytes to TNF-α (Ahmad *et al.*, 2012:)

2.5.3.5.1.3.6 Anti-diarrhoea activity

During a study that was done by Shamkuwar *et al.* (2012:48) on the anti-diarrheal, anti-motility and anti-secretory activity of an aqueous black pepper extract given at doses of 75, 150, 300 mg/kg in mice with diarrhoea induced by castor oil and magnesium sulphate, gastro-intestinal motility was assessed. The aqueous black pepper extract showed a significant dose dependant effect on diarrhoea, motility and secretion. The anti-motility effect as well as the anti-secretory effect of *P. nigrum,* could possibly be due to the presence of alkaloids and carbohydrates in

P. nigrum, while the anti-diarrheal effect could possibly be due to the anti-secretory and anti-motility effects of *P*. *nigrum* (Shamkuwar *et al.*, 2012:48).

2.5.3.5.1.3.7 Digestive activity

Numerous spices are known for their stimulating effect on the digestive system (Srivastava & Singh, 2017:4). Dietary piperine has the ability to enhance the digestive capacity by stimulating the secretion of digestive enzymes by the pancreas and reduction in food transit time in the gastro-intestinal tract (Srinivasan, 2007:735). Piperine increased the production of saliva and gastric secretions. It also increased the production and activation of salivary amylase (Ahmad *et al.*, 2012:1947). It was shown that orally administrated piperine or *P. nigrum* stimulated the secretion of bile acids by the liver, playing a key role in the digestion and absorption of fats (Damanhouri & Ahmad, 2014:4).

2.5.3.5.1.3.8 Anti-depressant activity

During a study that was done on mice that had corticosterone-induced depression, piperine was administrated to examine the possible mechanism of the antidepressant-like effect. When these animals were treated with piperine, the behavioural and biochemical changes caused by the administration of corticosterone were significantly reduced. The possible mechanism on which piperine works is by increasing brain-derived neurotrophic factor expression in the hippocampus of the brain (Mao *et al.*, 2014:36).

2.5.3.5.1.3.9 Immuno-modulatory activity

The *in vitro* immuno-modulatory activity of piperine was evaluated to enhance the effectiveness of rifampicin in a murine model of *Mycobacterium tuberculosis.* For the evaluation of the *in vitro* immune-modulatory effect of piperine, mouse splenocytes were used to measure cytokine production, macrophage activation and lymphocyte proliferation. Mouse splenocytes treated with piperine showed an increase in the secretion of Th-1 cytokines, which included IFN-γ and IL-2. An increase in macrophage activation and proliferation of T- and B-cells were observed as well. Piperine caused the upregulation of Th-1 immunity, therefore a synergistic effect can be obtained when rifampicin is given in a combination therapy with piperine to improve the therapeutically effectiveness of tuberculosis medication in patients that are immunocompromised (Sharma *et al.*, 2014:389).

2.5.3.5.1.3.10 Anticonvulsant activity

In a study where piperine was tested for its anticonvulsant activity in *in silico, in vivo* and *in vitro* models, the mechanism by which piperine mediated an anticonvulsant effect, was attributed to an antagonistic effect on Na^+ channels that inhibits convulsions (Mishra *et al.*, 2015:317).

2.5.3.5.1.3.11 Absorption enhancement characteristics

Possible absorption enhancement mechanisms of piperine that have been identified include the formation of polar complexes, altered membrane dynamics, inhibition of P-gp efflux, increased blood supply to the gastro-intestinal tract, increased gamma-glutamyl transpeptidase participation in active transport of nutrients and inhibition of gastrointestinal and hepatic metabolism. Some of the enzymes inhibited by piperine includes glucuronyltransferase, arylhydrocarbon hydroxylase and CYP (Ajazuddin *et al.*, 2014:2; Di *et al.*, 2015:144; Kang *et al.*, 2009:1209; Kesarwani & Gupta, 2013:255). Table 2.1 summarizes *in vivo* studies that have been done on the drug absorption enhancement properties of piperine.

Table 2.1: Summary of *in vivo* studies where the co-administration of piperine showed effects on drug pharmacokinetics

Drug	Model used	Bioavailability enhancement mechanism	Reference
Phenytoin	Healthy human volunteers	Phenytoin's absorption was enhanced possibly by increasing the absorption.	Dudhatra *et al.* (2012:6)
Pentobarbitone	Pentobarbitone-induced hypnosis in rats	The sleeping time was enhanced, possibly due to the inhibition of the liver microsomal enzyme system.	Dudhatra *et al.* (2012:5-6); Jhanwar and Gupta (2014:448)
Curcumin	Healthy human volunteers and rats	Enhanced the extent of absorption, serum concentration and bioavailability due to the inhibition of hepatic and intestinal glucuronidation.	Javed *et al.* (2016:151)
Rifampicin	Human	Increased bioavailability by 60% and reduced dose from 450 to 200 mg. The binding ability of Rifampicin to RNA polymerase is enhanced when administrated with piperine.	Dudhatra *et al.* (2012:8); Javed *et al.* (2016:151)
Epigallocatechin gallate	Albino mice	Inhibited glucoronidation and gastro-intestinal transit time. Increased the bioavailability of *Epigallocatechin gallate* 1.3 times.	Dudhatra *et al.* (2012:9); Jhanwar and Gupta (2014:448)
Nevirapine	Crossover, placebo-controlled pilot study	Enhanced the bioavailability when co-administered with Nevirapine.	Tatiraju *et al.* (2013a:57)
Resveratrol	Mice	Successfully improved the bioavailability of resveratrol in an *in vivo* study.	Johnson *et al.* (2011:1169)
β-Carotene	Mice	Changes the lipid dynamics and epithelial membrane of the gastro-intestinal tract	Veda and Srinivasan (2011:1429)

2.5.3.5.2 Capsaicin

The use of chilli pepper for medicinal and cooking purposes dates back to times before the birth of Christ when these peppers were used by the Mexican Indians from South America (Barceloux, 2009:380; Singletary, 2011:33). The active component in chilli peppers is capsaicin, which is responsible for the pungency of spices. The capsaicin in the chilli is produced as a secondary

metabolite and helps to protect the plant against certain herbivores and fungi (Srinivasan, 2016:1488).

2.5.3.5.2.1 Botany of *Capsicum* species

Capsicum, the genus of peppers, belongs to the botanical family Solanaceae, which is closely related to tomato, potatoes, eggplants, tobacco and petunias. The genus *Capsicum* consists of at least twenty species that originate from the tropical areas of America (Omolo *et al.*, 2014:1-3). The following species were used by native Americans *C. annuum* L. *C. baccatum* L., *C. chinense* Jacq., *C. frutescens* L. and *C. pubescens* (Stoica *et al*., 2016:93). *C. annuum* is the red pepper species that is most commonly known under the cultivated species with the highest morphological variety. This red pepper species is also rated as most economically important in the *Capsicum* genus (Aguilar *et al.*, 2009:1192; Csilléry, 2006:153). Different red peppers can be identified according to their fruit shape; size and colour (Qin *et al.*, 2014:5135). *Capsicum anuum* has densely branched stems that reach up to 1.5 m in height. During autumn, a single, white flower produces a small fruit that transform from white to shades of yellow, orange and red as the fruit ripens. This species originated from South America, but it is now grown worldwide in dry, warm climates (Barceloux, 2009:380-381). Figure 2.6 illustrates the geographical distribution, plant, flower and fruits of *Capsicum anuum.*

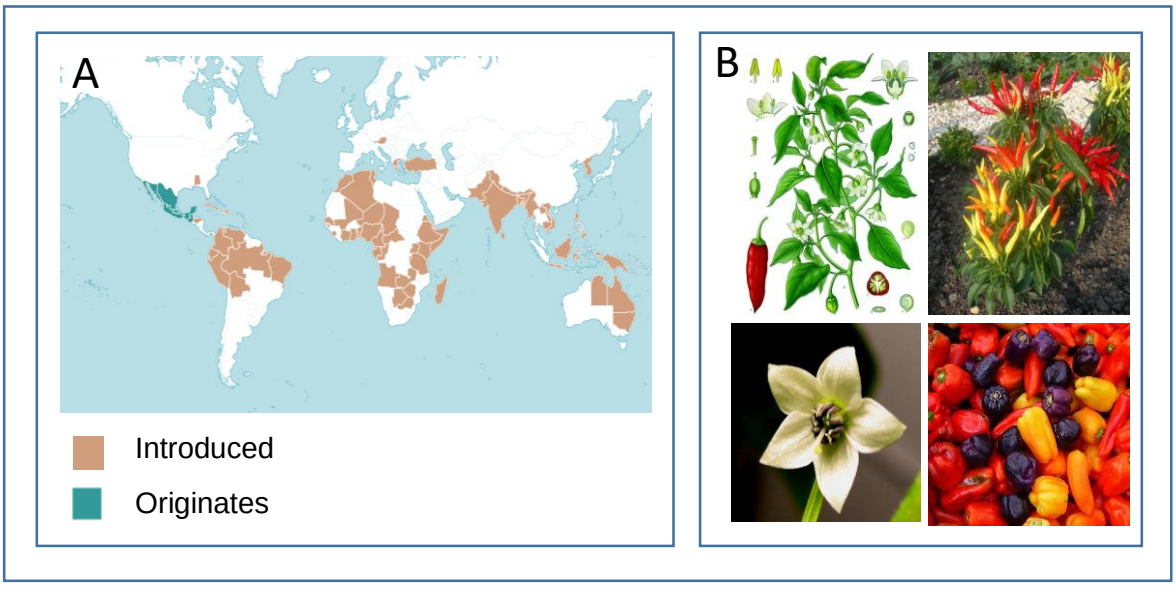

Figure 2.6: A) Geographical distribution of *Capsicum anuum* (KEW-Science:Plants-of-the-world-online, 2017). B) Image showing the plant, flower and fruits of *Capsicum anuum* (Adapted from (Wikipedia, 2018).

2.5.3.5.2.2 Chemistry of capsaicin

Capsaicin (trans-8-methyl-*N*-vanillyn-6-noneamide), the major alkaloid from the genus *Capsicum,* has a molecular weight of 305.4 Da and its molecular formula is $C_{18}H_{27}NO_3$. Capsaicin is insoluble in cold water, but soluble in fat-, oil-, ethanol- and acetone (Barceloux, 2009:382). The chemical

structure comprises an aromatic ring, amide bond and a hydrophobic side chain (Reyes-Escogido *et al.*, 2011:1254). When capsaicin is crystallized from the peppers it is a hydrophobic, colourless, odourless, crystalline compound (Srinivasan, 2016:1488). Figure 2.7 illustrates the chemical structure of capsaicin, indicating the three different regions of the molecule.

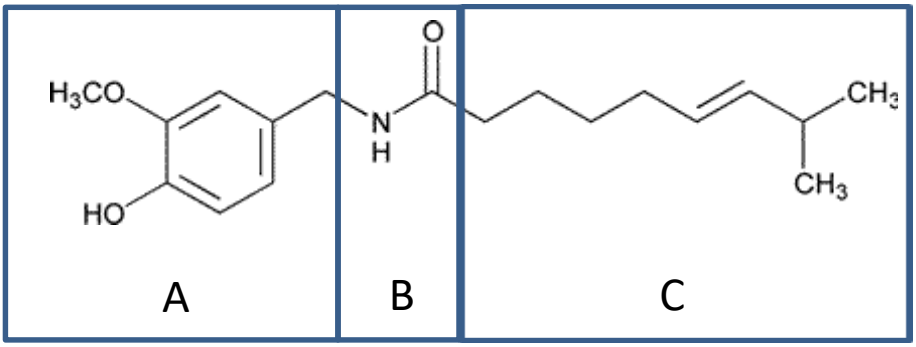

Figure 2.7: Chemical structure of capsaicin showing the different parts with distinctive characteristics: A) Aromatic ring, B) Amide bond, C) Hydrophobic side chain. (Adapted from (Reyes-Escogido et al., 2011:1254).

2.5.3.5.2.3 Medicinal properties of Capsaicin

2.5.3.5.2.3.1 Cardiovascular benefits of capsaicin

Capsaicin has the potential to help with the treatment of cardiovascular diseases including hypertension, myocardial infarction, coronary heart diseases and atherosclerosis (Peng & Li, 2010:2-4). Capsaicin sensitive sensory nerves are present in the cardiovascular system, playing a major role in cardiovascular function through the release of numerous neurotransmitters such as calcitonin gene-related peptide (CGRP) through the activation of transient receptor potential vanilloid (TRPV) and Substance P. Platelet aggregation and the activity of clotting factor seven and nine is blocked by capsaicin. This is due to the presence of TRPV1 in human platelets. Atherosclerosis is caused by the oxidation of low density lipoprotein. Capsaicin, an anti-oxidant, has the ability to reduce the amount of oxidation taking place by delaying the oxidation process or by stopping the initial oxidation process (Arora *et al.*, 2011:283-284).

2.5.3.5.2.3.2 Protective effect on erythrocyte integrity

The fluidity of red blood cells is affected by hyperlipidemic conditions such as uncontrolled diabetes mellitus or the intake of atherogenic diets (Kempaiah & Srinivasan, 2002:155; Srinivasan, 2016:1491). Capsaicin consumedas part of a diet may have beneficial protective effects on the integrity of the erythrocyte membranes due to its hypolipedemic effects. During a study that was done by Kempaiah and Srinivasan in 2002, they observed that after giving rats a cholesterol-enriched diet for eight weeks, the erythrocyte membranes, were enriched with cholesterol that led to an elevated cholesterol:phospholipid ratio of the membranes causing a

change in the structural integrity of erythrocytes (Kempaiah & Srinivasan, 2002:156-157). When capsaicin is given in combination with the cholesterol-enriched diet, hypolipedemic results were observed as well as the erythrocyte membrane lipid profile was corrected that led to the correction of the increased osmotic fragility of erythrocytes (Srinivasan, 2016:1491).

2.5.3.5.2.3.3 Anti-oxidant effect of capsaicin

Capsaicin's anti-oxidant activity is due to the binding of the OH-group with food components. When capsaicin is consumed with food, it has the ability to reduce the absorption of fat, resulting in the anti-oxidative effects (Akyuz *et al.*, 2018:438).

The inhibition of iron-mediated lipid peroxidation in human erythrocyte membranes and the inhibition of copper-dependent oxidation of human low-density lipoprotein is proven by using capsaicin. This effect is due to the formation of complexes with reduced metals and acting as hydrogen bond donors. (Kumar *et al.*, 2015:583; Rosa *et al.*, 2002:7396; Srinivasan, 2016:1491-1492).

2.5.3.5.2.3.4 Antinociceptive effects of capsaicin

The action of blocking a painful stimulus by making use of capsaicin does not involve neurotoxicity, but the depletion of sensory neuropeptides and activity at the peripheral receptors. Systemic capsaicin blocks pain stimuli by making use of the activation of capsaicin receptors on the afferent nerves of the spinal cord. C-fibre conduction and inactive neuropeptide release from peripheral nerve endings are blocked by the application of local and topical capsaicin (Chhabra *et al.*, 2012:9). A wide range of chronic pain conditions could be treated with topical applications of capsaicin. These conditions include postherapeutic neuralgia and diabetic neuropathy, rheumatoid arthritis, osteoarthritis, psoriasis, mastectomy pain and cluster headaches (Derry *et al.*, 2009:2).

2.5.3.5.2.3.5 Chemopreventive activity of capsaicin

A study was done on the chemopreventive activity of capsaicin, but the role of capsaicin in tumorgenesis is still a debatable topic due to their anti-tumorgenesis effects (Singletary, 2011:38; Srinivasan, 2016:1492). Capsaicin has chemopreventive activity on the following cancer cell lines namely, leukemic, prostate, colon, hepatoma, breast and gastric cancer cells, but capsaicin may increase the risk of stomach, liver, bladder and pancreatic cancer if consumed in lerge quantities (Liu *et al.*, 2012:2758; Singletary, 2011:38). The chemopreventive activity of capsaicin is based on the inactivation of CYPHE1 and other isoforms by irreversibly binding to the active sites of the enzymes. Furthermore, microsomal mono-oxygenases is inhibited by capsaicin. Since this enzyme is involved in carcinogen activation, it can be assumed that capsaicin is chemopreventive (Srinivasan, 2016:1492).

2.5.3.5.2.3.6 Anti-diabetic potential

Capsaicin has an insulinotropic effect, causing an indirect effect on the β cells. Capsaicin activates adenosine monophosphate-activated protein kinase. Type 2 diabetes mellitus is most probably prevented *via* a regulation of insulin resistance and β cells (Chang *et al.*, 2013:22).

2.5.3.5.2.3.7 Thermogenic and weight reducing influence of capsaicin

Capsaicin has a thermogenic effect as well as an effect on the energy metabolism of the human body that could possibly lead to the reduction in the frequency and severity of obesity (Srinivasan, 2016:1494). Capsaicin causes a reduction in the accumulation of body fat and enhances the amount of energy burned in the body. Capsaicin has anti-obesity properties but the potential adverse effects, namely the burning sensation, limits the use of it for this purpose (Arora *et al.*, 2011:283).

2.5.3.5.2.3.8 Anti-ulcer activity of capsaicin

Capsaicin is a substance that has the ability to control primary afferent neurons. In the stomach, capsaicin stimulates the afferent neurons and inhibits the secretion of acid to such a level to protect the gastric mucosa, increases mucus secretion as well as the mucosal blood flow. These actions help to prevent ulcers or help with the healing process of ulcers (De Sousa Falcão *et al.*, 2008:3201).

2.5.3.5.2.3.9 Anti-inflammatory effect of capsaicin

Capsaicin can be considered as one of the most powerful anti-inflammatory spices. Capsaicin reduces inflammation by the inhibition of the cyclo-oxygenase-2 (COX-2) and nitric oxide synthases (i-NOX). The activity of pro-inflammatory cytokines is reduced, while the activity of anti-inflammatory cytokines is enhanced (Jungbauer & Medjakovic, 2012:232).

2.5.3.5.2.3.10 Absorption enhancement characteristics

During a study that was done by Kanda and colleagues (Kanda *et al.*, 2018:3), reversible opening of tight junctions was observed when capsaicin was administered. The mechanism of the opening of tight junctions was described by the influx of calcium that leads to cofilin activation and F-actin alteration. A decrease in F-actin was observed at the bi-cellular junctions and an increase was observed at the tri-cellular junctions. Capsaicin had no effect on the tight junction protein localization, but the amount of occludin decreased significantly. Cofilin activation and a decrease in occludin is responsible for the opening of tight junctions (Kanda *et al.*, 2018:3). An inhibitory effect of P-gp function was observed with application of capsaicin when efflux of rhodamine 123 decreased in a Caco-2 cell culture model (Han *et al.*, 2006:1728).

2.6 Summary

Protein and peptide drug molecules have low membrane permeability due to their large molecular structure and susceptibility to enzymatic degradation, therefore these drugs are usually administrated by injections. Due to the pain and infections that could be caused by injection, patient compliancy is reduced. Patient compliance would increase if these drug molecules could be administered by the oral route, but the above mentioned properties of protein and peptide drugs are problematic.

Absorption enhancers can be co-administrated with protein and peptide drug molecules via the oral route to increase their bioavailability. Mechanisms by which absorption is enhanced by drug absorption-enhancing agents include the opening of tight junctions between epithelial cells, changing of membrane fluidity, lowering the viscosity of the mucous layer, inhibition of enzymes and targeting specific transporter proteins. Examples of absorption enhancers that have been investigated and that showed potential include bile salts, fatty acids, *Aloe vera*, chitosan, piperine, capsaicin, naringin, quercetin and turmeric. It has been shown that certain compounds of natural origin could enhance the absorption of drug molecules without damaging the epithelial cells.

During this study, the absorption enhancement properties of piperine and capsaicin were investigated on an *ex vivo* pig intestinal jejunum transport model by making use of the Sweetana-Grass diffusion apparatus.

Chapter 3: Materials and Methods

3.1 Introduction

During this study, excised pig intestinal tissues mounted in a Sweetana-Grass diffusion apparatus, was used as a model to determine if selected pepper extract compounds (i.e. piperine and capsaicin) have an effect on the transport of selected marker molecules. The effect of the selected pepper extract compounds on the bi-directional transport of a known P-gp substrate, Rhodamine 123 (RH-123), was investigated to determine if modulation of efflux transporters can be detected (Zhao *et al.*, 2016:1526-1527). The effect of selected pepper extract compounds on the absorptive transport of fluorescein isothiocyanate dextran (FITC-dextran), a macromolecule marker, was investigated to determine if tight junction modulation can be detected (Galipeau & Verdu, 2016:958; Woting & Blaut, 2018:685). Lucifer Yellow (LY) was used as exclusion marker to determine membrane integrity of the excised tissues utilized in the *ex vivo* model. Transport studies in the apical to basolateral (AP-BL) direction was used to determine absorptive transport, while transport in the basolateral to apical (BL-AP) direction was used to determine secretory transport that is representative of P-gp-related efflux. Excised pig intestinal jejunum tissue obtained from an abattoir was used for all the *ex vivo* transport studies conducted in this study. Pig intestinal tissue has various anatomical, physiological and biochemical similarities to the gastro-intestinal tract of humans (Sjögren *et al.*, 2014:109). This is considered to be a cost-effective method to investigate drug permeation and absorption modulation effects, because it is less labour intensive and the tissue may be collected as a waste product from the local abattoir where animals are slaughtered routinely for meat production purposes (Antunes *et al.*, 2013:7).

Validation forms an essential part in the development of an experimental design and the implementation of reliable and reproducible analytical methods. Validation of an analytical procedure is defined by the United States Pharmacopoeia (USP) as a "*process by which it is established, by making use of laboratory studies, that the performance characteristics of the procedure meet the requirements for the intended analytical applications USP (2018a:1)*". The performance characteristics that were measured in this study included linearity, precision, accuracy, detection limit, quantification limit and specificity (USP, 2018b:6653).

3.2 Materials

Rhodamine 123 (RH-123) (lot number BCBN 7838 V), Krebs-Ringer bicarbonate buffer (lot number SLBW3493), sodium bicarbonate (lot number 021M01014V), capsaicin (lot number SLBW 2890), piperine (lot number MKCC0339), European Pharmacopoeia reference standard Capsaicin CRS (lot number Y0000671), European Pharmacopoeia reference standard Piperine CRS (lot number Y0001217), Lucifer Yellow (lot number MKBS 3318V) and fluorescein isothiocyanate (FITC) dextran (4000 Da) (lot number BSBM4054V) were purchased from Sigma

Aldrich (Johannesburg, South Africa). Costar® 96-well plates were purchased from The Scientific Group (Randburg, South Africa). Excised pig intestinal jejunum tissue was collected from the local abattoir in Potchefstroom, South Africa.

3.3 Fluoroscence spectroscopic analytical method validation for Rhodamine 123 (RH-123), FITC-dextran (FD-4) and Lucifer Yellow (LY)

The marker molecules used in the transport experiments of this study namely RH-123, FITC-dextran and LY were analysed by means of fluorescence spectroscopy by using a Spectramax Paradigm® multi-mode detection platform plate reader with excitation and emission wavelengths set at 480 nm and 520 nm for RH-123, 490 nm and 520 nm for FITC-dextran and 485 nm and 535 nm for LY, respectively (Kaprelyants & Kell, 1992:412; Pinton *et al.*, 2009:42; Wahlang *et al.*, 2011:277). The fluorescence spectroscopic analytical methods used for the marker molecules were validated in terms of linearity, accuracy, precision, specificity, limit of detection and limit of quantification as described in the sections below.

3.3.1 Linearity

Linearity is defined as the ability of an analytical method to obtain detection values that are directly proportional to the concentration of the test samples within a specific concentration range (Shabir, 2003:63; USP, 2018a:4). The correlation coefficient (R^2) value should be equal to or higher than 0.995 to prove acceptable linearity. This was determined by measuring the detector responses of at least five solutions with different concentrations of each selected marker molecule covering the applicable concentration range for each molecule (USP, 2018b:6654).

The linearity for the RH-123 fluoroscopic analytical method was determined by preparing a stock solution of 5.00 µM. Serial dilutions were prepared from this stock solution with the following concentrations: 5.00 µM, 2.50 µM, 1.25 µM, 0.63 µM, 0.31 µM, 0.16 µM, 0.08 µM, 0.04 µM, 0.02 µM and 0.01 µM. A FITC-dextran stock solution was prepared with a concentration of 100.00 ug/mg. Serial dilutions were prepared from this stock solution with the following concentrations: 100.00 ug/mg, 50.0 ug/mg, 25.0 ug/mg, 12.5 ug/mg, 6.25 ug/mg, 3.13 ug/mg, 1.56 ug/mg, 0.78 ug/mg, 0.39 ug/mg and 0.20 ug/mg. A stock solution of LY was prepared with a concentration of 50.00 ug/mg. Serial dilutions were prepared from this stock solution with the following concentrations: 50.0 ug/mg, 25.0 ug/mg, 12.5 ug/mg, 6.25 ug/mg, 3.13 ug/mg, 1.56 ug/mg, 0.78 ug/mg, 0.39 ug/mg, 0.20 g/mg and 0.10 ug/ml.

Regression analysis of the calibration curves obtained for each marker molecule was done using Microsoft Excel® and the correlation coefficient values (R^2) as well as the equations ($y = mx + c$) that describe the curves were determined.

3.3.2 Accuracy

Accuracy can be defined as how close the analysed concentration values are to the real concentration values (Shabir, 2003:61; USP, 2018a:2).

Accuracy was determined by carrying out nine measurements at three different concentrations of each selected marker molecule that covered the entire concentration range, i.e. three samples of a high concentration, 3 samples of a medium concentration and 3 samples of a low concentration. The experimental concentration values were converted to a percentage of the theoretical concentration value, which were considered the recovery values. For the analytical method to be considered accurate, the mean recovery must be 100 ± 2% (Shabir, 2003:61; USP, 2018a:2; USP, 2018b:6653).

The percentage recovery for RH-123 was determined by making use of ten samples from each of the following concentrations: 5 µM, 2.5 µM and 0.125 µM. For FITC-dextran, ten samples from each of the following concentrations: 100 ug/ml, 50 ug/ml, 25 ug/ml were used to calculate the percentage recovery. To determine the percentage recovery of LY, ten samples from each of the following concentrations: 50 ug/ml, 25 ug/ml, 12.5 ug/ml were used.

3.3.3 Limit of detection (LOD) and limit of quantification (LOQ)

Limit of detection (LOD) is defined as the lowest concentration of the analyte that could be detected by the analytical method, but not necessary quantified (Shrivastava & Gupta, 2011:22). Equation 1 was used to determine the limit of detection of the fluorescence spectroscopic method for the selected marker molecules (Shabir, 2003:62-63).

$$LOD = 3.3 \times (\frac{SD}{S}) \qquad \textbf{Equation 1}$$

Where SD represents the standard deviation of the solvent blank readings and S represents the slope of the standard curve (i.e. the line on which regression was performed to determine linearity).

The lowest concentration of an analyte that could be quantified with precision and accuracy by means of an analytical method is known as the limit of quantification (LOQ). The LOQ was calculated using Equation 2 (Shabir, 2003:63; Shrivastava & Gupta, 2011:22):

$$LOQ = 10 \times (\frac{SD}{S}) \qquad \textbf{Equation 2}$$

Where SD represents the standard deviation of the solvent blank readings and S represents the slope of the standard curve (i.e. the line on which regression was performed to determine linearity).

The fluorescence values of six replicates of blank solutions (i.e. solvent only, namely Krebs Ringer Bicarbonate buffer) were used to determine the SD values for the LOD and LOQ equations (USP, 2018b:6653).

3.3.4 Precision

Precision is defined as the correspondence between individual test samples that are analysed at different time points. Precision is therefore used to determine the reliability of the method of analysis. Precision of the fluorescence spectroscopic methods was determined by means of intra-day and inter-day analysis as described below (Shabir, 2003:61). To determine the precision of an analytical procedure, a sufficient number of samples need to be assayed to be able to determine the standard deviation and percentage relative standard deviation (%RSD) of the measurements (USP, 2018a:3).

$$\%\,\mathrm{RSD} = \frac{\mathrm{SD}}{\mathrm{Ave}} \times 100 \qquad \textbf{Equation 3}$$

Where %RSD is the percentage relative standard deviation, SD is the standard deviation between fluorescence detection values and Ave is the average of the fluorescence detection values at each time point.

3.3.4.1 Intra-day precision

Intra-day precision analyses were done over a relatively short time period during the same day under the same operating conditions (Rambla-Alegre *et al.*, 2012:106). To confirm the precision of the analytical method, the percentage %RSD must be equal to or less than 2% (Shabir, 2003:62).

During this study, three different concentrations of RH-123, FITC-dextran and LY were prepared for determination of the intra-day precision. The concentrations utilised for the intra-day precision testing were as follows: 5.00 µM, 2.50 µM and 0.125 µM for RH-123, 100 µg/ml, 50 µg/ml and 25 µg/ml for FITC-dextran and 50.0 ug/ml, 25.0 ug/ml and 12.5 ug/ml for LY, respectively. These concentrations were analysed in triplicate at three different time intervals (i.e. 11:00, 14:00 and 17:00) and the %RSD was calculated for each time point (USP, 2018a:3).

3.3.4.2 Inter-day precision

Inter-day precision is used to express variations within the same laboratory and with the same analytical instrument when samples are measured on different days (Rambla-Alegre *et al.*, 2012:106).

The concentrations utilised for the inter-day precision testing were as follows: 5.00 µM, 2.50 µM and 0.125 µM for RH-123, 100 µg/ml, 50 µg/ml and 25 µg/ml for FITC-dextran and 50.0 µg/ml, 25.0 µg/ml and 12.5 µg/ml for LY, respectively. The samples were analysed on three consecutive

days at the same time (i.e. 11:00) every day. The %RSD for these samples must be equal to or less than 2% (Shabir, 2003:62).

3.3.5 Specificity

Specificity is the ability to assess an analyte in the presence of other components that may have the ability to possibly influence the detection of that specific analyte (Depani *et al.*, 2018:744).

Solutions were prepared containing 5.00 µM of RH-123 and 100 µg/ml of FITC-dextrin, respectively, which were used as reference solutions. Test solutions were prepared containing the highest concentration of a particular pepper extract compound (i.e. 200 µM capsaicin or 200 µM piperine) that was used in any experiment in the 5.00 µM of RH-123 solution or 100 ug/ml FITC-dextran solution. The reference solutions' mean fluorescence values were each compared with the test solutions fluorescence value. The same criteria for accuracy, namely 100 ± 2% recovery of RH-123 and FITC-dextran were used to determine acceptable specificity in the presence of specific plant material (USP, 2018b:6653).

Since acceptable specificity could not be obtained for RH-123 in the presence of piperine, an alternative method was used for analysis of RH-123 in the presence of piperine. A calibration curve was constructed for RH-123 in the presence of piperine according to the method for linearity described in Section 3.3.1. This calibration curve was used to determine RH-123 concentration in the presence of piperine (Patel *et al.*, 2017:251).

3.4 Characterisation of pepper raw materials by making use of a HPLC method

The quality of the pepper extract raw materials (i.e. piperine and capsaicin) used in this study were determined by means of high performance liquid chromatography (HPLC) analysis in terms of piperine and capsaicin content, as determined with respect to piperine and capsaicin reference standards (i.e. European Pharmacopoeia reference standards). The HPLC method published by Upadhyay *et al.* (2013:6-8) was adapted for the determination of the piperine content in the piperine raw material. The HPLC methods published by Suresh *et al.* (2007:347-348) and Randviir *et al.* (2013:2972) were adapted for the determination of capsaicin content in the capsaicin raw material. Tables 3.1 and 3.2 illustrate the chromatographic conditions used for the determination of pure piperine and capsaicin in the pepper extract raw materials (i.e. capsaicin raw material and piperine raw material).

Table 3.1: Summary of the chromatographic conditions for the piperine determination

Analytical instrument	Agilent 1100 series HPLC equipped with a gradient pump, auto-sampler, UV detector and OpenLab CDS Chemstation Rev. C.01.07 SR3 data acquisition and analysis software (Agilent Technologies, Palo Alto, CA).
Column	USP L1, Venusil XBP C18, 150 x 4.6 mm, 5 µm particle diameter (Agela Technologies, Newark, DE)
Mobile phase	acetonitrile/water:0.1% H_3PO_4, 60:40
Flow rate	1.0 ml/min.
Injection volume	10 µl
Detection	UV at 325 nm
Retention time	± 5.18 minutes

Table 3.2: Summary of the chromatographic conditions for the capsaicin determination

Analytical instrument	Agilent 1100 series HPLC equipped with a gradient pump, autosampler, UV detector and OpenLab CDS Chemstation Rev. C.01.07 SR3 data acquisition and analysis software (Agilent Technologies, Palo Alto, CA).
Column	USP L1, Venusil XBP C18, 150 x 4.6 mm, 5 µm particle diameter (Agela Technologies, Newark, DE)
Mobile phase	acetonitrile/water:0.1% H_3PO_4, 60:40
Flow rate	1.0 ml/min
Injection volume	10 µl
Detection	UV at 225 nm
Retention time	± 5.28 minutes

The reference standard solutions of capsaicin and piperine were prepared in methanol, respectively. The concentration of the piperine reference standard solution was 150 µg/ml and for capsaicin reference standard solution, it was 250 µg/ml. The piperine raw material and capsaicin raw material that were used in the *ex vivo* transport studies, were weighed and solutions of each were prepared in methanol. The concentration for the piperine extract solution was 150.8 µg/ml and the capsaicin extract solution was 244 µg/ml.

The reference standard solutions of capsaicin and piperine were injected in duplicate into the chromatograph at volumes of 5.00 µl, 10.00 µl, 15.0 µl, 20.0 µl, 25.0 µl. The peak areas on the chromatograms were plotted as a function of concentration and linear regression was performed on each curve, (Upadhyay *et al.*, 2013:7). An R^2 value of ≥ 0.99 was required for each of the reference standard calibration curves for the analytical method to be deemed acceptable.

The concentration of piperine and capsaicin was calculated from the HPLC peak areas obtained from experimental solutions of each extract powder (150 µg/ml) prepared in methanol by using the calibration curves that was drawn from the reference standards. The weight of piperine extract raw material that was dissolved in a specific volume of solvent (i.e. methanol) was used to express the concentration of the experimental solution. A percentage of pure piperine and capsaicin in each of the pepper extract powders (raw materials) was calculated from the ratio of the

experimental solution concentration to concentration calculated from the references standard curve as defined by Equation 4.

$$\% \text{ piperine or capsaicin} = \frac{\text{experimental concentration}}{\text{concentration from reference standard curve}} \times 100 \qquad \textbf{Equation 4}$$

3.5 *Ex vivo* transport studies

3.5.1 Preparation of buffer solution for the transport studies

A quantity of 1.2 g of sodium bicarbonate, used to adjust the pH, was added to the contents of each container of Krebs Ringer bicarbonate buffer powder mixture (Sigma Aldrich, Johannesburg, South Africa) to prepare the final powder mixture for buffer solution for the transport studies. This final powder mixture was transferred into a 1000 ml volumetric flask and made up to volume with distilled water.

3.5.2 Preparation of experimental solutions for the transport studies

3.5.2.1 Preparation of FITC-dextran solutions

Solutions of FITC-dextran, a marker molecule used in this study to determine if tight junctions were opened by the selected pepper extract compounds (Galipeau & Verdu, 2016:958; Woting & Blaut, 2018:685), were prepared as described below.

A stock solution of FITC-dextran was prepared in Krebs Ringer bicarbonate buffer solution with a concentration of 200 ug/ml. In addition to the FITC-dextran stock solution, stock solutions of the selected pepper extract raw materials in KRB buffer solution containing ethanol (4% v/v) were prepared at concentrations of 100 µM, 200 µM and 400 µM. Ethanol was added to the pepper extract compounds due to their poor solubility properties in water (Alomrani *et al.*, 2018:164; Kaiser *et al.*, 2015:2). These stock solutions were used to prepare the experimental test solutions, which consisted of FITC-dextran stock solution and one specific pepper extract stock solution. The final experimental test solution was prepared by combining the pepper extract solution and FITC-dextran solution in a 1:1 ratio. The control group consisted of a 100 µg/ml FITC-dextran in KRB buffer solution, without any other compound present. A volume of 7 ml of each experimental test solution and control solution was added respectively to the apical side (donor chamber) of the mounted intestinal tissue in the Sweetana-Grass diffusion apparatus.

3.5.2.2 Preparation of experimental solutions of Rhodamine-123

RH-123, a known substrate of P-gp, was used as a model compound in determining the extent of P-gp-related efflux modulation by the selected pepper extract compounds (Zhao *et al.*, 2016:1526-1527).

The RH-123 stock solution was prepared by adding the correct amount of RH-123 to KRB buffer (25 ml), producing a double strength solution with a concentration of 10 µM (a RH-123 solution

containing 5 µM was obtained when diluted to 50 ml in the final solution containing the pepper extract compound). Stock solutions of the selected pepper extract raw materials in KRB buffer solution containing ethanol (4% v/v) with concentrations of 400 µM, 200 µM, 100 µM were prepared. The final experimental test solutions were prepared by mixing the stock solutions of each pepper extract compound with the RH-123 stock solution in a 1:1 ratio to provide a final concentration of 5 µM of RH-123. The control group consisted of a 5 µM RH-123 solution in KRB buffer solution without any other component present. A volume of 7 ml, of the experimental test solution and control solution respectively was added to the apical side (donor chamber) of the mounted intestinal tissue in the Sweetana-Grass diffusion apparatus.

Transport studies in the basolateral to apical direction required two individual solutions. The pepper extract solutions were prepared in concentrations of 50 µM, 100 µM and 200 µM in KRB buffer. Aliquots of 7 ml of each of the selected pepper extract solutions were added to the apical side (acceptor chamber) of the mounted intestinal tissue in the Sweetana-Grass diffusion apparatus. Aliquots of 7 ml of the 5 µM RH-123 solution were added to the basolateral side (donor chamber) of the diffusion apparatus.

Transport experiments for RH-123 were designed in such a manner to ensure that the solution containing the selected pepper extract compound, was always added to the apical side of the intestinal tissue in the Sweetana-Grass diffusion apparatus.

3.5.3 Collection and preparation of pig intestinal tissue for *ex* vivo transport studies

For each transport experiment, fresh pig intestinal tissue was collected from the local abattoir (Potchefstroom, South Africa) (Atlabachew *et al.*, 2016:310). Directly after the slaughtering of the pigs, a piece of 30 cm in length was cut from the proximal jejunum of the pig's gastro-intestinal tract approximately 50 cm from the stomach. The excised pig intestinal jejunum tissue was washed and placed in ice cold KRB buffer and immediately taken to the laboratory. The process from getting the pig intestinal tissue, identification of the specific region required for transport studies and transferring the tissue to the laboratory did not exceed 30 min.

In the laboratory, the intestinal tissue was pulled over a wetted glass tube as shown in Figure 3.1 (A). The overlaying serosal layer (outer most layer on the basolateral side) was stripped off by blunt dissection as illustrated in Figure 3.1(B) (Aucamp *et al.*, 2015:1102).

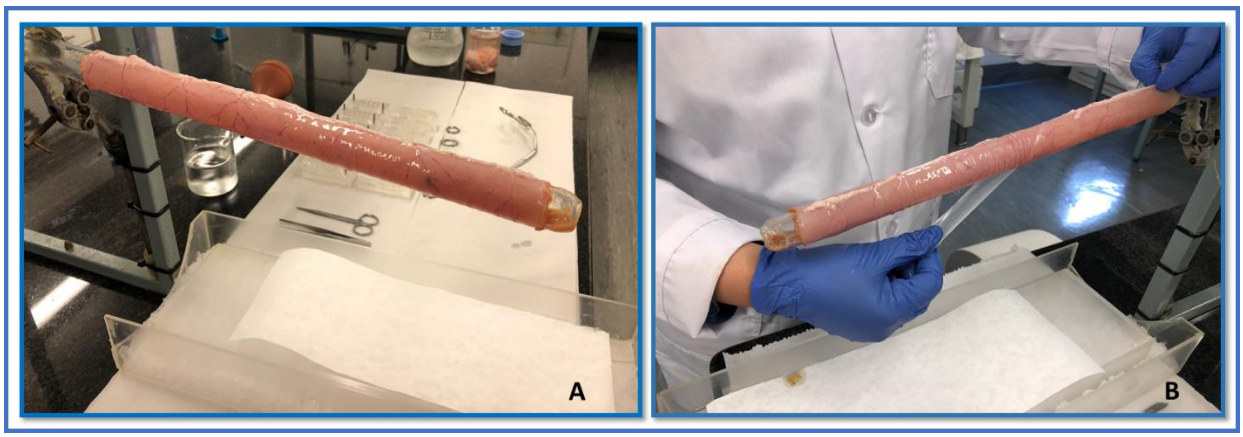

Figure 3.1: Photographic images showing A) excised pig intestinal jejunum tissue mounted on a glass tube, B) removal of the serosal layer from the excised pig jejunum tissue

After the removal of the serosal layer, the intestinal tissue on the glass tube was inspected for Peyer's patches (thickened areas) as shown in Figure 3.2. Areas with Peyer's patches were excluded from tissue mounted in the diffusion apparatus due to the negative influence that they could have on the permeation of compounds.

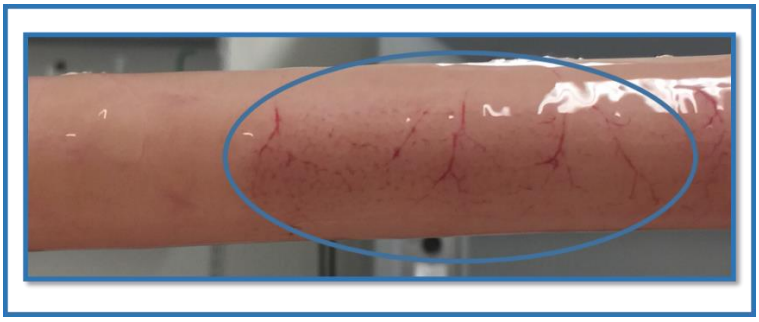

Figure 3.2: Photographic image illustrating a Peyer's patch in the excised jejunal intestinal tissue

After removal of the serosa, the intestinal tissue was removed from the glass tube by cutting it with a scalpel blade along the mesenteric border and the tissue sheet was washed from the glass tube with KRB buffer onto filter paper as shown in Figure 3.3 (Shikanga *et al.*, 2012:261-262). The tissue was continuously kept moist with cold KRB buffer and the excised tissue sheet was kept on a Perspex plate that was positioned on ice to keep the tissue cold during the preparation procedure (Figure 3.3 C).

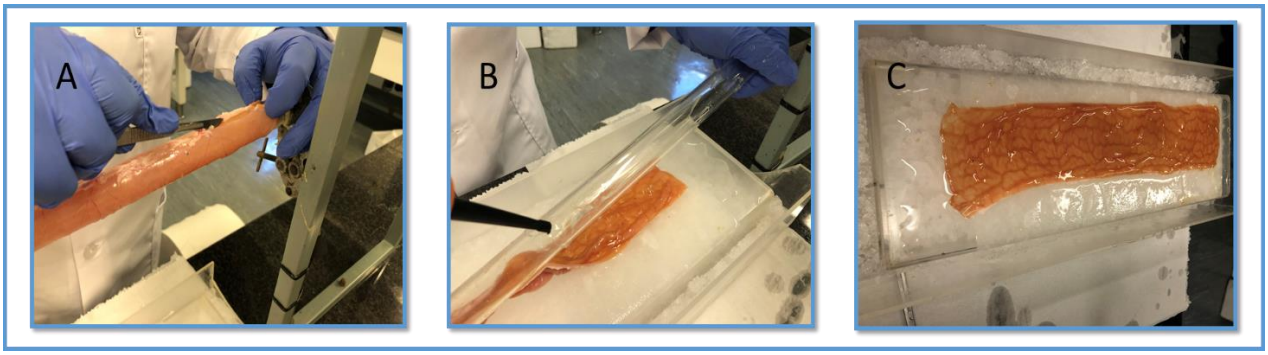

Figure 3.3.: Photographic images of A) the jejunum being cut along the mesenteric border, B) the jejunum being washed from the glass tube with Krebs Ringer bicarbonate buffer and C) the jejunum tissue sheet being transferred onto heavy duty filter paper

The excised jejunum tissue sheet on the filter paper was cut into smaller sections of ± 2 cm in width and mounted onto the pins of the Sweetana-Grass diffusion half-cells (Figure 3.4 A-E). Two diffusion half-cells were clamped together to form a chamber (Figure 3.4 F-G). The surface area available on the mounted tissue sheet for absorption of the model compound in each chamber was 1.78 cm^2. (Figure 3.4) (Aucamp *et al.*, 2015:1102; Nunes *et al.*, 2015b:214).

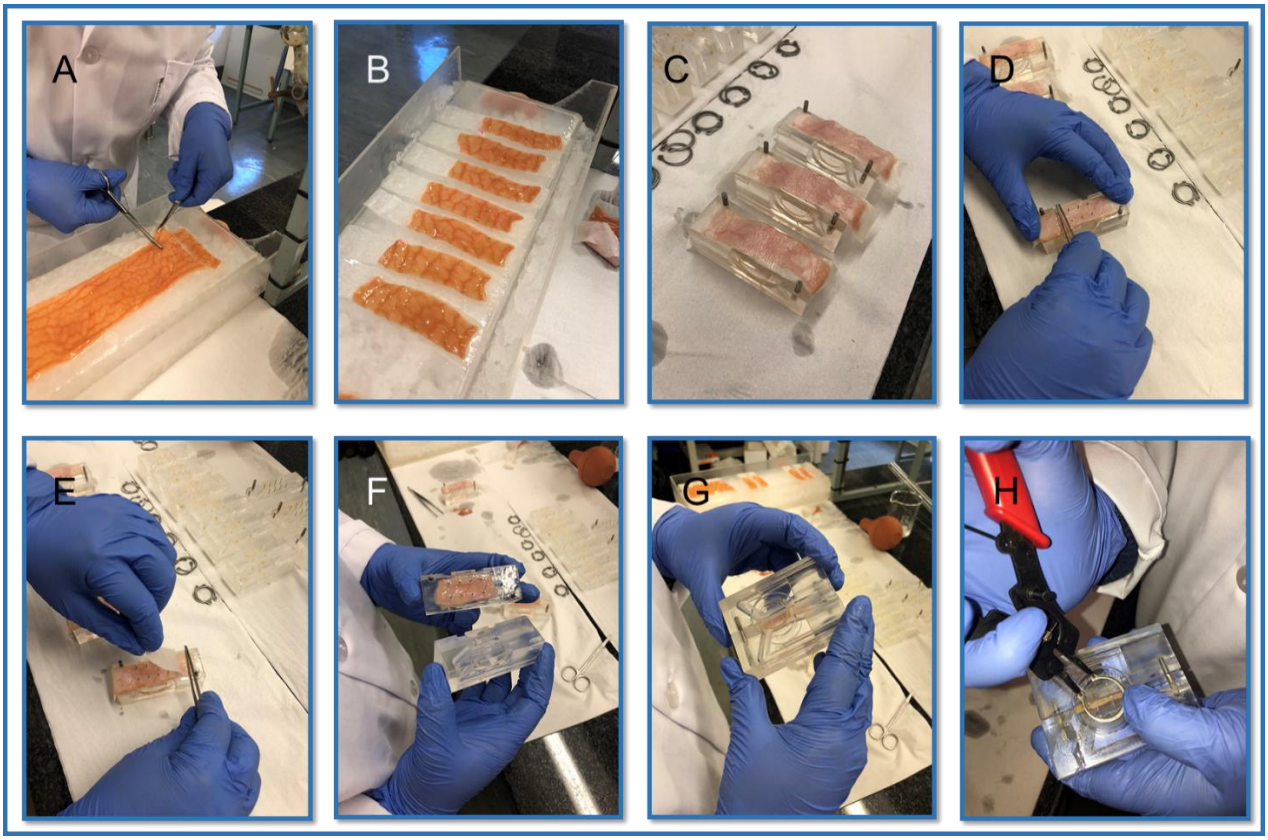

Figure 3.4: Photographic images illustrating A) and B) the cutting into smaller sections of the excised jejunal tissue sheet, C) and D) the mounting of the segments onto the pins of the diffusion half-cells, E) the removal of the heavy duty filter paper, F), G) and (H) the assembling of two half-cells into a single diffusion chamber.

Six diffusion cambers mounted with excised pig intestinal tissue were inserted into a diffusion apparatus that was linked to a heating block. The mucosal side of the excised tissue faced the

apical chamber. A volume of 7 ml of freshly prepared KRB buffer, pre-heated to 37 ºC, was added to each apical chamber as well to each basolateral chamber, which was kept for 15 min before starting the transport studies to allow the intestinal tissue to adapt to its new environment. Carbogen, a mixture of oxygen and carbon dioxide (5% CO_2:95% O_2), was bubbled continuously through the medium in each compartment as seen in Figure 3.5. The continuous flow of carbogen helped with the constant mixing of the medium in the cambers as well as keeping the tissue viable (Aucamp *et al.*, 2015:1102; Zhao *et al.*, 2016:1527).

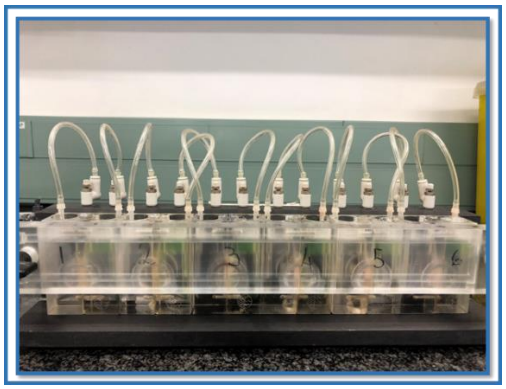

Figure 3.5: Photographic image showing a complete assembly of the Sweetana-Grass diffusion chamber apparatus with six chambers loaded into the heating block and the connected carbogen supply

3.5.4 Transport studies using the Sweetana-Grass diffusion chamber technique

The trans-epithelial electrical resistance (TEER) of the mounted excised tissue sheets were measured during the transport studies at 20 min time intervals as shown in Figure 3.6. TEER measurement was used to monitor the membrane integrity of the excised jejunal tissues and in addition to also determine if a specific pepper extract compound had the ability to open tight junctions. TEER was measured by making use of a Warner Instruments® EC-825A epithelial voltage clamp (Serial no. 211) (Atlabachew *et al.*, 2016:310; Shikanga *et al.*, 2012:262). All the transport studies conducted with all the marker molecules (i.e. RH-123, LY and FITC-dextran) and control groups were performed in triplicate.

Figure 3.6: Photographic image illustrating the setup for trans-epithelial electrical resistance measurement in the Sweetana-Grass diffusion chamber apparatus

Transport studies for RH-123 were performed in two directions across the excised intestinal tissues namely in the AP-BL direction and BL-AP direction. For AP-BL transport, the KRB was removed from the apical chambers of the Sweetana-Grass diffusion cells and replaced by the experimental test solutions. Samples (200 µl) were removed every 20 min from the basolateral chambers for a period of 2 h. The volume removed from the basolateral chambers for each sample was replenished after every withdrawal by an equal volume of KRB buffer.

For transport in the BL-AP direction, KRB buffer was removed from both chambers after the 15 min exposure period. The apical chambers were filled with test solutions containing a specific pepper extract compound, while the basolateral chambers were filled with test solution containing RH-123. Samples (200 µl) were withdrawn every 20 min from the apical chambers for a period of 2 h. The volume of the sample withdrawn from the apical chamber was replaced at every time interval by the test solution containing a specific pepper extract compound concentration dissolved in KRB buffer.

Both the FITC-dextran and LY transport studies were conducted in the same way as described for RH-123, but only in the AP-BL direction.

3.6 Assessment of intestinal tissue integrity

A fluorescent stain, Lucifer Yellow (MW:457.25 g/mol), was used as hydrophilic exclusion marker to evaluate the membrane integrity of the excised pig jejunal intestinal tissue mounted in the Sweetana-Grass diffusion apparatus over the entire period (2 h) that the transport studies were conducted (Hanani, 2012:26). For the membrane integrity test, LY was dissolved in KRB buffer in a volumetric flask with a concentration of 50 ug/ml. The effect of ethanol (4% v/v) on the membrane integrity was also investigated, in which case 2 ml ethanol were added to the LY solution in KRB buffer before making up to volume (50 ml). The membrane integrity studies were conducted by testing LY transport in the AP-BL direction over a 2 h time period where 200 µl samples were taken every 20 min from the basolateral chamber, and the samples withdrawn were replenished with the same amount of KRB buffer at every time point. The percentage transport and apparent permeability (P_{app}) values were calculated. To prove that membrane integrity was maintained, the % transport of LY in an apical to basolateral direction has to be less than 2% cumulative transport in total over the entire period (Prajapati *et al.*, 2013:360; Wahlang *et al.*, 2011:277). Similarly, the membrane is considered to be intact if the P_{app} of LY was in the range of 0.66 - 0.75 $\times 10^{-6}$ cm/s (Bhushani *et al.*, 2016:375).

3.7 Analysis of the transport samples

The concentrations of RH-123, FITC-dextran and LY in the experimental transport samples were determined by fluorescence spectroscopy using a Spectramax Paradigm® (Serial no. 33270-1142) multi-mode detection platform reader set at wavelengths as described earlier for each

marker molecule. The validated fluorescence spectroscopic methods as described in Section 3.3 were used for quantification of the marker molecule concentrations in the transport samples.

3.8 Data processing and statistical analysis

3.8.1 Percentage transport (% transport)

The fluorescence values obtained with the plate reader for each marker molecule sampled at specific withdrawal time points were corrected for dilution by two correction factors. The first correction factor compensated for the loss of the marker molecules as a result of each removal of a sample from the acceptor chamber. The second correction factor compensated for the dilution of the remaining maker molecule in solution as a result of continuous replenishment of the acceptor chamber directly after sample withdrawal with KRB to keep the volume constant. The percentage transport for each marker molecule was calculated using Equation 5 and plotted as a function of time on transport graphs.

$$\%\,\text{Transport} = \frac{\text{Mean value at specific time}}{\text{Mean value of donor solution}} \times 100 \qquad \textbf{Equation 5}$$

3.8.2 Apparent permeability coefficient (P_{app})

The apparent permeability coefficient (P_{app}) value can be defined as the flow rate of a compound from a donor chamber across a membrane into the receiver camber, normalised by the surface area of the membrane and concentration applied (Palumbo *et al.*, 2008:236). The P_{app} values for each marker molecule was calculated according to Equation 6 (Kotzé *et al.*, 1998:38).

$$P_{app} = {}^{dQ}\!/_{dt}\left(\frac{1}{A.60.C_0}\right) \qquad \textbf{Equation 6}$$

Where P_{app} is the apparent permeability coefficient (cm/s), ${}^{dQ}\!/_{dt}$ is the permeability rate (concentration/min), A is the diffusion area (cm^2) and C_0 is the initial concentration in the donor chamber (mg/ml).

3.8.3 Efflux ratio (ER)

The efflux ratio (ER) for the transport experiments that were conducted in two directions was determined by using Equation 7 (Troutman & Thakker, 2003:1202).

$$ER = \frac{P_{app}(BL - AP)}{P_{app}(AP - BL)} \qquad \textbf{Equation 7}$$

Where P_{app} (BL-AP) is the apparent permeability coefficient values in the basolateral-to-apical or secretory direction and P_{app} (AP-BL) is the apparent permeability coefficient values in the apical-to-basolateral or absorptive direction.

3.8.4 Statistical analysis of results

A Kruskal-Wallis test was done and differences were considered statistically significant when $p < 0.05$. The Statistical Consultation Services of North West University assisted with the statistical analysis of the experimental data.

Chapter 4: Results and discussion

4.1 Introduction

During this study, the potential intestinal drug absorption enhancement effects and mechanism of action of selected pepper extract compounds (i.e. capsaicin and piperine) were investigated. Different concentrations of the pepper extract compounds in combination with Rhodamine-123 (RH-123) and FITC-dextran (FD-4) were applied to excised pig intestinal jejunum tissue, which were mounted in Sweetana-Grass diffusion chambers. Rhodamine-123 was used as model compound to investigate the effect that the selected pepper extract compound may have on P-gp related efflux. Transport studies with RH-123 as model compound were done bi-directionally (i.e. both in the absorptive or AP-BL direction and secretory or BL-AP direction). FITC-dextran with a molecular size of 4000 Da was used as model compound to investigate the possibility of enhancement of paracellular transport by the selected pepper extract compounds. These studies were done in the absorptive or AP-BL direction only. All the data generated from the *ex vivo* transport studies were expressed as cumulative transport over a period of 120 min followed by the calculation of apparent permeability (P_{app}) values. The efflux ratio (ER) values were calculated for RH-123.

Trans-epithelial electrical resistance (TEER) was measured at each pre-determined time interval during all the transport experiments. Changes in the TEER values during the transport experiment may indicate changes in the tight junction integrity, which was possibly mediated by the added pepper extract compound. A lower TEER value, which is an indication of the opening of tight junctions, may cause an increase in the paracellular transport of FITC-dextran and RH-123.

The fluorometric analytical methods for RH-123, FD-4 and Lucifer Yellow (LY) were validated to confirm their accuracy and reliability. The validation process of the analytical method was done at the beginning of the study to ensure that all the analytical parameters applicable were compliant to the standards for accuracy and reliability.

Transport studies with LY were used to ensure that the method used to prepare and mount the excised jejunum intestinal tissue onto the Sweetana-Grass half cells were appropriate and to determine if the intestinal membranes were intact over the specific time period that the transport studies were done. To determine if a concentration of 4% v/v ethanol would have any effect on the intestinal membrane, a LY transport study was also conducted in the presence of 4% v/v ethanol.

Control groups for FITC-dextran and RH-123 were included in the experimental design and were used as a baseline to compare all the other transport studies with. This inclusion was used to determine if the pepper extract compounds in different concentrations had any effect on the

improvement of transport. P_{app} values calculated from the transport studies done with RH-123 (bi-directional transport studies) and FD-4 were compared to those of the control groups. A statistical analysis of the data was done to determine if differences were statistically significant or not.

4.2 Fluorescence spectrometry analytical method validation for Rhodamine 123 (RH-123), FITC-dextran (FD-4) and Lucifer Yellow (LY)

4.2.1 Method validation results for Rhodamine 123 (RH-123)

4.2.1.1 Linearity

The fluorescence values obtained for a series of solutions containing different concentrations of RH-123 are shown in Table 4.1. A standard curve was constructed by plotting the fluorescence values obtained as a function of RH-123 concentration as shown in Figure 4.1 on which a regression analysis was done to obtain the slope and correlation coefficient (R^2) value.

Table 4.1: Fluorescence values of Rhodamine-123 recorded over a specific concentration range, slope and correlation coefficient (R^2) value

R123 concentration (µM)	Fluorescence value
5.00	1591174144
2.50	798982784
1.25	384365216
0.63	194846000
0.31	92973176
0.16	45058716
0.08	21641080
0.04	10856774
0.02	5410601
0.01	3300751
Slope	317816437.76
R^2	0.9999

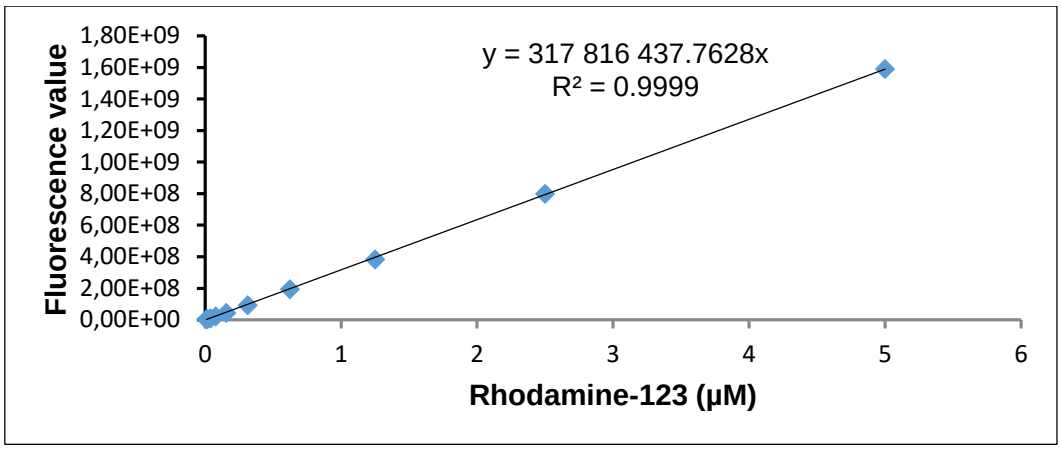

Figure 4.1: Linear regression curve of Rhodamine-123 with the straight line equation and correlation coefficient (R^2) value

According to the United States Pharmacopoeia (USP), an acceptable correlation coefficient (R^2) value for a standard curve is ≥ 0.995 (USP, 2018b:6654). It is evident from the data obtained for RH-123 that the fluorometric analytical method did meet the specific criteria for linearity since a R^2 value of 0.9999 was obtained.

4.2.1.2 Accuracy

Table 4.2 gives the results regarding the accuracy measurements (in terms of percentage Recovery) of three different concentrations of RH-123 determined by means of the fluorometric analytical method. The data obtained confirmed that the standard for accuracy was achieved with the analytical method, since the % Recovery of RH-123 was within the range of 100 ± 2% (Shabir, 2003:61; USP, 2018a:2; USP, 2018b:6653).

Table 4.2: Results obtained during determination of accuracy of the fluorometric analytical method for Rhodamine-123

Theoretical concentration (µM)	**5**	**2,5**	**0,125**
Fluorescence values	**1558070016**	**840289024**	**42938024**
	1557591552	823597888	43385904
	1585792256	780446144	42269668
	1574967168	787879104	43970516
	1561397248	782470208	41411212
	1556433024	791686144	42491984
	1546617472	833127744	42212912
	1546858112	804817920	43321284
	1543484800	836547968	40955660
	1565458944	847143360	43423044
Average fluorescence values	1559667059,20	812800550,40	42638020,80
Actual concentration (µM)	4,91	2,47	0,13
Accuracy (% Recovery)	98,15	98,66	101,63

4.2.1.3 Limit of detection (LOD) and limit of quantification (LOQ)

The standard deviation of the blank test samples (Krebs-Ringer bicarbonate buffer), also known as the background noise, as well as the calculated LOD and LOQ values are shown in Table 4.3.

Table 4.3: Average blank fluorescence detection values together with the standard deviation, limit of detection (LOD) and limit of quantification (LOQ) values for the fluorometric analytical method for Rhodamine-123

Blank fluorescence values	Average	Standard deviation	LOD (µM)	LOQ (µM)
35381	35016,83	1185,98	1,23E-05	3,73E-05
36102				
34216				
34354				
33285				
36763				

The concentrations of RH-123 obtained during the transport studies were all higher than the LOD and LOQ, therefore the RH-123 concentrations could be accurately quantified during the transport studies.

4.2.1.4 Precision

4.2.1.4.1 Intra-day precision

Three different solutions of RH-123 (i.e. 5 µM, 2.5 µM and 0.125 µM) were analysed in triplicate on the same day at three different time points (11:00, 14:00 and 17:00). The standard deviation and % RSD were calculated from the fluorescence values of each solution. Table 4.4 provides a summary of the data obtained during determination of the intra-day precision of the specific analytical method.

Table 4.4: Data obtained for intra-day precision of the fluorometric analytical method for Rhodamine-123

Theoretical concentration (µM)	Mean Fluoresence detection value			Average	Standard deviation	% RSD
	11:00	14:00	15:00			
5	1559667059,00	1554723632,00	1545382251,00	1553257647,33	5923161,78	0,38
2,5	812800550,00	807395168,00	808531354,00	809575690,67	2015256,55	0,25
0,125	42489965,78	43050711,00	42726917,00	42755864,59	229836,57	0,54

The analytical method complied within the standard of % RSD ≤ 2% as seen in Table 4.4 (Shabir, 2003:62).

4.2.1.4.2 Inter-day precision

The same concentrations used to determine intra-day precision for RH-123 (i.e. 5 µM, 2.5 µM and 0.125 µM) were used to determine inter-day precision over a time period of three days. These samples were analysed by means of fluorescence spectrometry in triplicate from which the standard deviation and % RSD were calculated. Table 4.5 summarises the results obtained.

Table 4.5: Data obtained for inter-day precision of the fluorometric analytical method for Rhodamine-123

Theoretical concentration (µM)	Mean Fluoresence detection value			Average	Standard deviation	% RSD
	Day1	Day 2	Day 3			
5	1559667059,00	1554612907,00	1576732245,00	1563670737,00	9463556,64	0,61
2,5	812800550,40	838841514,70	830210272,00	827284112,37	9379625,87	1,13
0,125	42638020,80	43098964,00	44150709,30	43295898,03	633058,13	1,46

The results showed that the fluorometric analytical method complied to the standards set in the literature (% RSD ≤ 2%) for inter-day precision as seen in Table 4.5 (Shabir, 2003:62).

4.2.1.5 Specificity

The analytical method was able to accurately quantify the concentration of RH-123 in a solution containing each of the pepper extract compounds. The standards set in the literature for specificity is 100 ± 2 % recovery (USP, 2018b:6653). Neither capsaicin nor piperine interfered with the accuracy of the RH-123 concentration measurement as seen in Table 4.6.

Table 4.6: Percentage recovery (% Recovery) of Rhodamine-123 in the presence of different pepper extracts

Pepper extract	Theoretical concentration (µM)	Actual concentration measured (µM)	% Recovery	R^2	% RSD
Capsaicin	5.00	4.92	98.33	N/A	0.10
Piperine	5.00	4.99	99.72	0.99997*	1.85

* A standard curve was constructed for Rhodamine 123 in the presence of piperine as described in the methods chapter

4.2.2 Method validation results: FITC-dextran (FD-4)

4.2.2.1 Linearity

The standard curve where fluorescence values of a series of FD-4 solutions were plotted as a function of FD-4 concentration is illustrated in Figure 4.2, while the values are listed in Table 4.7.

Table 4.7: Fluorescence values of FITC-dextran recorded over a specific concentration range, slope and correlation coefficient (R^2) value

FITC-Dextran concentration (µg/ml)	Fluorescence value
99.2	1764166272
49.6	924062208
24.8	469330304
12.4	249424944
6.20	122690400
3.10	65992076
1.55	31365100
0.78	15185896
0.39	7535498
0.19	3929550
Slope	18032408
R^2	0.999

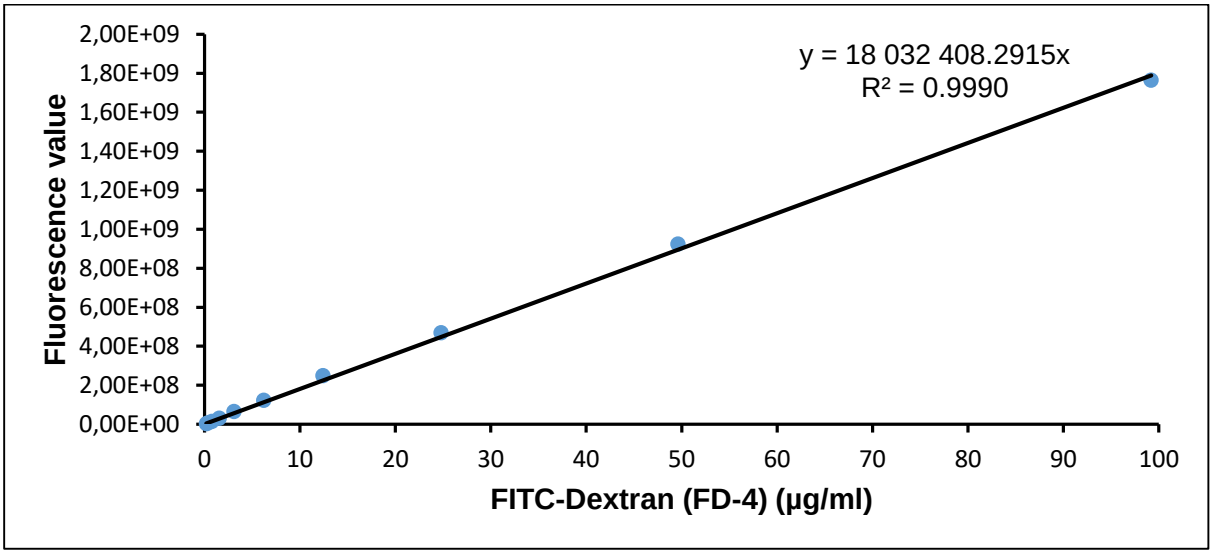

Figure 4.2: Linear regression curve of FITC-dextran (FD-4) with the straight line equation and correlation coefficient (R^2) value

The results outlined in Figure 4.2 and Table 4.7 showed that the fluorometric analytical method complied to the standards for linearity ($R^2 \geq 0.995$) (USP, 2018b:6654).

4.2.2.2 Accuracy

Table 4.8 provides results obtained for the accuracy (% Recovery) of three solutions of FITC-dextran with different concentrations by making use of a fluorometric analytical method. The results obtained indicate that the fluorometric analytical method for FD-4 complied with the standards set in the literature (% Recovery 100 ± 2%) for accuracy (Shabir, 2003:61; USP, 2018a:2; USP, 2018b:6653).

Table 4.8: Results obtained during determination of accuracy of the fluorometric analytical method for FITC-dextran

	Theoretical concentration (µg/ml)		
	99.2	**49.6**	**0.99**
Fluorescence values	1647087616	900118656	18894536
	1664007680	891533632	18938332
	1659893888	894780992	18661926
	1641839104	896923584	18451098
	1661406720	898038976	18352134
	1658442368	906092608	18355482
	1662264192	896052672	18449296
	1662500480	898464640	18452018
	1628820992	887211264	18431010
	1602278784	884619904	18584608
Average fluorescence values	1648854182	895383692	18557044
Actual concentration (µM)	98.1	49.7	0.99
Accuracy (% Recovery)	98.9	100,1	99,9

4.2.2.3 Limit of detection (LOD) and limit of quantification (LOQ)

The LOD and LOQ were determined from the blank test samples (Krebs-Ringer bicarbonate buffer) and the slope of the standard curve as shown in Figure 4.2 and Table 4.9.

Table 4.9: Average blank fluorescence detection values with the standard deviation, limit of detection (LOD) and limit of quantification (LOQ) values for the fluorometric analytical method for FITC-dextran

Blank fluorescence values	**Average**	**Standard deviation**	**LOD (µg/ml)**	**LOQ (µg/ml)**
42054	42578	1329	2.61E-04	7.91E-04
43828				
44330				
43140				
41680				
40439				

The FD-4 concentrations reported during the transport studies were much higher than the LOD and LOQ, making it possible to accurately quantify the values obtained during the transport studies.

4.2.2.4 Precision

4.2.2.4.1 Intra-day precision

Three different solutions of FITC-dextran (i.e. 99.2 µg/ml, 49.6 µg/ml and 0.99 µg/ml) were analysed in triplicate on the same day at three different time points (11:00, 14:00, 17:00). The standard deviation and % RSD were calculated from the fluorescence values of each solution. Table 4.10 provides a summary of the data obtained during determination of the intra-day precision of the specific analytical method.

Table 4.10: Data obtained for intra-day precision of the flurometric analytical method for FITC-dextran

Theoretical concentration (µg/ml)	Mean Fluoresence detection value			Average	Standard deviation	% RSD
	11:00	14:00	15:00			
99,20	1648854182,40	1619153356,80	1630374160,00	1632793899,73	12245437,67	0,75
49,60	897322856,73	894613641,14	893964644,57	895300380,81	1259584,41	0,14
0,99	18557044,00	18687159,56	18599649,33	18614617,63	54163,65	0,29

The analytical method complied within the standards of % RSD ≤ 2% as seen in Table 4.10 (Shabir, 2003:62; USP, 2018a:3).

4.2.2.4.2 Inter-day precision

The same concentrations used to determine intra-day precision for FITC-dextran (i.e. 99.2 µg/ml, 49.6 µg/ml and 0.99 µg/ml) were used to determine inter-day precision over a time period of three days. These samples were analysed by means of fluorescence spectroscopy in triplicate from which the standard deviation and % RSD were calculated. The obtained results are summarised in Table 4.11.

Table 4.11: Data obtained for inter-day precision of the fluorometric analytical method for FITC-dextran

Theoretical concentration (µg/ml)	Mean Fluoresence detection value			Average	Standard deviation	% RSD
	Day1	Day 2	Day 3			
99,20	1648854182,40	1619153356,80	1641723463,11	1636577000,77	12659629,18	0,77
49,60	897322856,73	901163072,00	909096172,80	902527367,18	4245510,50	0,47
0,99	18557044,00	18549525,80	18591782,00	18566117,27	18405,43	0,10

The results showed that the fluorometric analytical method complied with the standards set in the literature (%RSD ≤ 2 %) for inter-day precision as seen in Table 4.11 (Shabir, 2003:62; USP, 2018a:3).

4.2.2.5 Specificity

The analytical method was able to accurately quantify the concentration of FD-4 in a solution containing each of the pepper extract compounds. The standards set in the literature for

specificity is 100 ± 2% recovery (USP, 2018b:6653). Neither capsaicin nor piperine interfered with the accuracy of the FD-4 concentration measurements as seen in Table 4.12.

Table 4.12: Percentage recovery (% Recovery) of FITC-dextran in the presence of different pepper extracts

Pepper extract	Theoretical concentration (µg/ml)	Actual concentration (µg/ml)	% Recovery	% RSD
Capsaicin	99.4	99.4	100.0	1.68
Piperine	99.4	99.4	100.0	1.72

4.2.3 Method validation results: Lucifer Yellow

4.2.3.1 Linearity

The fluorescence values obtained for a series of solutions containing different concentrations of LY are shown in Table 4.13. A standard curve was constructed by plotting the fluorescence values obtained as a function of LY concentration as shown in Figure 4.3 on which a regression analysis was done to obtain the slope and correlation coefficient (R^2) value.

Table 4.13: Fluorescence values of Lucifer Yellow recorded over a specific concentration range, slope and correlation coefficient (R^2) value

Lucifer Yellow concentration (µg/ml)	Fluorescence value
49.4	113239928
24.7	56163448
12.4	27390988
6.18	13568873
3.09	6402873
1.54	3002172
0,.77	1266991
0.39	470716
0.19	214041
0.10	111386
Slope	2283164
R^2	0.9999

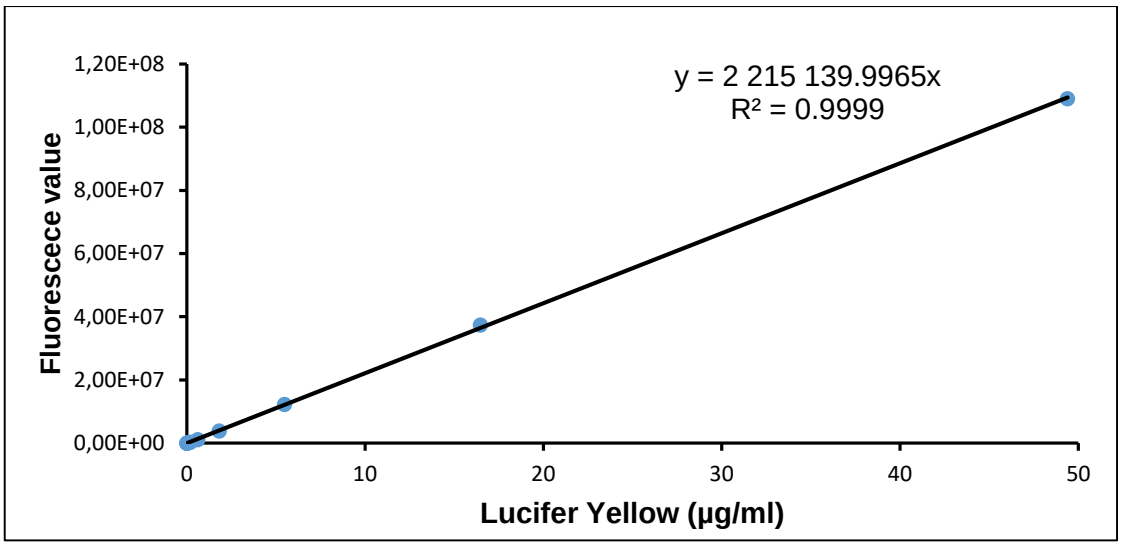

Figure 4.3: Linear regression curve of Lucifer Yellow with the straight line equation and correlation coefficient (R^2) value

According to the United States Pharmacopoeia (USP, 2018b:6654), an acceptable correlation coefficient (R^2) value for a standard curve is ≥ 0.995 (USP, 2018b:6654). It is evident from the data obtained for LY that the fluorometric analytical method did meet the specific criteria for linearity since a R^2 value of 0.9999 was obtained.

4.2.3.2 Accuracy

Table 4.14 gives the results regarding the accuracy measurements (in terms of % recovery) of three different concentrations of LY determined by means of the fluorometric analytical method. The data obtained confirms that the standards for accuracy was achieved with the analytical method, since the % recovery was within the range of 100 ± 2% (Shabir, 2003:61; USP, 2018a:2; USP, 2018b:6653).

Table 4.14: Results obtained during determination of accuracy of the fluorometric analytical method for Lucifer Yellow

Theoretical concentration (µg/ml)	**49.4**	**24.7**	**12.4**
Fluorescence values	111388024	58994780	27960306
	111148736	57311556	27695060
	107838672	58675744	27419306
	107816904	56950012	27340096
	106026184	57504668	27189250
	106022088	57372532	27157480
	109583344	57249632	27459234
	108442264	57813600	27704446
	106831008	59289612	27065400
	107019608	57419092	27126692
Average fluorescence values	108211683	57858122	27411727
Actual concentration (µg/ml)	48.9	24.6	12.3
Accuracy (% Recovery)	98.9	99.4	99.4

4.2.3.3 Limit of detection and limit of quantification

The standard deviation of the blank test samples (Krebs-Ringer bicarbonate buffer), also known as the background noise, as well as the calculated LOD and LOQ values are shown in Table 4.15.

Table 4.15: Average blank fluorescence detection values together with the standard deviation, Limit of detection (LOD) and Limit of quantification (LOQ) values for the fluorometric analytical method for Lucifer Yellow

Blank fluorescence values	Average	Standard deviation	LOD (µg/ml)	LOQ (µg/ml)
23186	23641,33	640,85	9,26E-04	2,81E-03
23434				
23210				
23054				
24115				
24849				

The concentrations of LY obtained during the transport studies were all higher than the LOD and LOQ, therefore the LY concentrations could be accurately quantified during the transport studies.

4.2.3.4 Precision

4.2.2.3.1 Intra-day precision

Three different solutions of LY (i.e. 99.5 µg/ml, 49.6 µg/ml, 0.99 µg/ml) were analysed in triplicate on the same day at three different time points (11:00, 14:00 and 17:00). The standard deviation and % RSD were calculated from the fluorescence values of each solution. Table 4.16 provides a summary of the data obtained during determination of the intra-day precision of the specific analytical method.

Table 4.16: Data obtained for intra-day precision of the fluorometric analytical method for Lucifer Yellow

Theoretical concentration (µg/ml)	Mean Fluoresence detection value			Average	Standard deviation	% RSD
	11:00	14:00	15:00			
49,4	108211683,20	107644265,60	106498740,00	107451562,90	712457,90	0,66
24,7	57785951,00	56594358,00	56418279,11	56932862,70	526103,90	0,92
12,35	27496753,60	27039436,20	26825780,80	27120656,87	279879,40	1,03

The analytical method complied within the standards of % RSD ≤ 2% as seen in Table 4.16 (Shabir, 2003:62; USP, 2018a:3).

4.2.2.3.2 Inter-day precision

The same concentrations used to determine intra-day precision for Lucifer Yellow (i.e. 99.2 µg/ml, 49.6 µg/ml and 0.99 µg/ml) were used to determine inter-day precision over a time period of three days. These samples were analysed by means of fluorescence spectrometry in triplicate from which the standard deviation and % RSD were calculated. The obtained results are summarised in Table 4.17.

Table 4.17: Data obtained for inter-day precision of the florometric analytical method for Lucifer Yellow

Theoretical concentration (µg/ml)	Mean Fluoresence detection value			Average	Standard deviation	% RSD
	Day1	Day 2	Day 3			
49,40	108211683,20	110514439,33	110859846,00	109861989,51	1175431,73	1,07
24,70	57785951,00	57647100,86	57959672,67	57797574,84	110739,83	0,19
12,35	27496753,60	27560700,00	27766473,00	27607975,53	115074,96	0,42

The results showed that the fluorometric analytical method complied with the standards set in the literature (%RSD ≤ 2 %) for inter-day precision as seen in Table 4.17 (Shabir, 2003:62; USP, 2018a:3).

4.2.4 Summary of validation results

The fluorometric analytical method complied with the criteria for validation parameters (i.e. linearity, accuracy, precision and specificity) as set in the literature. Therefore, the suitability of the fluorometric analytical method with the Spectramax Paradigma® plate reader was confirmed for the measurements of Rhodamine 123, FITC-dextran and Lucifer Yellow concentrations in the *ex vivo* transport studies.

4.3 Characterisation of pepper raw materials by making use of a HPLC method

4.3.1 Characterisation of piperine

4.3.1.1 Linearity of the Pharmacopoeia reference standard piperine CRS (Chemical Reference standard)

Linearity was obtained by applying a regression analysis to a standard curve where the peak areas of a series of piperine reference standard solutions with varying concentrations were plotted as a function of concentration as shown in Figure 4.4.

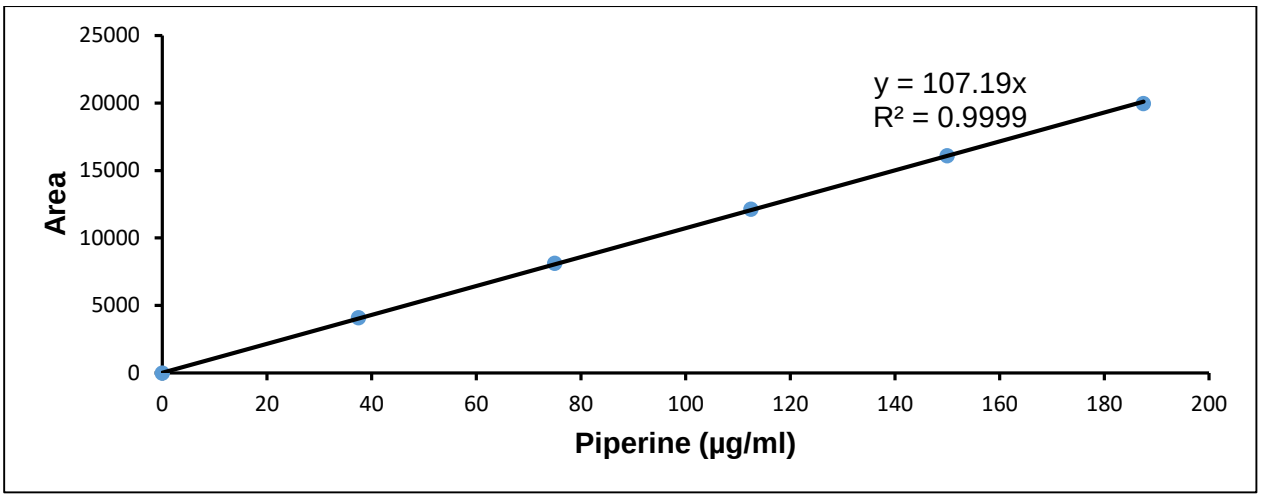

Figure 4.4: Linear regression curve of the Pharmacopoeia reference standard piperine illustrating the straight line equation as well as the correlation coefficient (R^2) value obtained with high performance liquid chromatography

According to Shabir (2003:63), an analytical method meets the requirements for linearity if the correlation coefficient (R^2) ≥ 0.999 of the curve obtained by plotting the response (i.e. peak area for HPLC) as a function of concentration. This requirement for linearity was achieved with the HPLC method used for the piperine reference standard since the R^2 value was 0.9999 for the linear regression curve.

4.3.1.2. Determining the purity of the piperine raw material used in the transport studies

The concentration of pure piperine in the piperine raw material experimental solution was determined from the HPLC peak area of the piperine experimental solution by using the piperine reference standard calibration curve (Figure 4.4). The purity of the piperine raw material determined with HPLC is shown in Table 4.18.

Table 4.18: Percentage purity of the piperine raw material

Theoretical concentration (µg/ml)	Mean area	Actual concentration (µg/ml)	% Purity
150.8	15769	147.1	97.6

The purity for the piperine raw material used during the transport studies was 97.6 % as seen in Table 4.18.

4.3.2 Characterisation of capsaicin

4.3.2.1 Linearity of the Pharmacopoeia reference standard capsaicin

Linearity was obtained by applying a regression analysis to a standard curve where the peak areas of a series of capsaicin reference standard solutions with varying concentrations were plotted as a function of concentration as shown in Figure 4.5.

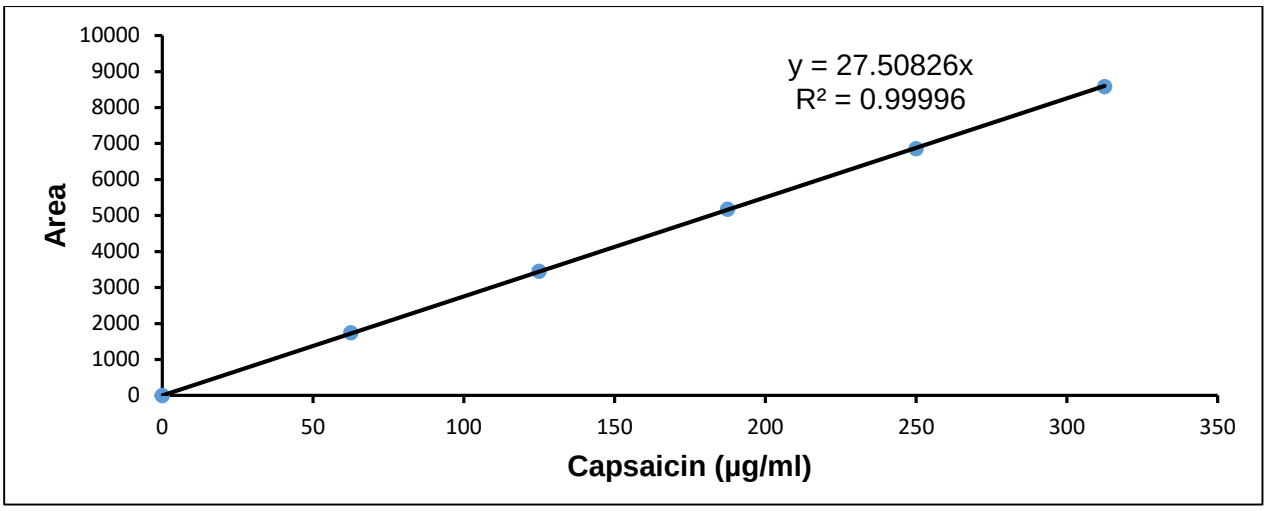

Figure 4.5: Linear regression curve of the Pharmacopoeia reference standard Capsaicin Chemical Reference Standard (CRS) illustrating the straight line equation as well as the correlation coefficient (R^2) value

According to Shabir (2003:63) a validation method meets the requirements for linearity if the correlation coefficient (R^2) ≥ 0.999. As seen in Figure 4.5 and Table 4.19 this requirement was met.

4.3.2.2 Determining the purity of the capsaicin raw material used in the transport studies

The concentration of pure capsaicin in the capsaicin raw material experimental solution was determined from the HPLC peak area of the capsaicin experimental solution by using the capsaicin reference standard calibration curve (Figure 4.4) as shown in Table 4.19.

Table 4.19: Percentage purity of the Sigma Standard for capsaicin

Theoretical concentration (µg/ml)	Mean area	Actual concentration (µg/ml)	% Purity
244	6164	224.1	91.8

The purity of the capsaicin raw material used during transport studies was 91.8% as seen in Table 4.19.

4.4 *Ex vivo* transport studies

4.4.1 Bi-directional transport studies with Rhodamine 123

Ex vivo transport studies with RH-123, a highly selective P-gp substrate, were conducted bi-directionally across excised pig intestinal jejunum tissue to determine if the selected pepper extract compounds had any effect on efflux transporters (Zhao *et al.*, 2016:1526-1527). RH-123 without any pepper extract compound served as the control group for the bi-directional transport studies.

4.4.1.1 Bi-directional transport studies in the presence of piperine

Figure 4.6 represents the average percentage transport of RH-123 in the AP-BL direction and Figure 4.7 represents the average percentage transport of RH-123 in the BL-AP direction across excised pig jejunum tissue in the presence of different concentrations of piperine.

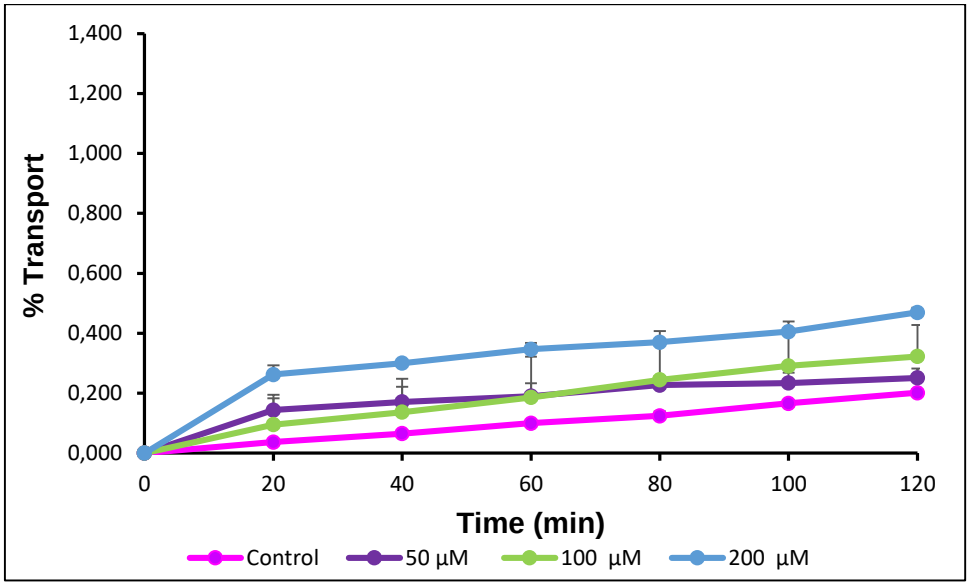

Figure 4.6: Apical-to-basolateral transport of Rhodamine-123 in the presence of different concentrations of piperine across excised pig jejunum tissue plotted as a function of time

A concentration dependent increase in RH-123 transport was mediated in the AP-BL direction when piperine was added. When the percentage transport of RH-123 in the presence of piperine is compared to RH-123 alone (control group), it is evident that the highest concentration of piperine (200 µM) had the largest increasing effect on the RH-123 transport (2.3 fold). This could possibly be due to inhibition of P-gp-related efflux of RH-123 by the piperine (Ajazuddin *et al.*, 2014:2). In addition, a concentration dependent decrease in TEER was observed in the presence of piperine (Table 4.21)**.** The highest concentration of piperine exhibited a decrease in TEER of 10.37%, which could possibly indicate a slight opening of tight junctions and thereby causing an increase in paracellular transport of Rhodamine 123 (Du Toit *et al.*, 2016:576).

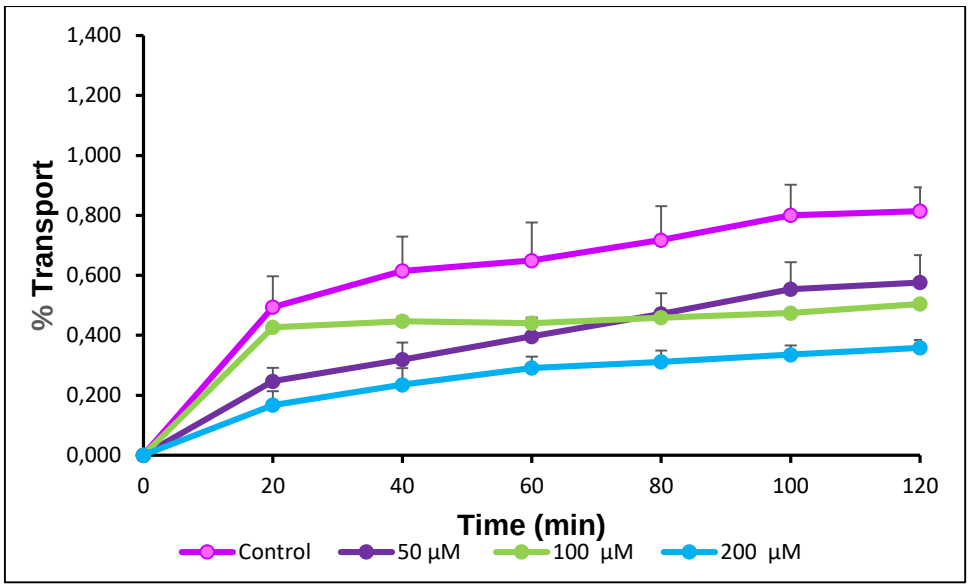

Figure 4.7: Basolateral-to-apical transport of Rhodamine-123 in the presence of different concentrations of piperine across excised pig jejunum tissue plotted as a function of time

Figure 4.7 shows that the percentage transport of RH-123 alone (control group) in the BL-AP (secretory) direction was four times higher than the transport in the AP-BL (absorptive) direction (as shown in Figure 4.6). This confirms that the *ex vivo* model used in this study, namely the excised pig jejunum tissue, was able to efflux RH-123 actively and therefore contained functional active efflux transporters. A decrease in secretory transport of RH-123 was observed when piperine was added, which was concentration dependent. The highest concentration of piperine (200 µM) decreased RH-123 secretory transport 2.3 fold. This could be explained by the inhibition of active efflux of RH-123 by the piperine (Di *et al.*, 2015:144).

A summary of the P_{app} values for RH-123 in the absence (control) and presence of different piperine concentrations in the AP-BL and BL-AP directions is given in Figure 4.8. The P_{app} values indicate the flux of RH-123 across the excised jejunum tissue normalized by taking the surface area and drug concentration on the donor side of the membrane into consideration (Du Toit *et al.*, 2016:579). The results indicated that piperine inhibited efflux of RH-123 causing a decrease in secretory transport in a concentration dependent manner and thereby enhanced the absorptive transport of RH-123. Statistically significant differences were evident when the P_{app} values of the control groups were compared to the P_{app} values in the presence of piperine and a $p \leq 0.05$ was obtained. The only statistically significant difference obtained was in the presence of 200 µM piperine in the BL-AP direction.

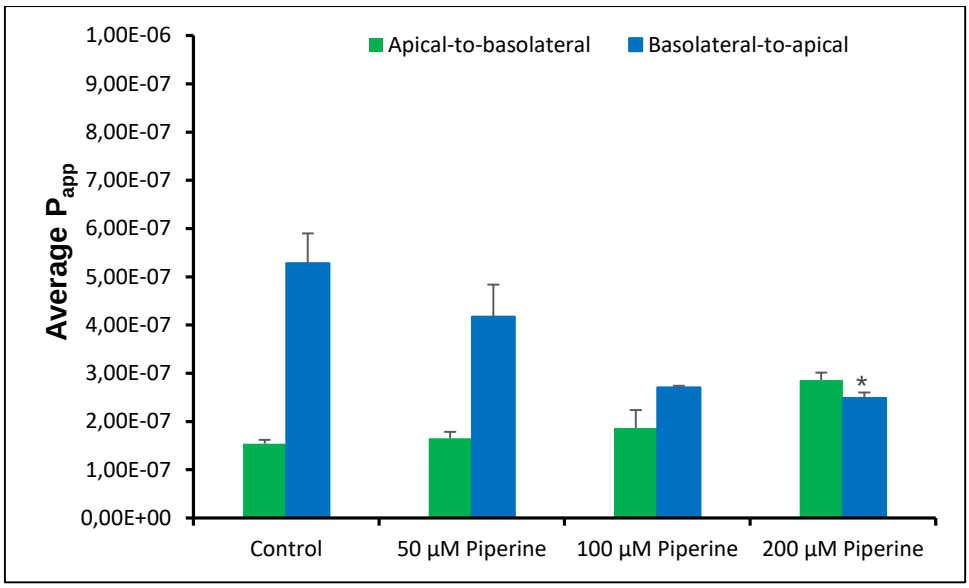

Figure 4.8: Average P_{app} values for bi-directional transport of Rhodamine-123 in the presence of different concentrations of piperine across excised pig jejunum tissue (*statistically significant difference, $p \leq 0.05$)

4.4.1.2 Bi-directional transport studies in the presence of capsaicin

Figure 4.9 represents the average percentage transport of RH-123 in the AP-BL direction and Figure 4.10 represents the average percentage transport in the BL-AP direction in the presence of different concentrations of capsaicin.

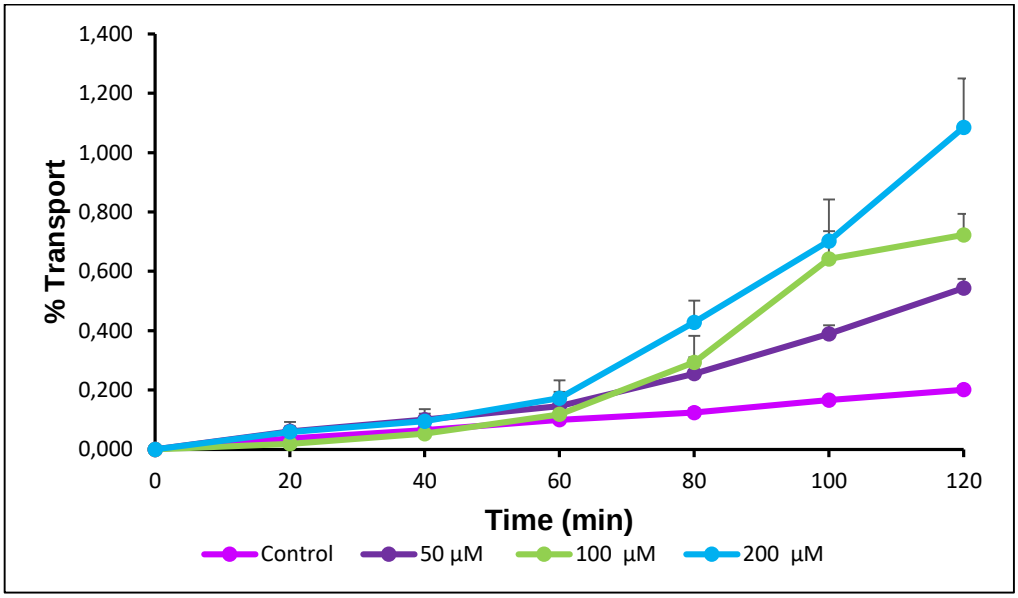

Figure 4.9: Apical-to-basolateral transport of Rhodamine-123 in the presence of different concentrations of capsaicin across excised pig jejunum tissue plotted as a function of time

Capsaicin yielded a concentration dependent increase in RH-123 transport in the AP-BL direction as seen in Figure 4.9. A concentration of 200 µM capsaicin exhibited a 5.4-fold increase in the absorption of RH-123 when compared to the control group. This is most probably due to the inhibition of efflux of RH-123 by capsaicin (Han *et al.*, 2006:1733). A slight decrease in the TEER

values was observed for capsaicin when applied at concentrations of 50 and 100 µM and a slight increase took place in the average TEER value when applied at a concentration of 200 µM.

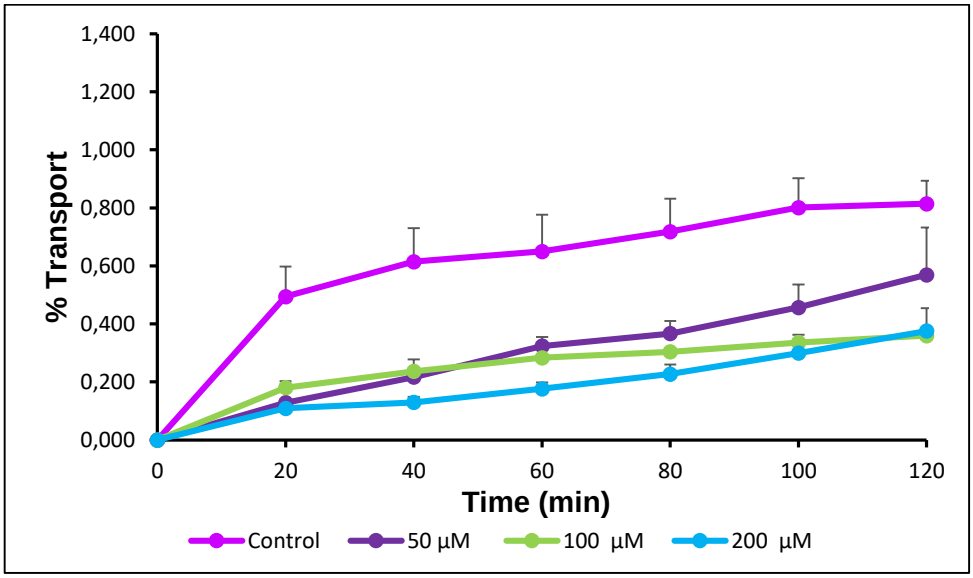

Figure 4.10: Basolateral-to-apical transport of Rhodamine-123 in the presence of different concentrations of capsaicin across excised pig jejunum tissue plotted as a function of time

As seen in Figure 4.10, there was a concentration dependent decrease in the secretory transport of Rhodamine 123 when considering the 50 µM and the 100 µM concentrations of the co-applied capsaicin. The medium concentration of 100 µM capsaicin and the highest concentration of 200 µM did not cause a pronounced difference in RH-123 transport when compared to each other, but decreased the RH-123 transport by more than 2-fold when compared to the control group.

A summary of the P_{app} values for RH-123 in the AP-BL and BL-AP directions in the presence of capsaicin at different concentrations is shown in Figure 4.11. An increase in RH-123 transport took place in the AP-BL direction as the concentration of capsaicin increased. In the BL-AP direction there was a decrease in the transport of RH-123 compared to the control group, but this decrease was lower when capsaicin was co-applied at a 200 µM concentration. Since transport of RH-123 was higher in the absorptive direction than in the secretory direction as seen in Table 4.22 (ER values), which is most probably due to the inhibition of efflux (Han *et al.*, 2006:1733). The only statistically significantly difference obtained was between the control group and the 200 µM capsaicin in the AP-BL direction.

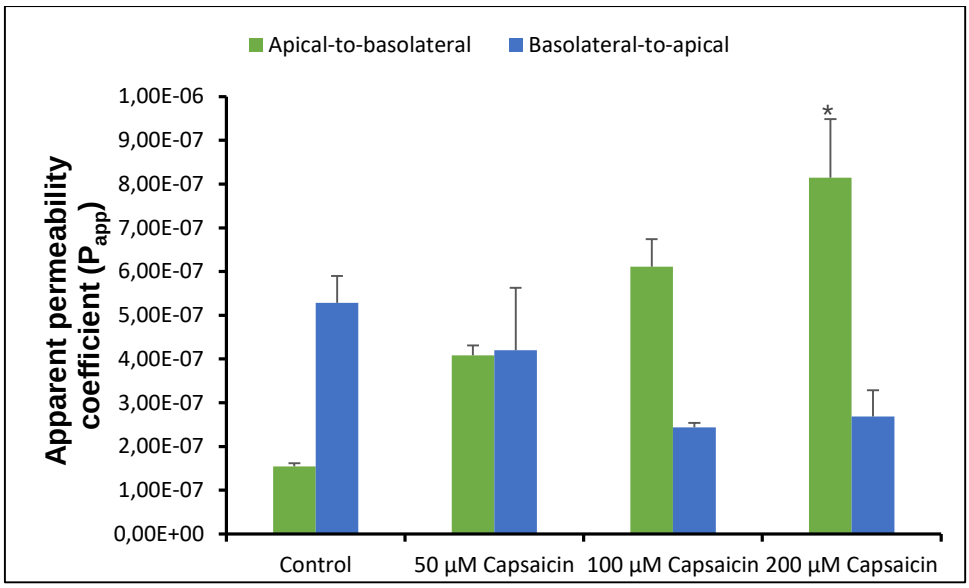

Figure 4.11: P_{app} values for bi-directional transport of Rhodamine-123 in the presence of different concentrations of capsaicin across excised pig jejunum tissue (*statistically significant difference, $p \leq 0.05$)

4.4.1.3 Evaluation of efflux ratios

Efflux ratio (ER) values can give an indication of the transport mechanism by which drug absorption enhancement occurs during co-administration of a selected pepper extract compound. An ER value > 1 indicates that a permeant is subjected to active efflux transport, ER < 1 indicates that active absorption took place and a ER = 1 indicates that passive diffusion is the main transport mechanism (Gerber *et al.*, 2018:118). Table 4.20 represents the ER values calculated for RH-123 in the presence of selected pepper extract compounds at different concentrations.

Table 4.20: Summary of the P_{app} values and efflux ratio (ER) values for the selected pepper extracts at selected concentrations

	Piperine		
	50 µM	**100 µM**	**200 µM**
Mean P_{app} (AP-BL)	1.654E-07	1.862E-07	2.859E-07
Mean P_{app} (BL-AP)	4.173E-07	2.709E-07	2.488E-07
Efflux Ratio (ER)	2.52	1.45	0.87
	Capsaicin		
	50 µM	**100 µM**	**200 µM**
Mean P_{app} (AP-BL)	4.085E-07	6.110E-07	8.150E-07
Mean P_{app} (BL-AP)	4.201E-07	2.437E-07	2.682E-07
Efflux Ratio (ER)	1.03	0.40	0.33

Piperine as well as capsaicin showed a concentration dependant inhibition of the efflux of RH-123. It is important to note that piperine might have enhanced the transport of RH-123 by means of another mechanism in addition to efflux inhibition, which is the opening of tight junctions based on the TEER results. Piperine also enhanced the transport of FITC-dextran, which confirmed transport enhancement by means of the modulation of tight junctions. Capsaicin, on the other hand, caused a slight increase in TEER values (Table 4.21) and had almost no effect on FITC-

dextran transport (Figure 4.14 and 4.15), indicating that P-gp efflux inhibition is the only possible mechanism by which RH-123 transport was enhanced in the AP-BL direction.

4.4.1.4 Comparison and evaluation of TEER

Trans-epithelial electrical resistance (TEER) is used as a guideline that indicates changes in the epithelial barrier in terms of the paracellular permeability of ions. The TEER value quantifies the transport of ions over cell barriers, helping to evaluate the integrity of epithelial membranes and tight junction dynamics (Assunção *et al.*, 2014:984; Srinivasan *et al.*, 2015:107).

During this study, TEER measurements were taken at 20 min intervals, and the average percentage change in TEER values was calculated at T_{120} as given in Table 4.21.

Table 4.21: Percentage trans-epithelial electrical resistance (TEER) across excised tissue exposed to each of the selected pepper extracts at 120 min after administration (T_{120}) during the Rhodamine-123 transport studies

		TEER Values		
		Piperine		
		50 µM	100 µM	200 µM
Direction of transport	Apical-basolateral	96.2196	928780	89.6630
	Standard deviation	1.51	2.04	1.28
	Basolateral-apical	96.0	92.7	89.0
	Standard deviation	1.60	1.08	1.13
		Capsaicin		
		50 µM	100 µM	200 µM
	Apical-basolateral	98.0	96.3	97.3
	Standard deviation	4.73	1.94	0.88
	Basolateral-apical	98.1	96.8	100.1
	Standard deviation	1,41	1,05	2,18

		TEER Values		
		Piperine		
		50 µM	100 µM	200 µM
Direction of transport	Apical-basolateral	96,196	92,780	89,630
	Standard deviation	1,513	2,040	1,279
	Basolateral-apical	96,052	92,737	89,032
	Standard deviation	1,601	1,075	1,127
		Capsaicin		
		50 µM	100 µM	200 µM
	Apical-basolateral	98,018	96,345	97,274
	Standard deviation	4,734	1,936	0,882
	Basolateral-apical	98,112	96,815	100,071
	Standard deviation	1,410	1,047	2,181

Table 4.21 shows that there was a concentration dependant decrease in the TEER values of the Rhodamine 123 experiments containing piperine. This indicates that piperine possibly opened intercellular tight junctions. In the presence of capsaicin there was a slight decrease in TEER values from the 50 µM to the 100 µM, and from the 100 µM to the 200 µM there were an increase in TEER values, indicating that the integrity of the tight junctions increased.

4.4.2. Transport studies with FITC-dextran (FD-4)

Ex vivo transport studies with FITC-dextran (FD-4) were conducted in an AP-BL direction across excised pig intestinal jejunum tissue to determine if the selected pepper extract compounds had any effect on the transport of the macromolecular model compound. These transport studies investigated paracellular transport and tight junction modulation (Galipeau & Verdu, 2016:958; Woting & Blaut, 2018:685). FD-4 in the absence of pepper extract compound served as the control group for these transport studies. A P_{app} value (Addendum B) for each individual transport study was calculated and the TEER values (Addendum C) were measured.

4.4.2.1 Transport studies in the presence of piperine

Figure 4.12 represents the percentage transport of FD-4 in the AP-BL direction in the presence of different concentrations of piperine.

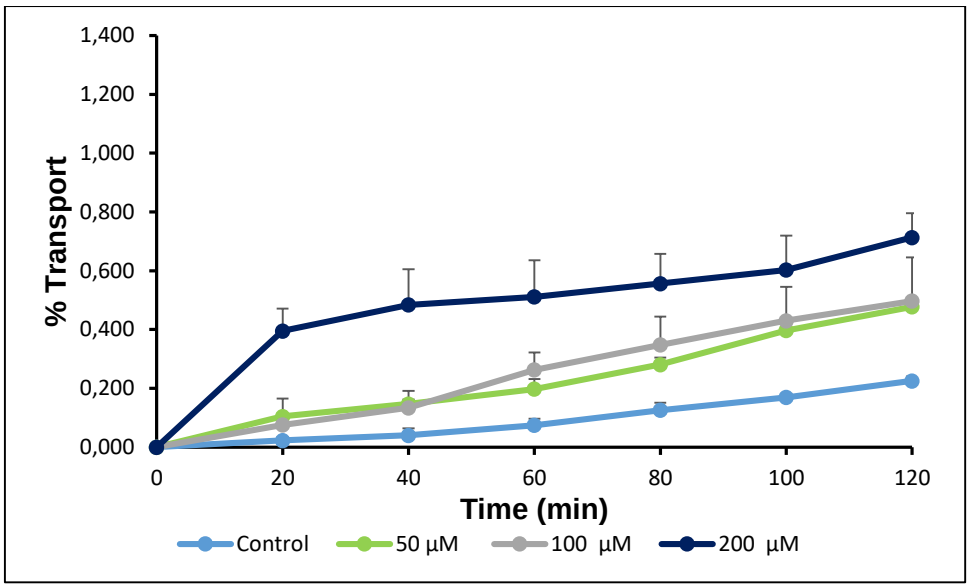

Figure 4.12: Transport of FITC-dextran in the presence of different concentrations of piperine across excised pig jejunum tissue plotted as a function of time

A concentration dependent increase in FD-4 transport was mediated in the AP-BL direction when piperine was added. Comparing the transport of FD-4 in the presence of piperine with FD-4 alone (control group), it is clear that the highest piperine concentration caused a transport enhancement effect of more than 3-fold on the FD-4 transport. This could possibly be due to the opening of tight junctions due to the fact that there was a concentration dependent decrease in the TEER values as seen in Table 4.22. The highest concentration of piperine exhibited a decrease in TEER of more than 18%, which indicates the opening of tight junctions.

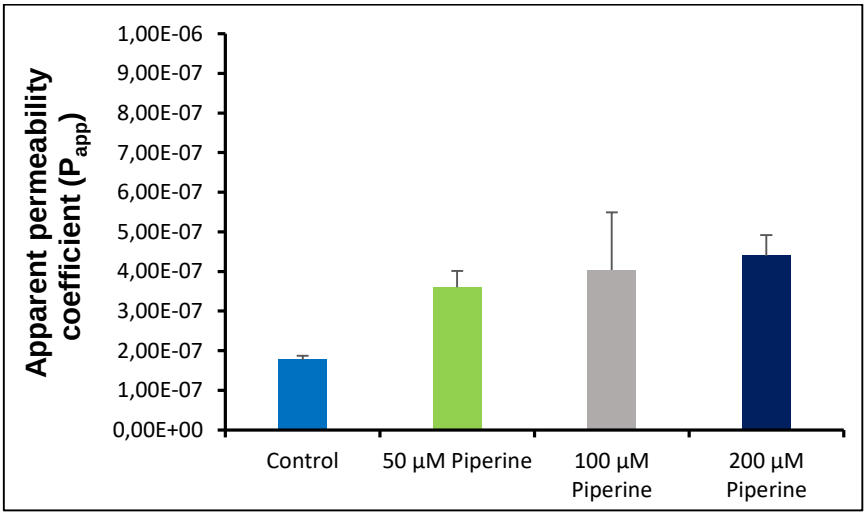

Figure 4.13: P_{app} values for transport of FITC-dextran in the presence of different concentrations of piperine across excised pig jejunum tissue

From Figure 4.13, an approximate 2.5-fold increase in FD-4 transport can be observed for the highest concentration of piperine. This increase in transport occurred in a concentration dependent manner from the 50 µM concentration of piperine to the 200 µM concentration of piperine.

4.4.2.2 Transport studies in the presence of capsaicin

Figure 4.14 represents the percentage transport of FD-4 in the AP-BL direction in the presence of different concentrations of capsaicin.

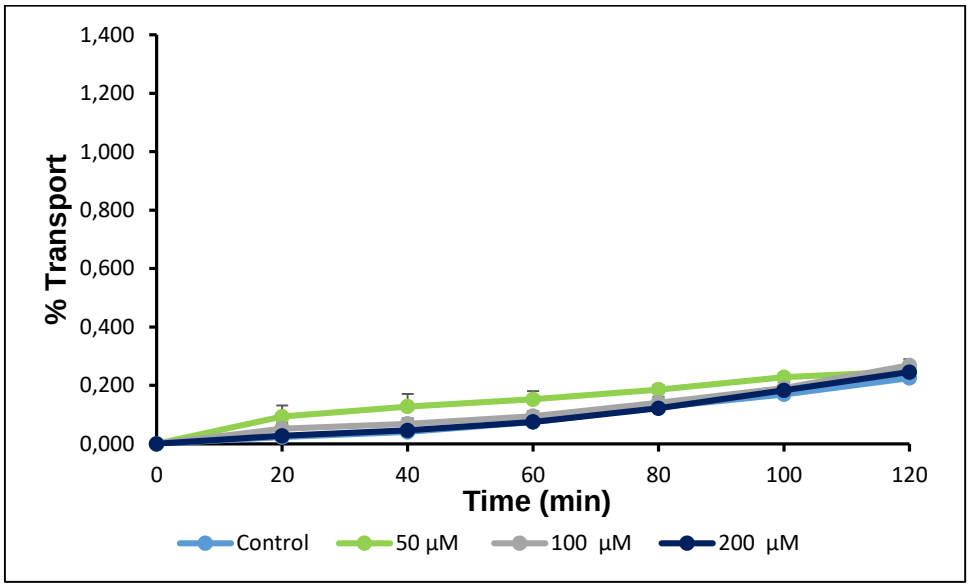

Figure 4.14: Transport of FITC-dextran in the presence of different concentrations of capsaicin across excised pig jejunum tissue plotted as a function of time

From Figure 4.14, it is evident that almost no change in the percentage transport took place when capsaicin in specific concentrations was added to the FD-4. The value of 100 µM of capsaicin had the largest FD-4 transport enhancement effect when compared to FD-4 alone (control group). An absorption enhancement effect of 1.2-fold was observed at this concentration of capsaicin. The TEER values over the concentration range of capsaicin stayed stable at 97%. These results indicate that modulation of the tight junctions did not take place.

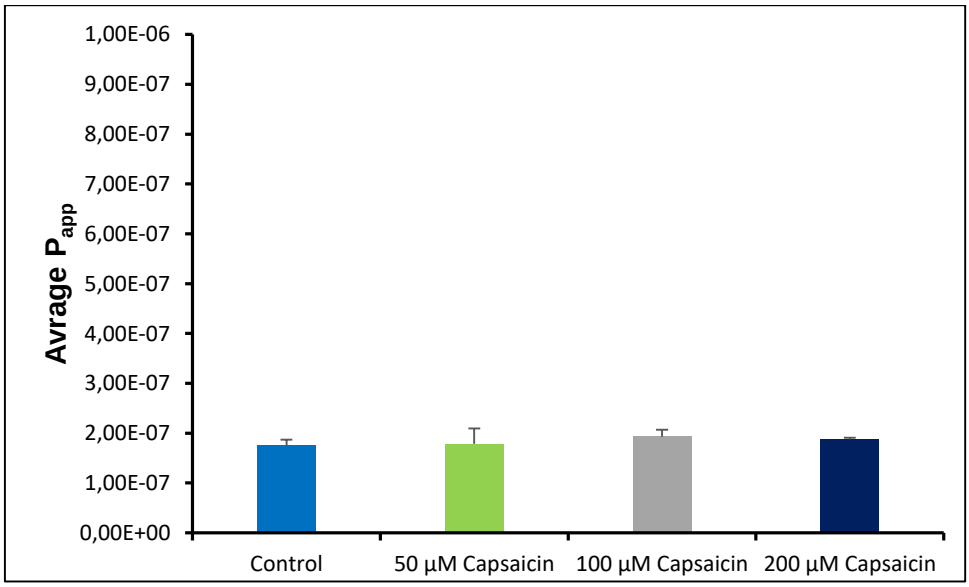

Figure 4.15: Average P_{app} values for transport of FITC-dextran in the presence of different concentrations of capsaicin across excised pig jejunum tissue

From Figure 4.15, it is evident that there was almost no change in the P_{app} values from the FD-4 alone (control group) until the concentration of 200 µM capsaicin was applied, indicating that capsaicin had almost no effect on the transport of FITC-dextran at the selected concentrations.

4.4.2.3 Comparison and evaluation of TEER

During this study, TEER readings were taken at 20-minute time intervals, and the average percentage TEER values were calculated between the T_0 and T_{120} readings as seen in Table 4.22.

Table 4.22.: Average percentage trans-epithelial electrical resistance (TEER) for excised tissue exposed to each of the selected pepper extracts over a two-hour period in the presence of FITC-dextran (FD-4) (all the values are expressed as average percentage change from the initial T_0 to the T_{120} value)

		TEER values		
		Piperine		
		50 µM	100 µM	200 µM
Direction of transport	Apical-basolateral	90,626	82,921	81,444
	Standard deviation	2,481753	1,112704	3,848
		Capsaicin		
		50 µM	100 µM	200 µM
	Apical-basolateral	97,497	97,020	97,883
	Standard deviation	0,091	0,174	1,497

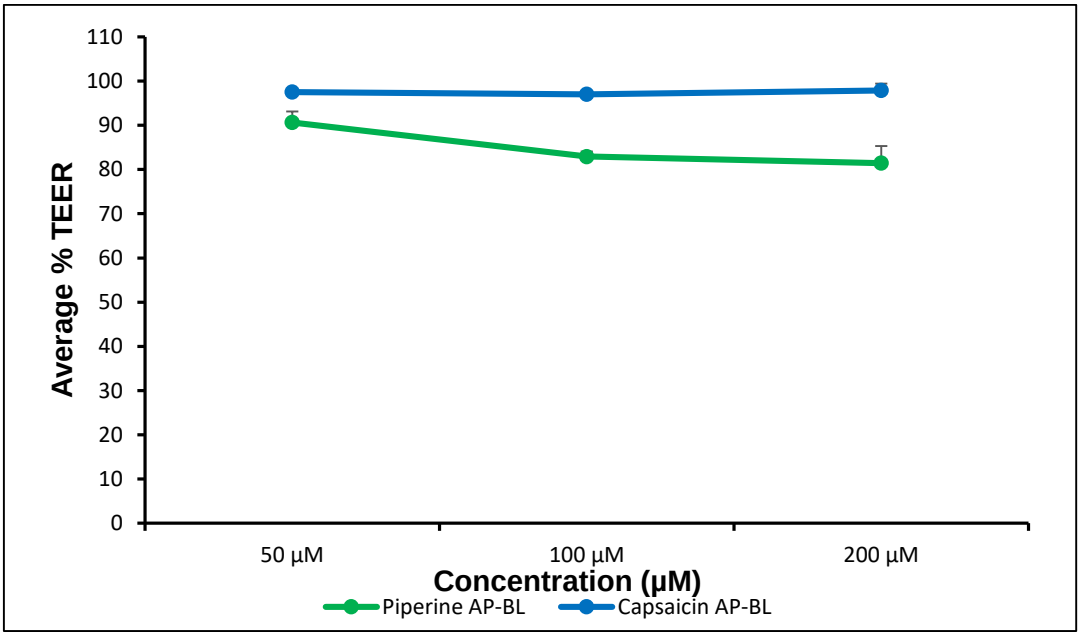

Figure 4.16: Average percentage TEER reduction plotted as a function of concentration over a two-hour period (Error bars represent the standard deviation)

As seen in Table 4.22 and Figure 4.16, there were a significant concentration dependent decrease in TEER values as the concentration of piperine increased, indicating that piperine modulated the opening of tight junctions as the concentration increased, resulting in a significant effect. The TEER values of capsaicin stayed relatively constant as seen in the above mentioned table and

figure. This indicated that capsaicin at this specific concentration range had no effect on tight junctions.

4.5 Assessment of intestinal tissue integrity

To prove that membrane integrity of the intestinal tissue was maintained for the duration of the transport experiments, the % transport of LY must be less than 2% over the entire period of the transport study and the P_{app} value must be in the range of 0.66-0.75 × 10^{-6} cm/s (Bhushani *et al.*, 2016:375; Prajapati *et al.*, 2013:360; Wahlang *et al.*, 2011:277). The percentage cumulative transport of LY was 0.773% (therefore < 2%), for LY without ethanol and the percentage cumulative transport was 0.742% for the LY with 4% ethanol. The average P_{app} value for the LY without ethanol was 5.3×10^{-7} cm/s and for LY with 4% ethanol, it was 5.38×10^{-7} cm/s. Both of these values complied with the standards set in the literature for membrane integrity. These results therefore indicated that the method used to mount the intestinal tissue and the 4% ethanol did not influence the integrity of the excised tissue membrane of the jejunum.

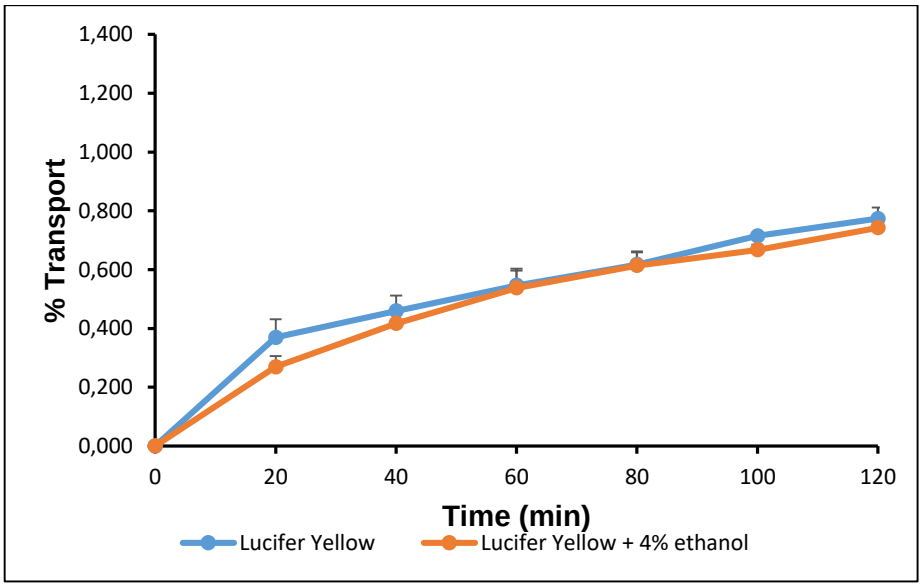

Figure 4.17: Apical to basolateral transport of Lucifer Yellow and Lucifer Yellow + 4% ethanol across excised pig intestinal jejunum tissue plotted as a function of time

Table 4.23: The permeability coefficient values for Lucifer Yellow and Lucifer Yellow + 4% ethanol across excised pig intestinal jejunum tissue

Chamber	Lucifer Yellow Papp (×10-7)	Lucifer Yellow + 4% ethanol Papp (×10-7)
Chamber 1	5.28	5.40
Chamber 2	4.95	5.38
Chamber 3	5.67	5.36
Average	5.30	5.38

4.6 Conclusions

The analytical method used to measure and quantify the value of Rhodamine 123, FITC-dextran and Lucifer Yellow in the test samples complied with the validation standards set in the literature for linearity, accuracy, specificity and precision. Piperine improved the absorption of RH-123 in the absorptive direction and decreased the absorption of RH-123 in the secretory direction, indicating that piperine has the ability to inhibit P-gp related efflux. A decrease in TEER values were observed as the piperine concentration increased, indicating that piperine possibly mediated a slight opening of tight junctions and in turn, improved paracellular transport of RH-123. A statistically significant difference was observed between the RH-123 control group and the 200 µM piperine in the BL-AP direction. Piperine improved FD-4 transport as the concentration of piperine increased. These results indicate that piperine opens tight junctions and improves paracellular transport in the gastro-intestinal tract. Capsaicin improved the absorption of RH-123 in the absorptive direction as the capsaicin concentration increased, and decreased the RH-123 absorption in the secretory direction, indicating that capsaicin has the ability to inhibit P-gp efflux. A statistically significant difference was observed between the RH-123 control group and the 200 µM capsaicin in the AP-BL direction. Capsaicin had almost no effect on the absorption of FD-4 indicating that capsaicin does not improve paracellular transport.

Chapter 5: Final conclusions and future recommendations

5.1 Final conclusions

The main aim of this study was to investigate if selected pepper extract compounds (i.e. capsaicin and piperine) had the ability to enhance drug absorption by the inhibition of P-gp efflux transporters or by the opening of tight junctions. These drug absorption enhancement mechanisms were investigated by the co-administration of model compounds, Rhodamine 123 (RH-123) and FITC-dextran (FD-4) with the pepper extract compounds. *Ex vivo* transport studies with RH-123, a known P-gp substrate, across excised pig intestinal tissue in the Sweetana-Grass diffusion apparatus were conducted bi-directionally in the presence of the selected pepper extract compounds in varying concentrations to investigate the ability of each pepper extract compound to inhibit P-gp efflux transporters. Transport studies with FD-4 (4000 Da) were conducted in the AP-BL (absorptive) direction across excised intestinal jejunum tissue to investigate the ability of the selected pepper extract compound in varying concentrations to open tight junctions and thereby improve the paracellular transport of drug molecules.

The fluorometric analytical methods for RH-123 and FD-4 were validated and they complied with all the specifications set in the literature when considering linearity, specificity, precision and accuracy. The fluorometric analytical method for Lucifer Yellow (LY) was validated in the same manner as RH-123 and FD-4, except it was not evaluated in terms of specificity because it was applied alone. By validating the fluorometric analytical methods for RH-123, FD-4 and LY ensured that the method of analysis was accurate and that the concentrations determined for these compounds in the samples collected during transport studies were trustworthy and accurate. Two transport studies with LY were done in the AP-BL direction. One of these transport studies were done in the presence of 4% ethanol that proved the ethanol had no effect on the membrane integrity and that membrane integrity had been maintained throughout the experiments. It was clearly shown by the results of this study that piperine and capsaicin had a concentration dependant effect when compared to the control group (RH-123 alone) on the efflux transport of RH-123 due to the inhibition of P-gp. Piperine increased the absorptive transport of FD-4 in a concentration dependant manner, when compared to the control group (FD-4 alone), indicating that tight junctions are opened by the co-administration of piperine. Piperine had the ability to enhance the transport of drug molecules by means of the paracellular transport route. Capsaicin had almost no effect on the transport of FD-4 atthe concentrations investigated. This indicated that capsaicin at concentrations of 50 µM, 100 µM and 200 µM did not open tight junctions.

Piperine showed a concentration dependant decrease in TEER values of the excised pig intestinal tissues, which indicated that tight junctions were opened, confirming enhanced transport of drug molecules by the paracellular route. Excised pig intestinal tissues to which capsaicin was applied showed a relatively constant TEER reading over the three concentrations. This lack of a tight

junction opening effect of capsaicin at the specific concentrations investigated could be a possible reason why FD-4 transport across the excised pork intestinal tissue did not take place.

This study confirmed that the selected pepper extract compounds (i.e. piperine and capsaicin) had the ability to enhance the absorption of drug molecules across intestinal epithelial membranes by different mechanisms including the inhibition of efflux transporters and opening of tight junctions.

5.2 Future recommendations

During this study, the use of selected pepper extract compounds displayed promising results regarding the delivery of macromolecular drug molecules. This study proved that intestinal drug absorption enhancement of macromolecular drug molecules is possible by pepper extract compounds, however, the following recommendations are made for future studies:

- The possibility of inter-individual variation between pigs slaughtered at the abattoir exists. It is important to make sure that the pigs from which the excised intestinal jejunum tissues are being collected are approximately the same weight and age. This minimise the chance of variation during transport studies caused by physiological differences between the animals from which intestinal jejunum tissue are being collected.
- Additional *ex vivo* permeation studies can be conducted in the presence of pepper extract compounds with clinically relevant macromolecules (i.e. human growth hormone, parathyroid hormone, calcitonin and insulin).
- *In vivo* studies in appropriate animal and human models are required to confirm oral macromolecular delivery efficacy in terms of bioavailability and to verify if the absorption enhancing effects shown by *ex vivo* permeation studies are sufficient to provide effective blood plasma levels that is clinically significant.
- Liposomes, micelles, nanoemulsions or a sustained-release solid preparation can be formulated to improve the solubility of capsaicin and piperine and to achieve a prolonged therapeutic effect.
- A wider range of testing can be done on different models used during transport studies, including cell monolayer (i.e. MDCK and Caco-2) as well as tissue from different species of animals.
- The potential damaging effect of prolonged exposure of absorption enhancers to the intestinal tissue can be evaluated by means of long term toxicity studies.

Addendum A: Ethics Approval

NORTH-WEST UNIVERSITY
YUNIBESITI YA BOKONE-BOPHIRIMA
NOORDWES-UNIVERSITEIT

Private Bag X6001, Potchefstroom
South Africa 2520

Tel: (018) 299-4900
Faks: (018) 299-4910
Web: http://www.nwu.ac.za

Ethics Committee
Tel +27 18 299 4849
Email Ethics@nwu.ac.za

ETHICS APPROVAL OF PROJECT

The North-West University Research Ethics Regulatory Committee (NWU-RERC) hereby approves your project as indicated below. This implies that the NWU-RERC grants its permission that provided the special conditions specified below are met and pending any other authorisation that may be necessary, the project may be initiated, using the ethics number below.

Project title: **Excised pig buccal and intestinal tissues as in vitro models for pharmacokinetic studies**

Project Leader: **Prof Sias Hamman**

Ethics number:

N	W	U	-	0	0	0	2	5	-	1	5	-	A	5
Institution				Project Number						Year			Status	

Status: S = Submission; R = Re-Submission; P = Provisional Authorisation; A = Authorisation

Approval date: 2015-04-16 **Expiry date**: 2020-04-15

Special conditions of the approval (if any): None

General conditions:

While this ethics approval is subject to all declarations, undertakings and agreements incorporated and signed in the application form, please note the following:

- *The project leader (principle investigator) must report in the prescribed format to the NWU-RERC:*
  - *annually (or as otherwise requested) on the progress of the project,*
  - *without any delay in case of any adverse event (or any matter that interrupts sound ethical principles) during the course of the project.*
- *The approval applies strictly to the protocol as stipulated in the application form. Would any changes to the protocol be deemed necessary during the course of the project, the project leader must apply for approval of these changes at the NWU-RERC. Would there be deviated from the project protocol without the necessary approval of such changes, the ethics approval is immediately and automatically forfeited.*
- *The date of approval indicates the first date that the project may be started. Would the project have to continue after the expiry date, a new application must be made to the NWU-RERC and new approval received before or on the expiry date.*
- *In the interest of ethical responsibility the NWU-RERC retains the right to:*
  - *request access to any information or data at any time during the course or after completion of the project;*
  - *withdraw or postpone approval if:*
    - *any unethical principles or practices of the project are revealed or suspected,*
    - *it becomes apparent that any relevant information was withheld from the NWU-RERC or that information has been false or misrepresented,*
    - *the required annual report and reporting of adverse events was not done timely and accurately,*
    - *new institutional rules, national legislation or international conventions deem it necessary.*

The Ethics Committee would like to remain at your service as scientist and researcher, and wishes you well with your project. Please do not hesitate to contact the Ethics Committee for any further enquiries or requests for assistance.

Yours sincerely

Linda du Plessis

Digitally signed by Linda du Plessis
DN: cn=Linda du Plessis, o=NWU, Vaal Triangle Campus, ou=Vice-Rector: Academic, email=linda.duplessis@nwu.ac.za, c=US
Date: 2015.04.20 20:35:13 +02'00'

Prof Linda du Plessis
Chair NWU Research Ethics Regulatory Committee (RERC)

Addendum B: *Ex vivo* transport data of Rhodamine-123, Lucifer Yellow and FITC-dextran (FD-4) across excised pig jejunum tissue and apparent permeability coefficient (P_{app}) values

Table B.1: Apical-to-basolateral cumulative percentage transport of Rhodamine-123 alone across excised pig jejunum tissue

Time (min)	Percentage transport: Chamber 1	Percentage transport: Chamber 2	Percentage transport: Chamber 3	Standard deviation	Mean percentage transport
0	0.00	0.00	0.00	0.00	0.00
20	0.03	0.05	0.03	0.01	0.04
40	0.05	0.08	0.06	0.01	0.07
60	0.08	0.10	0.11	0,01	0.10
80	0.10	0.13	0.14	0.02	0.12
100	0.16	0.17	0.17	0.01	0.17
120	0.19	0.22	0.20	0.01	0.20
P_{app} ($\times 10^{-7}$)	1.44	1.57	1.62	0.08	

Table B.2: Basolateral-to-apical cumulative percentage transport of Rhodamine-123 alone across excised pig jejunum tissue

Time (min)	Percentage transport: Chamber 1	Percentage transport: Chamber 2	Percentage transport: Chamber 3	Standard deviation	Mean percentage transport
0	0.00	0.00	0.00	0.00	0.00
20	0.40	0.64	0.45	0.10	0.49
40	0.52	0.78	0.55	0.12	0.62
60	0.54	0.83	0.58	0.13	0.65
80	0.64	0.88	0.64	0.11	0.72
100	0.79	0.93	0.68	0.10	0.80
120	0.89	0.85	0.70	0.08	0.81
P_{app} ($\times 10^{-7}$)	5.96	5.42	4.47	0.62	

Table B.3: Apical-to-basolateral cumulative percentage transport of Rhodamine-123 in the presence of 50 µM piperine across excised pig jejunum tissue

Time (min)	Percentage transport: Chamber 1	Percentage transport: Chamber 2	Percentage transport: Chamber 3	Standard deviation	Mean percentage transport
0	0.00	0.00	0.00	0.00	0.00
20	0.10	0.12	0.22	0.05	0.14
40	0.13	0.14	0.24	0.05	0.17
60	0.15	0.17	0.25	0.04	0.19
80	0.20	0.22	0.27	0.03	0.23
100	0.19	0.23	0.28	0,03	0.23
120	0.21	0.26	0.29	0,03	0.25
P_{app} ($\times 10^{-7}$)	1.48	1.79	1.69	0.13	

Table B.4: Basolateral-to-apical cumulative percentage transport of Rhodamine-123 in the presence of 50 µM Piperine across excised pig jejunum tissue

Time (min)	Percentage transport: Chamber 1	Percentage transport: Chamber 2	Percentage transport: Chamber 3	Standard deviation	Mean percentage transport
0	0.00	0.00	0.00	0.00	0.00
20	0.31	0.21	0.22	0.04	0.25
40	0.40	0.27	0.29	0.06	0.32
60	0.48	0.33	0.38	0.06	0.40
80	0.57	0.43	0.42	0.07	0.47
100	0.67	0.54	0.45	0.09	0.55
120	0.69	0.57	0.47	0.09	0.58
P_{app} ($\times 10^{-7}$)	4.95	4.24	3.33	0.67	

Table B.5: Apical-to-basolateral cumulative percentage transport of Rhodamine-123 in the presence of 100 µM Piperine across excised pig jejunum tissue

Time (min)	Percentage transport: Chamber 1	Percentage transport: Chamber 2	Percentage transport: Chamber 3	Standard deviation	Mean percentage transport
0	0.00	0.00	0.00	0.00	0.00
20	0.03	0.04	0.22	0.09	0.10
40	0.04	0.08	0.29	0.11	0.14
60	0.07	0.11	0.38	0.14	0.19
80	0.18	0.13	0.42	0.13	0.24
100	0.24	0.18	0.45	0.12	0.29
120	0.28	0.22	0.47	0.11	0.32
P_{app} ($\times 10^{-7}$)	2.39	1.64	1.56	0.38	

Table B.6: Basolateral-to-apical cumulative percentage transport of Rhodamine-123 in the presence of 100 µM Piperine across excised pig jejunum tissue

Time (min)	Percentage transport: Chamber 1	Percentage transport: Chamber 2	Percentage transport: Chamber 3	Standard deviation	Mean percentage transport
0	0.00	0.00	0.00	0.00	0.00
20	0.44	0.42	0.43	0.01	0.43
40	0.46	0.42	0.46	0.02	0.45
60	0.45	0.42	0.45	0.01	0.44
80	0.48	0.44	0.46	0.01	0.46
100	0.47	0.47	0.48	0.01	0.47
120	0.50	0.50	0.51	0.00	0.51
P_{app} ($\times 10^{-7}$)	2.67	2.71	2.75	0.03	

Table B.7: Apical-to-basolateral cumulative percentage transport of Rhodamine-123 in the presence of 200 µM Piperine across excised pig jejunum tissue

Time (min)	Percentage transport: Chamber 1	Percentage transport: Chamber 2	Percentage transport: Chamber 3	Standard deviation	Mean percentage transport
0	0.00	0.00	0.00	0.00	0.00
20	0.28	0.29	0.22	0.03	0.26
40	0.30	0.31	0.29	0.01	0.30
60	0.33	0.34	0.38	0.02	0.35
80	0.34	0.35	0.42	0.04	0.37
100	0.37	0.39	0.45	0.03	0.41
120	0.49	0.45	0.47	0.02	0.47
P_{app} ($\times 10^{-7}$)	2.83	2.68	3.06	0.16	

Table B.8: Basolateral-to-apical cumulative percentage transport of Rhodamine-123 in the presence of 200 µM Piperine across excised pig jejunum tissue

Time (min)	Percentage transport: Chamber 1	Percentage transport: Chamber 2	Percentage transport: Chamber 3	Standard deviation	Mean percentage transport
0	0.00	0.00	0.00	0.00	0.00
20	0.11	0.21	0.18	0.05	0.17
40	0.16	0.27	0.28	0.06	0.24
60	0.24	0.31	0.33	0.04	0.29
80	0.26	0.33	0.35	0.04	0.31
100	0.29	0.35	0.36	0.03	0.34
120	0.32	0.37	0.38	0.03	0.36
P_{app} ($\times 10^{-7}$)	2.42	2.39	2.65	0.11	

Table B.9: Apical-to-basolateral cumulative percentage transport of Rhodamine-123 in the presence of 50 µM capsaicin across excised pig jejunum tissue

Time (min)	Percentage transport: Chamber 1	Percentage transport: Chamber 2	Percentage transport: Chamber 3	Standard deviation	Mean percentage transport
0	0.00	0.00	0.00	0.00	0.00
20	0.11	0.05	0.03	0.03	0.06
40	0.14	0.11	0.05	0.04	0.10
60	0.20	0.16	0.08	0.05	0.15
80	0.32	0.25	0.19	0.06	0.26
100	0.41	0.41	0.35	0.03	0.39
120	0.52	0.59	0.51	0.03	0.54
P_{app} ($\times 10^{-7}$)	3.99	4.40	3.87	0.23	

Table B.10: Basolateral-to-apical cumulative percentage transport of Rhodamine-123 ithe presence of 50 µM Capsaicin across excised pig jejunum tissue

Time (min)	Percentage transport: Chamber 1	Percentage transport: Chamber 2	Percentage transport: Chamber 3	Standard deviation	Mean percentage transport
0	0.00	0.00	0.00	0.00	0.00
20	0.08	0.08	0.24	0.07	0.13
40	0.18	0.17	0.30	0.06	0.22
60	0.36	0.28	0.30	0.03	0.32
80	0.43	0.32	0.35	0.04	0.37
100	0.49	0.53	0.35	0.08	0.46
120	0.75	0.61	0.35	0.16	0.57
P_{app} ($\times 10^{-7}$)	5.58	4.84	2.22	1.43	

Table B.11: Apical-to-basolateral cumulative percentage transport of Rhodamine-123 in the presence of 100 µM Capsaicin across excised pig jejunum tissue

Time (min)	Percentage transport: Chamber 1	Percentage transport: Chamber 2	Percentage transport: Chamber 3	Standard deviation	Mean percentage transport
0	0.00	0.00	0.00	0.00	0.00
20	0.02	0.02	0.02	0.00	0.02
40	0.06	0.04	0.06	0.01	0.05
60	0.14	0.13	0.09	0.02	0.12
80	0.25	0.42	0.21	0.09	0.29
100	0.53	0.64	0.76	0.09	0.64
120	0.66	0.69	0.82	0.07	0.72
P_{app} ($\times 10^{-7}$)	5.30	6.20	6.83	0.63	

Table B.12: Basolateral-to-apical cumulative percentage transport of Rhodamine-123 in the presence of 100 µM Capsaicin across excised pig jejunum tissue

Time (min)	Percentage transport: Chamber 1	Percentage transport: Chamber 2	Percentage transport: Chamber 3	Standard deviation	Mean percentage transport
0	0.00	0.00	0.00	0.00	0.00
20	0.19	0.17	0.19	0.01	0.18
40	0.23	0.23	0.25	0.01	0.24
60	0.28	0.28	0.29	0.00	0.28
80	0.31	0.30	0.30	0.00	0.30
100	0.34	0.34	0.33	0.00	0.34
120	0.37	0.37	0.34	0.00	0.36
P_{app} ($\times 10^{-7}$)	2.52	2.50	2.29	0.01	

Table B.13: Apical-to-basolateral cumulative percentage transport of Rhodamine-123 in the presence of 200 µM Capsaicin across excised pig jejunum tissue

Time (min)	Percentage transport: Chamber 1	Percentage transport: Chamber 2	Percentage transport: Chamber 3	Standard deviation	Mean percentage transport
0	0.00	0.00	0.00	0.00	0.00
20	0.04	0.06	0.08	0.02	0.06
40	0.06	0.11	0.11	0.03	0.10
60	0.09	0.18	0.24	0.06	0.17
80	0.45	0.33	0.50	0.07	0.43
100	0.69	0.54	0.88	0.14	0.70
120	0.99	0.95	1.32	0.17	1.09
P_{app} ($\times 10^{-7}$)	7.82	6.71	9.93	1.34	

Table B.14: Basolateral-to-apical cumulative percentage transport of Rhodamine-123 in the presence of 200 µM Capsaicin across excised pig jejunum tissue

Time (min)	Percentage transport: Chamber 1	Percentage transport: Chamber 2	Percentage transport: Chamber 3	Standard deviation	Mean percentage transport
0	0.00	0.00	0.00	0.00	0.00
20	0.09	0.12	0.12	0.01	0.11
40	0.12	0.11	0.16	0.02	0.13
60	0.15	0.17	0.21	0.02	0.18
80	0.18	0.24	0.26	0.03	0.23
100	0.21	0.33	0.35	0.06	0.30
120	0.26	0.42	0.44	0.08	0.38
P_{app} ($\times 10^{-7}$)	1.84	3.05	3.16	0.60	

Table B.15: Apical-to-basolateral cumulative percentage transport of FITC-dextran (FD-4) alone across excised pig jejunum tissue

Time (min)	Percentage transport: Chamber 1	Percentage transport: Chamber 2	Percentage transport: Chamber 3	Standard deviation	Mean percentage transport
0	0.00	0.00	0.00	0.00	0.00
20	0.02	0.04	0.01	0.01	0.02
40	0.03	0.07	0.02	0.02	0.04
60	0.08	0.10	0.05	0.02	0.08
80	0.15	0.13	0.09	0.03	0.13
100	0.18	0.17	0.15	0.01	0.17
120	0.21	0.21	0.25	0.02	0.23
P_{app} ($\times 10^{-7}$)	1.85	1.62	1.83	0.11	

Table B.16: Apical-to-basolateral cumulative percentage transport of FITC-dextran (FD-4) in the presence of 50 µM Piperine across excised pig jejunum tissue

Time (min)	Percentage transport: Chamber 1	Percentage transport: Chamber 2	Percentage transport: Chamber 3	Standard deviation	Mean percentage transport
0	0.00	0.00	0.00	0.00	0.00
20	0.06	0.06	0.19	0.06	0.11
40	0.13	0.11	0.21	0.05	0.15
60	0.16	0.20	0.24	0.03	0.20
80	0.31	0.26	0.27	0.02	0.28
100	0.43	0.38	0.38	0,03	0.40
120	0.50	0.48	0.46	0.02	0.48
P_{app} ($\times 10^{-7}$)	4.04	3.71	3.04	0.42	

Table B.17: Apical-to-basolateral cumulative percentage transport of FITC-dextran (FD-4) in the presence of 100 µM Piperine across excised pig jejunum tissue

Time (min)	Percentage transport: Chamber 1	Percentage transport: Chamber 2	Percentage transport: Chamber 3	Standard deviation	Mean percentage transport
0	0.00	0.00	0.00	0.00	0.00
20	0.06	0.06	0.10	0.02	0.08
40	0.13	0.10	0.17	0.03	0.13
60	0.29	0.18	0.32	0.06	0.26
80	0.34	0.24	0.47	0.10	0.35
100	0.41	0.30	0.58	0.12	0.43
120	0.46	0.34	0.70	0.15	0,50
P_{app} ($\times 10^{-7}$)	3.80	2.72	5.60	1.19	

Table B.18: Apical-to-basolateral cumulative percentage transport of FITC-dextran (FD-4) in the presence of 200 µM Piperine across excised pig jejunum tissue

Time (min)	Percentage transport: Chamber 1	Percentage transport: Chamber 2	Percentage transport: Chamber 3	Standard deviation	Mean percentage transport
0	0.00	0.00	0.00	0.00	0.00
20	0.39	0.31	0.49	0.08	0.40
40	0.44	0.36	0.65	0.12	0.48
60	0.46	0.39	0.68	0.13	0.51
80	0.51	0.46	0.70	0.10	0.56
100	0.58	0.47	0.76	0.12	0.60
120	0.65	0.66	0.83	0.08	0.71
P_{app} ($\times 10^{-7}$)	4.01	4.04	5.13	0.52	

Table B.19: Apical-to-basolateral cumulative percentage transport of FITC-dextran (FD-4) in the presence of 50 µM Capsaicin across excised pig jejunum tissue

Time (min)	Percentage transport: Chamber 1	Percentage transport: Chamber 2	Percentage transport: Chamber 3	Standard deviation	Mean percentage transport
0	0.00	0.00	0.00	0.00	0.00
20	0.14	0.10	0,05	0.04	0.09
40	0.17	0.15	0.07	0.04	0.13
60	0.18	0.16	0.12	0.03	0.15
80	0.20	0.20	0.17	0.02	0.19
100	0.22	0.23	0.23	0.01	0.23
120	0.23	0.22	0.29	0.03	0.25
P_{app} ($\times 10^{-7}$)	1.51	1.65	2.21	0.30	

Table B.20: Apical-to-basolateral cumulative percentage transport of FITC-dextran (FD-4) in the presence of 100 µM Capsaicin across excised pig jejunum tissue

Time (min)	Percentage transport: Chamber 1	Percentage transport: Chamber 2	Percentage transport: Chamber 3	Standard deviation	Mean percentage transport
0	0.00	0.00	0.00	0.00	0.00
20	0.04	0.04	0.08	0.02	0.05
40	0.06	0.05	0.10	0.02	0.07
60	0.08	0.09	0.12	0.02	0.10
80	0.12	0.14	0.17	0.02	0.14
100	0.16	0.20	0.21	0.02	0.19
120	0.24	0.27	0.30	0.02	0.27
P_{app} ($\times 10^{-7}$)	1.74	2.00	2.05	0.14	

Table B.21: Apical-to-basolateral cumulative percentage transport of FITC-dextran (FD-4) in the presence of 200 µM Capsaicin across excised pig jejunum tissue

Time (min)	Percentage transport: Chamber 1	Percentage transport: Chamber 2	Percentage transport: Chamber 3	Standard deviation	Mean percentage transport
0	0.00	0.00	0.00	0.00	0.00
20	0.04	0.02	0.02	0.01	0.03
40	0.06	0.04	0.04	0.01	0.05
60	0.08	0.07	0.07	0.01	0.08
80	0.13	0.12	0.12	0.01	0.12
100	0.19	0.19	0.17	0.01	0.18
120	0.26	0.23	0.24	0.01	0.25
P_{app} ($\times 10^{-7}$)	1.92	1.86	1.86	0.03	

Table B.22: Apical-to-basolateral cumulative percentage transport of Lucifer Yellow alone across excised pig jejunum tissue

Time (min)	Percentage transport: Chamber 1	Percentage transport: Chamber 2	Percentage transport: Chamber 3	Standard deviation	Mean percentage transport
0	0.00	0.00	0.00	0.00	0.00
20	0.31	0.45	0.34	0.06	0.37
40	0.43	0.53	0.42	0.05	0.46
60	0.50	0.63	0.51	0.06	0.55
80	0.59	0.68	0.59	0.04	0.62
100	0.72	0.71	0.71	0.00	0.72
120	0.73	0.77	0.82	0.04	0.77
P_{app} ($\times 10^{-7}$)	5.28	4.95	5.67	0.29	

Table B.23: Apical-to-basolateral cumulative percentage transport of Lucifer Yellow containing 4% ethanol across excised pig jejunum tissue

Time (min)	Percentage transport: Chamber 1	Percentage transport: Chamber 2	Percentage transport: Chamber 3	Standard deviation	Mean percentage transport
0	0.00	0.00	0.00	0.00	0.00
20	0.24	0.32	0.25	0.04	0.27
40	0.38	0.48	0.39	0.05	0.42
60	0.47	0.62	0.53	0.06	0.54
80	0.56	0.68	0.60	0.05	0.61
100	0.65	0.69	0.66	0.02	0.67
120	0.74	0.71	0.72	0.02	0.74
P_{app} ($\times 10^{-7}$)	5.41	5.38	5.36	0.02	

Addendum C: Efflux ratios of Rhodamine 123

Table C.1: Apparent permeability (P_{app}) values and efflux ratios for piperine at selected test concentrations

Concentration (μM)	Transport direction	P_{app} ($\times 10^{-7}$)	Average P_{app} ($\times 10^{-7}$)	Efflux ratio
50	**Apical-to-basolateral**	1.48	1.65	2.52
		1.79		
		1.69		
	Basolateral-to-apical	4.95	4.17	
		4.24		
		3.33		
100	**Apical-to-basolateral**	2.39	1.86	1.43
		1.64		
		1.56		
	Basolateral-to-apical	2.67	2.67	
		2.67		
		2.67		
200	**Apical-to-basolateral**	2.83	2.86	0.87
		2.68		
		3.06		
	Basolateral-to-apical	2.42	2.49	
		2.39		
		2.65		

Table C.2: Apparent permeability (P_{app}) values and efflux ratios for capsaicin at selected test concentrations

Concentration (μM)	Transport direction	P_{app} ($\times 10^{-7}$)	Average P_{app} ($\times 10^{-7}$)	Efflux ratio
50	**Apical-to-basolateral**	3.99	4.06	0.61
		4.40		
		3.87		
	Basolateral-to-apical	2.42	2.49	
		2.39		
		2.65		
100	**Apical-to-basolateral**	5.30	6.11	0.40
		6.20		
		6.83		
	Basolateral-to-apical	2.52	2.44	
		2.50		
		2.29		
200	**Apical-to-basolateral**	7.82	8.15	0.33
		6.71		
		9.93		
	Basolateral-to-apical	1.84	2.68	
		3.05		
		3.16		

Addendum D: Trans-Epithelial electrical resistance (TEER) measurements

Table D.1: Apical-to-basolateral TEER measurements across excised pig jejunum in the presence of Rhodamine-123 alone

	TEER (KΩ)			
Time (min)	**Chamber 1**	**Chamber 2**	**Chamber 3**	**Average**
0	33.00	35.00	35.00	34.33
20	33.00	35.00	32.00	33.33
40	34.00	32.00	37.00	34.33
60	33.00	35.00	35.00	34.33
80	33.00	34.00	32.00	33.00
100	33.00	34.00	34.00	33.67
120	32.00	33.00	34.00	33.00
% Change in TEER T_0 to T_{120}	96.97	94.29	97.14	96.13

Table D.2: Basolateral-to-apical TEER measurements across excised pig jejunum in the presence of Rhodamine-123 alone

	TEER (KΩ)			
Time (min)	**Chamber 1**	**Chamber 2**	**Chamber 3**	**Average**
0	44.00	49.00	49.00	47.33
20	42.00	48.00	49.00	46.33
40	43.00	49.00	48.00	46.67
60	45.00	48.00	49.00	47.33
80	46.00	49.00	48.00	47.67
100	44.00	48.00	47.00	46.33
120	42.00	47.00	47.00	45.33
% Change in TEER T_0 to T_{120}	95.46	95.92	95.92	95.76

Table D.3: Apical-to-basolateral TEER measurements across excised pig jejunum in the presence of Rhodamine-123 and 50 µM piperine

	TEER (KΩ)			
Time (min)	**Chamber 1**	**Chamber 2**	**Chamber 3**	**Average**
0	58.00	66.00	59.00	61.00
20	56.00	64.00	61.00	60.33
40	56.00	66.00	57.00	59.67
60	59.00	58.00	57.00	58.00
80	59.00	65.00	57.00	60.33
100	59.00	64.00	57.00	60.00
120	55.00	63.00	58.00	58.67
% Change in TEER T_0 to T_{120}	94.83	95.46	98.31	96.20

Table D.4: Basolateral-to-apical TEER measurements across excised pig jejunum in the presence of Rhodamine-123 and 50 µM piperine

	TEER (KΩ)			
Time (min)	**Chamber 1**	**Chamber 2**	**Chamber 3**	**Average**
0	51.00	50.00	51.00	50.67
20	51.00	51.00	51.00	51.00
40	51.00	50.00	51.00	50.67
60	51.00	49.00	48.00	49.33
80	50.00	50.00	51.00	50.33
100	51.00	51.00	50.00	50.67
120	48.00	48.00	50.00	48.67
% Change in TEER T_0 to T_{120}	94.12	96.00	98.04	96.05

Table D.5: Apical-to-basolateral TEER measurements across excised pig jejunum in the presence of Rhodamine-123 and 100 µM piperine

	TEER (KΩ)			
Time (min)	**Chamber 1**	**Chamber 2**	**Chamber 3**	**Average**
0	42.00	42.00	41.00	41.67
20	42.00	41.00	41.00	41.33
40	41.00	41.00	41.00	41.00
60	41.00	39.00	41.00	40.33
80	41.00	40.00	39.00	40.00
100	42.00	41.00	39.00	40.67
120	40.00	39.00	37.00	38.67
% Change in TEER T_0 to T_{120}	95.24	92.86	90.24	92.78

Table D.6: Basolateral-to-apical TEER measurements across excised pig jejunum in the presence of Rhodamine-123 and 100 µM piperine

	TEER (KΩ)			
Time (min)	**Chamber 1**	**Chamber 2**	**Chamber 3**	**Average**
0	63.00	60.00	57.00	60.00
20	60.00	62.00	58.00	60.00
40	61.00	61.00	56.00	59.33
60	65.00	59.00	55.00	59.67
80	60.00	59.00	55.00	58.00
100	60.00	58.00	53.00	57.00
120	59.00	56.00	52.00	55.67
% Change in TEER T_0 to T_{120}	93.65	93.33	91.23	92.74

Table D.7: Apical-to-basolateral TEER measurements across excised pig jejunum in the presence of Rhodamine-123 and 200 µM piperine

	TEER (KΩ)			
Time (min)	**Chamber 1**	**Chamber 2**	**Chamber 3**	**Average**
0	35.00	35.00	36.00	35.33
20	34.00	34.00	35.00	34.33
40	33.00	32.00	33.00	32.67
60	33.00	32.00	32.00	32.33
80	32.00	31.00	31.00	31.33
100	33.00	31.00	32.00	32.00
120	32.00	31.00	32.00	31.67
% Change in TEER T_0 to T_{120}	91.43	88.57	88.89	89.63

Table D.8: Basolateral-to-apical TEER measurements across excised pig jejunum in the presence of Rhodamine-123 and 200 µM piperine

	TEER (KΩ)			
Time (min)	**Chamber 1**	**Chamber 2**	**Chamber 3**	**Average**
0	34.00	32.00	34.00	33.33
20	34.00	31.00	35.00	33.33
40	33.00	32.00	35.00	33.33
60	32.00	32.00	34.00	32.67
80	33.00	33.00	33.00	33.00
100	32.00	30.00	32.00	31.33
120	30.00	29.00	30.00	29.67
% Change in TEER T_0 to T_{120}	88.24	90.63	88.24	89.03

Table D.9: Apical-to-basolateral TEER measurements across excised pig jejunum in the presence of Rhodamine-123 and 50 µM capsaicin

	TEER (KΩ)			
Time (min)	**Chamber 1**	**Chamber 2**	**Chamber 3**	**Average**
0	39.00	47.00	40.00	42.00
20	39.00	47.00	40.00	42.00
40	40.00	45.00	41.00	42.00
60	38.00	48.00	41.00	42.33
80	38.00	47.00	40.00	41.67
100	39.00	46.00	41.00	42.00
120	40.00	43.00	40.00	41.00
% Change in TEER T_0 to T_{120}	102.56	91.49	100.00	98.02

Table D.10: Basolateral-to-apical TEER measurements across excised pig jejunum in the presence of Rhodamine-123 and 50 µM capsaicin

	TEER (KΩ)			
Time (min)	**Chamber 1**	**Chamber 2**	**Chamber 3**	**Average**
0	59.00	43.00	44.00	48.67
20	56.00	43.00	45.00	48.00
40	52.00	44.00	46.00	47.33
60	56.00	46.00	46.00	49.33
80	57.00	46.00	44.00	49.00
100	59.00	46.00	45.00	50.00
120	57.00	43.00	43.00	47.67
% Change in TEER T_0 to T_{120}	96.61	100.00	97.73	98.11

Table D.11: Apical-to-basolateral TEER measurements across excised pig jejunum in the presence of Rhodamine-123 and 100 µM capsaicin

	TEER (KΩ)			
Time (min)	**Chamber 1**	**Chamber 2**	**Chamber 3**	**Average**
0	40.00	48.00	47.00	45.00
20	40.00	48.00	47.00	45.00
40	40.00	48.00	48.00	45.33
60	40.00	47.00	46.00	44.33
80	40.00	44.00	46.00	43.33
100	39.00	44.00	45.00	42.67
120	39.00	47.00	44.00	43.33
% Change in TEER T_0 to T_{120}	97.50	97.92	93.62	96.35

Table D.12: Basolateral-to-apical TEER measurements across excised pig jejunum in the presence of Rhodamine-123 and 100 µM capsaicin

	TEER (KΩ)			
Time (min)	**Chamber 1**	**Chamber 2**	**Chamber 3**	**Average**
0	44.00	38.00	43.00	41.67
20	43.00	38.00	43.00	41.33
40	43.00	39.00	44.00	42.00
60	43.00	39.00	44.00	42,00
80	44.00	38.00	43.00	41.67
100	44.00	38.00	44.00	42.00
120	43.00	37.00	41.00	40.33
% Change in TEER T_0 to T_{120}	97.73	97.37	95.35	96.82

Table D.13: Apical-to-basolateral TEER measurements across excised pig jejunum in the presence of Rhodamine-123 and 200 µM capsaicin

	TEER (KΩ)			
Time (min)	**Chamber 1**	**Chamber 2**	**Chamber 3**	**Average**
0	41.00	51.00	55.00	49.00
20	42.00	50.00	55.00	49.00
40	41.00	52.00	53.00	48.67
60	42.00	52.00	53.00	49.00
80	41.00	53.00	55.00	49.67
100	43.00	51.00	57.00	50.33
120	40.00	49.00	54.00	47.67
% Change in TEER T_0 to T_{120}	97.56	96.08	98.18	97.27

Table D.14: Basolateral-to-apical TEER measurements across excised pig jejunum in the presence of Rhodamine-123 and 200 µM capsaicin

	TEER (KΩ)			
Time (min)	**Chamber 1**	**Chamber 2**	**Chamber 3**	**Average**
0	36.00	39.00	34.00	36.33
20	36.00	38.00	33.00	35.67
40	37.00	37.00	34.00	36.00
60	35.00	40.00	33.00	36.00
80	37.00	38.00	35.00	36.67
100	36.00	39.00	35.00	36.67
120	37.00	38.00	34.00	36.33
% Change in TEER T_0 to T_{120}	102.78	97.44	100.00	100.07

Table D.15: Apical-to-basolateral TEER measurements across excised pig jejunum in the presence of FITC-dextran (FD-4) alone

	TEER (KΩ)			
Time (min)	**Chamber 1**	**Chamber 2**	**Chamber 3**	**Average**
0	35.00	34.00	33.00	34.00
20	35.00	35.00	33.00	34.33
40	35.00	34.00	31.00	33.33
60	35.00	34.00	31.00	33.33
80	35.00	35.00	32.00	34.00
100	36.00	34.00	33.00	34.33
120	33.00	33.00	32.00	32.67
% Change in TEER T_0 to T_{120}	94.29	97.06	96.97	96.11

Table D.16: Apical-to-basolateral TEER measurements across excised pig jejunum in the presence of FITC-dextran (FD-4) and 50 µM piperine

	TEER (KΩ)			
Time (min)	**Chamber 1**	**Chamber 2**	**Chamber 3**	**Average**
0	37.00	34.00	35.00	35.33
20	37.00	33.00	34.00	34.67
40	37.00	33.00	34.00	34.67
60	36.00	33.00	34.00	34.33
80	35.00	32.00	36.00	34.33
100	33.00	32.00	34.00	33.00
120	33.00	32.00	31.00	32.00
% Change in TEER T_0 to T_{120}	89.19	94.12	88.57	90.63

Table D.17: Apical-to-basolateral TEER measurements across excised pig jejunum in the presence of FITC-dextran (FD-4) and 100 µM piperine

	TEER (KΩ)			
Time (min)	**Chamber 1**	**Chamber 2**	**Chamber 3**	**Average**
0	40.00	44.00	45.00	43.00
20	39.00	44.00	44.00	42.33
40	39.00	42.00	44.00	41.67
60	36.00	34.00	42.00	37.33
80	33.00	36.00	39.00	36.00
100	32.00	35.00	37.00	34.67
120	33.00	36.00	38.00	35.67
% Change in TEER T_0 to T_{120}	82.50	81.82	84.44	82.92

Table D.18: Apical-to-basolateral TEER measurements across excised pig jejunum in the presence of FITC-dextran (FD-4) and 200 µM piperine

	TEER (KΩ)			
Time (min)	**Chamber 1**	**Chamber 2**	**Chamber 3**	**Average**
0	61.00	47.00	47.00	51.67
20	59.00	43.00	42.00	48.00
40	58.00	42.00	43.00	47.67
60	57.00	41.00	41.00	46.33
80	56.00	38.00	39.00	44.33
100	56.00	40.00	39.00	45.00
120	53.00	37.00	37.00	42.33
% Change in TEER T_0 to T_{120}	86.89	78.72	78.72	81.44

Table D.19: Apical-to-basolateral TEER measurements across excised pig jejunum in the presence of FITC-dextran (FD-4) and 50 µM capsaicin

	TEER (KΩ)			
Time (min)	**Chamber 1**	**Chamber 2**	**Chamber 3**	**Average**
0	41.00	38.00	41.00	40.00
20	42.00	37.00	41.00	40.00
40	42.00	39.00	40.00	40.33
60	42.00	37.00	42.00	40.33
80	40.00	39.00	41.00	40.00
100	42.00	36.00	41.00	39.67
120	40.00	37.00	40.00	39.00
% Change in TEER T_0 to T_{120}	97.56	97.37	97.56	97.50

Table D.20: Apical-to-basolateral TEER measurements across excised pig jejunum in the presence of FITC-dextran (FD-4) and 100 µM capsaicin

	TEER (KΩ)			
Time (min)	**Chamber 1**	**Chamber 2**	**Chamber 3**	**Average**
0	31.00	35.00	35.00	33.67
20	32.00	35.00	36.00	34.33
40	30.00	34.00	35.00	33.00
60	32.00	34.00	36.00	34.00
80	30.00	36.00	33.00	33.00
100	31.00	35.00	36.00	34.00
120	30.00	34.00	34.00	32.67
% Change in TEER T_0 to T_{120}	96.77	97.14	97.14	97.02

Table D.21: Apical-to-basolateral TEER measurements across excised pig jejunum in the presence of FITC-dextran (FD-4) and 200 µM capsaicin

	TEER (KΩ)			
Time (min)	**Chamber 1**	**Chamber 2**	**Chamber 3**	**Average**
0	32.00	31.00	35.00	32.67
20	34.00	31.00	33.00	32.67
40	30.00	30.00	34.00	31.33
60	35.00	31.00	36.00	34.00
80	33.00	31.00	32.00	32.00
100	31.00	31.00	34.00	32.00
120	31.00	30.00	35.00	32.00
% Change in TEER T_0 to T_{120}	96.88	96.77	100.00	97.88

Table D.22: Apical-to-basolateral TEER measurements across excised pig jejunum in the presence of Lucifer Yellow alone

	TEER (KΩ)			
Time (min)	**Chamber 1**	**Chamber 2**	**Chamber 3**	**Average**
0	36.00	34.00	40.00	36.67
20	36.00	34.00	39.00	36.33
40	37.00	34.00	40.00	37.00
60	36.00	33.00	40.00	36.33
80	37.00	33.00	40.00	36.67
100	36.00	33.00	40.00	36.33
120	36.00	33.00	39.00	36.00
% Change in TEER T_0 to T_{120}	100.00	97.06	97.50	98.19

Table D.23: Apical-to-basolateral TEER measurements across excised pig jejunum in the presence of Lucifer Yellow containing 4% ethanol

	TEER (KΩ)			
Time (min)	**Chamber 1**	**Chamber 2**	**Chamber 3**	**Average**
0	35.00	38.00	38.00	37.00
20	33.00	39.00	37.00	36.33
40	35.00	39.00	38.00	37.33
60	36.00	39.00	38.00	37.67
80	35.00	38.00	39.00	37.33
100	35.00	38.00	38.00	37.00
120	34.00	38.00	37.00	36.33
% Change in TEER T_0 to T_{120}	97.14	100.00	97.37	98.17

Addendum E: Statistical Analysis

Table E.1: Statistical analysis results of the transport data for the Kruskal-Wallis test: Comparison of FD-4 transport in the presence of capsaicin with the control group (FD-4 alone)

	Multiple Comparisons p values (2-tailed); Capsaicin+FD (VNiekerk_Papp_FD) Independent (grouping) variable: Var1 Kruskal-Wallis test: H (3, N= 12) =2.692308 p =.4415			
Depend.: Capsaicin+FD	Control R:4.3333	50 µM R:5.3333	100 µM R:8.3333	200 µM R:8.0000
Control		1.000000	1.000000	1.000000
50 µM	1.000000		1.000000	1.000000
100 µM	1.000000	1.000000		1.000000
200 µM	1.000000	1.000000	1.000000	

Table E.2: Statistical analysis results of the transport data for the Kruskal-Wallis test: Comparison of FD-4 transport in the presence of piperine with the control group (FD-4 alone)

	Multiple Comparisons p values (2-tailed); Piperine+FD (VNiekerk_Papp_FD) Independent (grouping) variable: Var1 Kruskal-Wallis test: H (3, N= 12) =6.897436 p =.0752			
Depend.: Piperine+FD	Control R:2.0000	50 µM R:7.0000	100 µM R:7.6667	200 µM R:9.3333
Control		0.536576	0.325473	0.076428
50 µM	0.536576		1.000000	1.000000
100 µM	0.325473	1.000000		1.000000
200 µM	0.076428	1.000000	1.000000	

Table E.3: Statistical analysis results of the transport data for the Kruskal-Wallis test: Comparison of RH-123 transport in the presence of piperine in the apical-to-basolateral direction with the control group (RH-123 alone)

	Multiple Comparisons p values (2-tailed); Piperine+R123 (A-B) (VNiekerk_Papp_R123) Independent (grouping) variable: Var1 Kruskal-Wallis test: H (3, N= 12) =7.205128 p =.0656			
Depend.: Piperine+R123 (A-B)	Control R:3.3333	50 µM R:5.6667	100 µM R:6.0000	200 µM R:11.000
Control		1.000000	1.000000	0.055247
50 µM	1.000000		1.000000	0.420248
100 µM	1.000000	1.000000		0.536576
200 µM	0.055247	0.420248	0.536576	

Table E.4: Statistical analysis results of the transport data for the Kruskal-Wallis test: Comparison of RH-123 transport in the presence of piperine in the basolateral-to-apical direction with the control group (RH-123 alone)

	Multiple Comparisons p values (2-tailed); Piperine+R123 (B-A) (VNiekerk_Papp_R123) Independent (grouping) variable: Var1 Kruskal-Wallis test: H (3, N= 12) =9.974359 p =.0188			
Depend.: Piperine+R123 (B-A)	Control R:10.667	50 µM R:8.3333	100 µM R:5.0000	200 µM R:2.0000
Control		1.000000	0.325473	0.019445
50 µM	1.000000		1.000000	0.188703
100 µM	0.325473	1.000000		1.000000
200 µM	0.019445	0.188703	1.000000	

Table E.5: Statistical analysis results of the transport data for the Kruskal-Wallis test: Comparison of RH-123 transport in the presence of capsaicin in the apical-to-basolateral direction with the control group (RH-123 alone)

	Multiple Comparisons p values (2-tailed); Capsaicin+R123 (A-B) (VNiekerk_Papp_R123) Independent (grouping) variable: Var1 Kruskal-Wallis test: H (3, N= 12) =9.974359 p =.0188			
Depend.: Capsaicin+R123 (A-B)	Control R:2.0000	50 µM R:5.0000	100 µM R:8.3333	200 µM R:10.667
Control		1.000000	0.188703	0.019445
50 µM	1.000000		1.000000	0.325473
100 µM	0.188703	1.000000		1.000000
200 µM	0.019445	0.325473	1.000000	

Table E.6: Statistical analysis results of the transport data for the Kruskal-Wallis test: Comparison of RH-123 transport in the presence of capsaicin in the basolateral-to-apical direction with the control group (RH-123 alone)

	Multiple Comparisons p values (2-tailed); Capsaicin+R123 (B-A) (VNiekerk_Papp_R123) Independent (grouping) variable: Var1 Kruskal-Wallis test: H (3, N= 12) =5.205128 p =.1574			
Depend.: Capsaicin+R123 (B-A)	Control R:10.000	50 µM R:7.3333	100 µM R:4.0000	200 µM R:4.6667
Control		1.000000	0.249240	0.420248
50 µM	1.000000		1.000000	1.000000
100 µM	0.249240	1.000000		1.000000
200 µM	0.420248	1.000000	1.000000	

References

Aguilar, M., Morrell, P.L., Roose, M.L. & Kim, S.-C. 2009. Genetic Diversity and Structure in Semiwild and Domesticated Chiles (*Capsicum annuum*; Solanaceae) from Mexico. *American Journal of Botany*, 96(6):1190-1202.

Ahmad, A., Othman, I., Zaini, A. & Chowdhury, E. 2014. Oral nano-insulin therapy: Current progress on nanoparticle-based devices for intestinal epithelium-targeted insulin delivery. *Journal of Nanomedicine & Nanotecnology*, 4:1-10.

Ahmad, N., Fazal, H., Abbasi, B.H., Farooq, S., Ali, M. & Khan, M.A. 2012. Biological role of *Piper nigrum* L.(Black pepper): A review. *Asian Pacific Journal of Tropical Biomedicine*, 2(3):1945-1953.

Ajazuddin, A., Qureshi, A., Kumari, L., Vaishnav, P., Sharma, M., Saraf, S. & Saraf, S. 2014. Role of herbal bioactives as a potential bioavailability enhancer for active pharmaceutical ingredients. *Fitoterapia*, 97:1-14.

Akyuz, L., Kaya, M., Mujtaba, M., Ilk, S., Sargin, I., Salaberria, A.M., Labidi, J., Cakmak, Y.S. & Islek, C. 2018. Supplementing capsaicin with chitosan-based films enhanced the anti-quorum sensing, antimicrobial, antioxidant, transparency, elasticity and hydrophobicity. *International Journal of Biological Macromolecules*, 115:438-446.

Alomrani, A.H., Alhazza, F.I., AlGhamdi, K.M. & El Maghraby, G.M. 2018. Effect of neat and binary vehicle systems on the solubility and cutaneous delivery of piperine. *Saudi Pharmaceutical Journal*, 26(2):162-168.

Amidon, S., Brown, J.E. & Dave, V.S. 2015. Colon-targeted oral drug delivery systems: design trends and approaches. *The American Association of Pharmaceutical Scientists Journal* 16(4):731-741.

Anilkumar, P., Badarinath, A., Naveen, N., Prasad, K., Reddy, B.R.S., Hyndhavi, M. & Nirosha, M. 2011. A rationalized description on study of intestinal barrier, drug permeability and permeation enhancers. *Journal of Global Trends in Pharmaceutical Sciences*, 2(4):431-449.

Antunes, F., Andrade, F., Ferreira, D., Morck Nielsen, H. & Sarmento, B. 2013. Models to predict intestinal absorption of therapeutic peptides and proteins. *Current Drug Metabolism*, 14(1):4-20.

Arora, R., Gill, N., Chauhan, G. & Rana, A. 2011. An overview about versatile molecule capsaicin. *International Journal of Pharmaceutical Sciences and Drug Research*, 3(4):280-286.

Artursson, P. & Knight, S.D. 2015. Breaking the intestinal barrier to deliver drugs. *Science*, 347(6223):716-717.

Assunção, R., Ferreira, M., Martins, C., Diaz, I., Padilla, B., Dupont, D., Bragança, M. & Alvito, P. 2014. Applicability of *in vitro* methods to study patulin bioaccessibility and its effects on intestinal membrane integrity. *Journal of Toxicology and Environmental Health, Part A*, 77(14-16):983-992.

Atlabachew, M., Combrinck, S., Viljoen, A.M., Hamman, J.H. & Gouws, C. 2016. Isolation and in vitro permeation of phenylpropylamino alkaloids from Khat (*Catha edulis*) across oral and intestinal mucosal tissues. *Journal of Ethnopharmacology*, 194:307-315.

Aucamp, M., Odendaal, R., Liebenberg, W. & Hamman, J. 2015. Amorphous azithromycin with improved aqueous solubility and intestinal membrane permeability. *Drug Development and Industrial Pharmacy*, 41(7):1100-1108.

Balimane, P.V., Chong, S. & Morrison, R.A. 2000. Current methodologies used for evaluation of intestinal permeability and absorption. *Journal of Pharmacological and Toxicological Methods*, 44(1):301-312.

Barceloux, D.G. 2009. Pepper and Capsaicin (Capsicum and Piper Species). *Medical Toxicology of Natural Substances: Foods, Fungi, Medicinal Herbs, Toxic Plants, and Venomous Animals*, 55(6):380-390.

Bhushani, J.A., Karthik, P. & Anandharamakrishnan, C. 2016. Nanoemulsion based delivery system for improved bioaccessibility and Caco-2 cell monolayer permeability of green tea catechins. *Food Hydrocolloids*, 56:372-382.

Billat, P.-A., Roger, E., Faure, S. & Lagarce, F. 2017. Models for drug absorption from the small intestine: where are we and where are we going? *Drug Discovery Today*, 22(5):761-775.

Bohdanowicz, M. & Grinstein, S. 2013. Role of phospholipids in endocytosis, phagocytosis, and macropinocytosis. *Physiological Reviews*, 93(1):69-106.

Bohets, H., Annaert, P., Mannens, G., Anciaux, K., Verboven, P., Meuldermans, W. & Lavrijsen, K. 2001. Strategies for absorption screening in drug discovery and development. *Current Topics in Medicinal Chemistry*, 1(5):367-383.

Brayden, D.J. & Mrsny, R.J. 2011. Oral peptide delivery: prioritizing the leading technologies. *Therapeutic Delivery*, 2(12):1567-1573.

Bruno, B.J., Miller, G.D. & Lim, C.S. 2013. Basics and recent advances in peptide and protein drug delivery. *Therapeutic Delivery*, 4(11):1443-1467.

Carsten, C.P., Fano, M., Saaby, L., Yang, M., Mørck, N.H. & Mu, H. 2015. Characterization of particulate drug delivery systems for oral delivery of peptide and protein drugs. *Current Pharmaceutical Design*, 21(19):2611-2628.

Cefalu, W.T. 2004. Concept, strategies, and feasibility of noninvasive insulin delivery. *Diabetes Care*, 27(1):239-246.

Challa, T., Vynala, V. & Allam, K.V. 2011. Colon specific drug delivery systems: a review on primary and novel approaches. *International Journal of Pharmaceutical Sciences Review and Research*, 7(2):171-181.

Chang, C.L., Lin, Y., Bartolome, A.P., Chen, Y.-C., Chiu, S.-C. & Yang, W.-C. 2013. Herbal therapies for type 2 diabetes mellitus: chemistry, biology, and potential application of selected plants and compounds. *Evidence-Based Complementary and Alternative Medicine*, 2013.

Che, C.-T., Wang, Z.J., Chow, M.S.S. & Lam, C.W.K. 2013. Herb-herb combination for therapeutic enhancement and advancement: theory, practice and future perspectives. *Molecules*, 18(5):5125-5141.

Chen, R., Khormaee, S., Eccleston, M.E. & Slater, N.K. 2009a. The role of hydrophobic amino acid grafts in the enhancement of membrane-disruptive activity of pH-responsive pseudo-peptides. *Biomaterials*, 30(10):1954-1961.

Chen, W., Lu, Z., Viljoen, A. & Hamman, J. 2009b. Intestinal drug transport enhancement by *Aloe vera*. *Planta Medica*, 75(06):587-595.

Chhabra, N., Aseri, M., Goyal, V. & Sankhla, S. 2012. Capsaicin: A promising therapy-A critical reappraisal. *International Journal of Nutrition, Pharmacology, Neurological Diseases*, 2(1):8.

Chongsiriwatana, N.P., Patch, J.A., Czyzewski, A.M., Dohm, M.T., Ivankin, A., Gidalevitz, D., Zuckermann, R.N. & Barron, A.E. 2008. Peptoids that mimic the structure, function, and mechanism of helical antimicrobial peptides. *Proceedings of the National Academy of Sciences*, 105(8):2794-2799.

Choonara, B.F., Choonara, Y.E., Kumar, P., Bijukumar, D., Du Toit, L.C. & Pillay, V. 2014. A review of advanced oral drug delivery technologies facilitating the protection and absorption of protein and peptide molecules. *Biotechnology Advances*, 32(7):1269-1282.

Chopra, B., Dhingra, A.K., Kapoor, R.P. & Prasad, D.N. 2016. Piperine and its various physicochemical and biological aspects: A Review. *Open Chemistry Journal*, 3(1):75-96.

Csilléry, G. 2006. Pepper taxonomy and the botanical description of the species. *Acta Agronomica Hungarica*, 54(2):151-166.

Damanhouri, Z.A. & Ahmad, A. 2014. A review on therapeutic potential of *Piper nigrum* L. (Black Pepper): The king of spices. *Medicinal & Aromatic Plants*, 3(161):1-6.

De Sousa Falcão, H., Leite, J.A., Barbosa-Filho, J.M., de Athayde-Filho, P.F., de Oliveira Chaves, M.C., Moura, M.D., Ferreira, A.L., De Almeida, A.B.A., Souza-Brito, A.R.M. & De Fátima Formiga Melo Diniz, M. 2008. Gastric and duodenal antiulcer activity of alkaloids: A review. *Molecules*, 13(12):3198-3223.

Depani, J.A., Chaudhary, A.B., Bhadani, S.M. & Patel, B.D. 2018. Development and validation of RP-HPLC method for simultaneous estimation of bimatoprost and timolol mealeate. *World Journal of Pharmacy and Pharmaceutical Science*, 7(5):741-750.

Derry, S., Lloyd, R., Moore, R.A. & McQuay, H.J. 2009. Topical capsaicin for chronic neuropathic pain in adults. *Europe PMC Funders Author Manuscripts*(4):1-39.

Di, L. 2015. Strategic approaches to optimizing peptide ADME properties. *The American Association of Pharmaceutical Scientists Journal*, 17(1):134-143.

Di, X., Wang, X., Di, X. & Liu, Y. 2015. Effect of piperine on the bioavailability and pharmacokinetics of emodin in rats. *Journal of Pharmaceutical and Biomedical Analysis*, 115:144-149.

Du Toit, T., Malan, M.M., Lemmer, H.J.R., Gouws, C., Aucamp, M.E., Breytenbach, W.J. & Hamman, J.H. 2016. Combining chemical permeation enhancers for synergistic effects. *European Journal of Drug Metabolism and Pharmacokinetics*, 41(5):575-586.

Dudhatra, G.B., Mody, S.K., Awale, M.M., Patel, H.B., Modi, C.M., Kumar, A., Kamani, D.R. & Chauhan, B.N. 2012. A comprehensive review on pharmacotherapeutics of herbal bioenhancers. *The Scientific World Journal*, 2012.

Estudante, M., Morais, J.G., Soveral, G. & Benet, L.Z. 2013. Intestinal drug transporters: an overview. *Advanced Drug Delivery Reviews*, 65(10):1340-1356.

Fearn, R.A. & Hirst, B.H. 2006. Predicting oral drug absorption and hepatobiliary clearance: human intestinal and hepatic in vitro cell models. *Environmental Toxicology and Pharmacology*, 21(2):168-178.

Fuhrmann, G. & Leroux, J.-C. 2014. Improving the stability and activity of oral therapeutic enzymes—Recent advances and perspectives. *Pharmaceutical Research*, 31(5):1099-1105.

Galipeau, H. & Verdu, E. 2016. The complex task of measuring intestinal permeability in basic and clinical science. *Neurogastroenterology & Motility*, 28(7):957-965.

Gamboa, J.M. & Leong, K.W. 2013. *In vitro* and *in vivo* models for the study of oral delivery of nanoparticles. *Advanced Drug Delivery Reviews*, 65(6):800-810.

Gaucher, G., Satturwar, P., Jones, M.-C., Furtos, A. & Leroux, J.-C. 2010. Polymeric micelles for oral drug delivery. *European Journal of Pharmaceutics and Biopharmaceutics*, 76(2):147-158.

Gedawy, A., Martinez, J., Al-Salami, H. & Dass, C.R. 2018. Oral insulin delivery: existing barriers and current counter-strategies. *Journal of Pharmacy and Pharmacology*, 70(2):197-213.

Gerber, W., Hamman, J.H. & Steyn, J.D. 2018. Excipient-drug pharmacokinetic interactions: Effect of disintegrants on efflux across excised pig intestinal tissues. *Journal of Food and Drug Analysis*, 26(2):115-124.

Gertsch, J. 2011. Botanical drugs, synergy, and network pharmacology: forth and back to intelligent mixtures. *Planta Medica*, 77(11):1086-1098.

Gorgani, L., Mohammadi, M., Najafpour, G.D. & Nikzad, M. 2017a. Piperine—the bioactive compound of black pepper: from isolation to medicinal formulations. *Comprehensive Reviews in Food Science and Food Safety*, 16(1):124-140.

Gorgani, L., Mohammadi, M., Najafpour, G.D. & Nikzad, M. 2017b. Sequential microwave-ultrasound-Assisted extraction for isolation of piperine from Black Pepper (*Piper nigrum* L.). *Food and Bioprocess Technology*, 10(12):2199-2207.

Griffin, B. & O'Driscoll, C. 2007. Models of the small intestine. In Carsten, E. & Kwang-Jin, K. (Eds.). *Drug absorption studies: In situ, in vitro and in silico models* (pp. 34). New York: Springer Science and Business media. https://books.google.co.za/books?id=3geWUtmDPxwC&pg=PA224&lpg=PA224&dq=definition+of+in+vitro+study+during+transportstudies&source=bl&ots=DPlL-FidGP&sig=ea8gVDLsi9Lavl-hNa6c1K7WmB4&hl=en&sa=X&ved=0ahUKEwjup43U65HSAhXpDMAKHVkJCfcQ6AEIHjAD#v=onepage&q=definition%20of%20in%20vitro%20study%20during%20transportstudies&f=false Date of access 15 Feb 2017.

Griffiths, P.C., Cattoz, B., Ibrahim, M.S. & Anuonye, J.C. 2015. Probing the interaction of nanoparticles with mucin for drug delivery applications using dynamic light scattering. *European Journal of Pharmaceutics and Biopharmaceutics*, 97:218-222.

Hamman, J.H., Enslin, G.M. & Kotzé, A.F. 2005. Oral delivery of peptide drugs. *BioDrugs*, 19(3):165-177.

Han, Y., Tan, T.M.C. & Lim, L.-Y. 2006. Effects of capsaicin on P-gp function and expression in Caco-2 cells. *Biochemical Pharmacology*, 71(12):1727-1734.

Hanani, M. 2012. Lucifer yellow–an angel rather than the devil. *Journal of Cellular and Molecular Medicine*, 16(1):22-31.

Hassani, L., Lewis, A. & Richard, J. 2015. Oral peptide delivery: technology landscape and current status. *OnDrugDelivery*, 59:12-17.

Hayman, M. & Kam, P.C. 2008. Capsaicin: a review of its pharmacology and clinical applications. *Current Anaesthesia and Critical Care*, 19(5):338-343.

Holmstock, N., Annaert, P. & Augustijns, P. 2012. Boosting of HIV protease inhibitors by ritonavir in the intestine: the relative role of cytochrome P450 and P-glycoprotein inhibition based on Caco-2 monolayers versus in situ intestinal perfusion in mice. *Drug Metabolism and Disposition*, 40(8):1473-1477.

Iyer, H., Khedkar, A. & Verma, M. 2010. Oral insulin–a review of current status. *Diabetes, Obesity and Metabolism*, 12(3):179-185.

Javed, S., Ahsan, W. & Kohli, K. 2016. The concept of bioavailability enhancement of drugs-A patent review. *Journal of Scientific Letters*, 1(3):143-165.

Jhanwar, B. & Gupta, S. 2014. Biopotentiation using herbs: Novel technique for poor bioavailable drugs. *International Journal of PharmTech Research*, 6(2):443-454.

Ji, H., Tang, J., Li, M., Ren, J., Zheng, N. & Wu, L. 2016. Curcumin-loaded solid lipid nanoparticles with Brij78 and TPGS improved *in vivo* oral bioavailability and in situ intestinal absorption of curcumin. *Drug Delivery*, 23(2):459-470.

Johnson, J.J., Nihal, M., Siddiqui, I.A., Scarlett, C.O., Bailey, H.H., Mukhtar, H. & Ahmad, N. 2011. Enhancing the bioavailability of resveratrol by combining it with piperine. *Molecular Nutrition & Food Research*, 55(8):1169-1176.

Jungbauer, A. & Medjakovic, S. 2012. Anti-inflammatory properties of culinary herbs and spices that ameliorate the effects of metabolic syndrome. *Maturitas*, 71(3):227-239.

Kaiser, M., Pereira, S., Pohl, L., Ketelhut, S., Kemper, B., Gorzelanny, C., Galla, H.-J., Moerschbacher, B.M. & Goycoolea, F.M. 2015. Chitosan encapsulation modulates the effect of capsaicin on the tight junctions of MDCK cells. *Scientific Reports*, 5:1-14.

Kanda, Y., Yamasaki, Y., Sasaki-Yamaguchi, Y., Ida-Koga, N., Kamisuki, S., Sugawara, F., Nagumo, Y. & Usui, T. 2018. TRPA1-dependent reversible opening of tight junction by natural compounds with an α, β-unsaturated moiety and capsaicin. *Scientific Reports*, 8(1):1-13.

Kang, M.J., Cho, J.Y., Shim, B.H., Kim, D.K. & Lee, J. 2009. Bioavailability enhancing activities of natural compounds from medicinal plants. *Journal of Medicinal Plants Research*, 3(13):1204-1211.

Kaprelyants, A. & Kell, D. 1992. Rapid assessment of bacterial viability and vitality by rhodamine 123 and flow cytometry. *Journal of Applied Bacteriology*, 72(5):410-422.

Karsha, P.V. & Lakshmi, O.B. 2010. Antibacterial activity of black pepper (*Piper nigrum* Linn.) with special reference to its mode of action on bacteria. *Indian Journal of Nutural Products and Resources*, 1(2):213-215.

Kempaiah, R. & Srinivasan, K. 2002. Integrity of erythrocytes of hypercholesterolemic rats during spices treatment. *Molecular and Cellular Biochemistry*, 236(1-2):155-161.

Kesarwani, K. & Gupta, R. 2013. Bioavailability enhancers of herbal origin: An overview. *Asian Pacific Journal of Tropical Biomedicine*, 3(4):253-266.

KEW-Science:Plants-of-the-world-online. 2018. *Piper nigrum* L. http://powo.science.kew.org/taxon/urn:lsid:ipni.org:names:682369-1 Date of access: 14 Aug. 2018.

Khafagy, E.-S. & Morishita, M. 2012. Oral biodrug delivery using cell-penetrating peptide. *Advanced Drug Delivery Reviews*, 64(6):531-539.

Khafagy, E.-S., Morishita, M., Onuki, Y. & Takayama, K. 2007. Current challenges in non-invasive insulin delivery systems: A comparative review. *Advanced Drug Delivery Reviews*, 59(15):1521-1546.

Khajuria, A., Thusu, N. & Zutshi, U. 2002. Piperine modulates permeability characteristics of intestine by inducing alterations in membrane dynamics: Influence on brush border membrane fluidity, ultrastructure and enzyme kinetics. *Phytomedicine*, 9(3):224-231.

Khan, M. & Siddiqui, M. 2007. Antimicrobial activity of piper fruits. *Natural Product Radiance*, 6(2):111-113.

König, J., Müller, F. & Fromm, M.F. 2013. Transporters and drug-drug interactions: important determinants of drug disposition and effects. *Pharmacological Reviews*, 65(3):944-966.

Kotzé, A.F., Lueßen, H.L., de Leeuw, B.J., de Boer, B.G., Coos Verhoef, J. & Junginger, H.E. 1998. Comparison of the effect of different chitosan salts and N-trimethyl chitosan chloride on the permeability of intestinal epithelial cells (Caco-2). *Journal of Controlled Release*, 51(1):35-46.

Kumar-Sarangi, M., Chandra-Joshi, B. & Ritchie, B. 2018. Natural bioenhancers in drug delivery: an overview. *Puerto Rico Health Sciences Journal*, 37(1):12-18.

Kumar, P., Chand, S., Chandra, P. & Maurya, P.K. 2015. Influence of dietary capsaicin on redox status in red blood cells during human aging. *Advanced Pharmaceutical Bulletin*, 5(4):583-586.

Lassmann-Vague, V. & Raccah, D. 2006. Alternatives routes of insulin delivery. *Diabetes & Metabolism*, 32(5):513-522.

Le Ferrec, E., Chesne, C., Artusson, P., Brayden, D., Fabre, G., Gires, P., Guillou, F., Rousset, M., Rubas, W. & Scarino, M.-L. 2001. In vitro models of the intestinal barrier. *Atla*, 29:649-668.

Li, W., Zhan, P., De Clercq, E., Lou, H. & Liu, X. 2013. Current drug research on PEGylation with small molecular agents. *Progress in Polymer Science*, 38(3-4):421-444.

Lin, Y.-H., Chen, C.-T., Liang, H.-F., Kulkarni, A.R., Lee, P.-W., Chen, C.-H. & Sung, H.-W. 2007. Novel nanoparticles for oral insulin delivery via the paracellular pathway. *Nanotechnology*, 18(10):1-11.

Liu, N.-C., Hsieh, P.-F., Hsieh, M.-K., Zeng, Z.-M., Cheng, H.-L., Liao, J.-W. & Chueh, P.J. 2012. Capsaicin-mediated tNOX (ENOX2) up-regulation enhances cell proliferation and migration in vitro and in vivo. *Journal of Agricultural and Food Chemistry*, 60(10):2758-2765.

Lopes, M.A., Abrahim, B.A., Seiça, R., Veiga, F., Rodrigues, C.R. & Ribeiro, A.J. 2014. Intestinal uptake of insulin nanoparticles: facts or myths? *Current Pharmaceutical Biotechnology*, 15(7):629-638.

Lundquist, P. & Artursson, P. 2016. Oral absorption of peptides and nanoparticles across the human intestine: Opportunities, limitations and studies in human tissues. *Advanced Drug Delivery Reviews*, 106:256-276.

Luo, Z., Liu, Y., Zhao, B., Tang, M., Dong, H., Zhang, L., Lv, B. & Wei, L. 2013. *Ex vivo* and in situ approaches used to study intestinal absorption. *Journal of Pharmacological and Toxicological Methods*, 68(2):208-216.

Madhav, N.S., Shakya, A.K., Shakya, P. & Singh, K. 2009. Orotransmucosal drug delivery systems: a review. *Journal of Controlled Release*, 140(1):2-11.

Maher, S. & Brayden, D.J. 2012. Overcoming poor permeability: translating permeation enhancers for oral peptide delivery. *Drug Discovery Today: Technologies*, 9(2):113-119.

Maher, S., Mrsny, R.J. & Brayden, D.J. 2016. Intestinal permeation enhancers for oral peptide delivery. *Advanced Drug Delivery Reviews*, 106, Part B:277-319.

Majeed, M. & Prakash, L. 2007. Targeting Optimal Nutrient Absorption with Phytonutrients. *Sabinsa Corporation*:1-12.

Mao, Q.-Q., Huang, Z., Zhong, X.-M., Xian, Y.-F. & Ip, S.-P. 2014. Piperine reverses the effects of corticosterone on behavior and hippocampal BDNF expression in mice. *Neurochemistry International*, 74:36-41.

Meghwal, M. & Goswami, T. 2013. *Piper nigrum* and piperine: an update. *Phytotherapy Research*, 27(8):1121-1130.

Mishra, A., Punia, J.K., Bladen, C., Zamponi, G.W. & Goel, R.K. 2015. Anticonvulsant mechanisms of piperine, a piperidine alkaloid. *Channels*, 9(5):317-323.

Morishita, M. & Peppas, N.A. 2006. Is the oral route possible for peptide and protein drug delivery? *Drug Discovery Today*, 11(19):905-910.

Moroz, E., Matoori, S. & Leroux, J.-C. 2016. Oral delivery of macromolecular drugs: Where we are after almost 100 years of attempts. *Advanced Drug Delivery Reviews*, 101:108-121.

Muheem, A., Shakeel, F., Jahangir, M.A., Anwar, M., Mallick, N., Jain, G.K., Warsi, M.H. & Ahmad, F.J. 2016. A review on the strategies for oral delivery of proteins and peptides and their clinical perspectives. *Saudi Pharmaceutical Journal*, 24(4):413-428.

Nakanishi, T. & Tamai, I. 2015. Interaction of drug or food with drug transporters in intestine and liver. *Current Drug Metabolism*, 16(9):753-764.

Niu, Z., Conejos-Sánchez, I., Griffin, B.T., O'Driscoll, C.M. & Alonso, M.J. 2016. Lipid-based nanocarriers for oral peptide delivery. *Advanced Drug Delivery Reviews*, 106, Part B:337-354.

Nunes, R., Silva, C. & Chaves, L. 2015a. Tissue-based *in vitro* and *ex vivo* models for intestinal permeability studies. (*In* Sarmento, B., Concepts and Models for Drug Permeability Studies: Cell and Tissue Based in Vitro Culture Models. Cambridge, UK: Woodhead Publishing. Available: https://scholar.google.co.za/scholar?hl=en&q=Concepts+and+Models+for+Drug+Permeability+Studies&btnG=&as_sdt=1%2C5&as_sdtp Date of access: 23 Mar. 2017.

Ölander, M., Wiśniewski, J.R., Matsson, P., Lundquist, P. & Artursson, P. 2016. The proteome of filter-grown Caco-2 cells with a focus on proteins involved in drug disposition. *Journal of Pharmaceutical Sciences*, 105(2):817-827.

Omolo, M.A., Wong, Z.-Z., Mergen, K., Hastings, J.C., Le, N.C., Reil, H.A., Case, K.A. & Baumler, D.J. 2014. Antimicrobial properties of chili peppers. *Journal of Infectious Diseases and Therapy*:1-8.

Owens, D.R., Zinman, B. & Bolli, G. 2003. Alternative routes of insulin delivery. *Diabetic Medicine*, 20(11):886-898.

Palumbo, P., Picchini, U., Beck, B., van Gelder, J., Delbar, N. & DeGaetano, A. 2008. A general approach to the apparent permeability index. *Journal of Pharmacokinetics and Pharmacodynamics*, 35(2):235.

Park, K., Kwon, I.C. & Park, K. 2011. Oral protein delivery: Current status and future prospect. *Reactive and Functional Polymers*, 71(3):280-287.

Pasut, G. & Veronese, F.M. 2012. State of the art in PEGylation: The great versatility achieved after forty years of research. *Journal of Controlled Release*, 161(2):461-472.

Patel, J., Patil, S. & Pawar, S. 2017. A review on method development and validation. *World Journal of Pharmacy and Pharmaceutical Science*, 6(3):245-259.

Patel, V.F., Liu, F. & Brown, M.B. 2011. Advances in oral transmucosal drug delivery. *Journal of Controlled Release*, 153(2):106-116.

Patil, V.M., Das, S. & Balasubramanian, K. 2016. Quantum chemical and docking insights into bioavailability enhancement of curcumin by piperine in pepper. *The Journal of Physical Chemistry A*, 120(20):3643-3653.

Pawar, V.K., Meher, J.G., Singh, Y., Chaurasia, M., Surendar Reddy, B. & Chourasia, M.K. 2014. Targeting of gastrointestinal tract for amended delivery of protein/peptide therapeutics: Strategies and industrial perspectives. *Journal of Controlled Release*, 196:168-183.

Peng, J. & Li, Y.-J. 2010. The vanilloid receptor TRPV1: Role in cardiovascular and gastrointestinal protection. *European Journal of Pharmacology*, 627(1):1-7.

Petit, C., Bujard, A., Skalicka-Woźniak, K., Cretton, S., Houriet, J., Christen, P., Carrupt, P.-A. & Wolfender, J.-L. 2016. Prediction of the passive intestinal absorption of medicinal plant extract constituents with the parallel artificial membrane permeability assay (PAMPA). *Planta Medica*, 82(05):424-431.

Pillay, V., Hibbins, A.R., Choonara, Y.E., Du Toit, L.C., Kumar, P. & Ndesendo, V.M. 2012. Orally administered therapeutic peptide delivery: enhanced absorption through the small intestine using permeation enhancers. *International Journal of Peptide Research and Therapeutics*, 18(3):259-280.

Pinton, P., Nougayrède, J.-P., Del Rio, J.-C., Moreno, C., Marin, D.E., Ferrier, L., Bracarense, A.-P., Kolf-Clauw, M. & Oswald, I.P. 2009. The food contaminant deoxynivalenol, decreases intestinal barrier permeability and reduces claudin expression. *Toxicology and Applied Pharmacology*, 237(1):41-48.

Prajapati, R., Singh, U., Patil, A., Khomane, K.S., Bagul, P., Bansal, A.K. & Sangamwar, A.T. 2013. In silico model for P-glycoprotein substrate prediction: insights from molecular dynamics and in vitro studies. *Journal of Computer-Aided Molecular Design*, 27(4):347-363.

Putnam, W.S., Pan, L., Tsutsui, K., Takahashi, L. & Benet, L.Z. 2002. Comparison of bidirectional cephalexin transport across MDCK and Caco-2 cell monolayers: Interactions with peptide transporters. *Pharmaceutical Research*, 19(1):27-33.

Qin, C., Yu, C., Shen, Y., Fang, X., Chen, L., Min, J., Cheng, J., Zhao, S., Xu, M., Luo, Y., Yang, Y., Wu, Z., Mao, L., Wu, H., Ling-Hu, C., Zhou, H., Lin, H., González-Morales, S., Trejo-Saavedra, D.L., Tian, H., Tang, X., Zhao, M., Huang, Z., Zhou, A., Yao, X., Cui, J., Li, W., Chen, Z., Feng, Y., Niu, Y., Bi, S., Yang, X., Li, W., Cai, H., Luo, X., Montes-Hernández, S., Leyva-González, M.A., Xiong, Z., He, X., Bai, L., Tan, S., Tang, X., Liu, D., Liu, J., Zhang, S., Chen, M., Zhang, L., Zhang, L., Zhang, Y., Liao, W., Zhang, Y., Wang, M., Lv, X., Wen, B., Liu, H., Luan, H., Zhang, Y., Yang, S., Wang, X., Xu, J., Li, X., Li, S., Wang, J., Palloix, A., Bosland, P.W., Li, Y., Krogh, A., Rivera-Bustamante, R.F., Herrera-Estrella, L., Yin, Y., Yu, J., Hu, K. & Zhang, Z. 2014. Whole-genome sequencing of cultivated and wild peppers provides insights into Capsicum domestication and specialization. *Proceedings of the National Academy of Sciences*, 111(14):5135-5140.

Rambla-Alegre, M., Esteve-Romero, J. & Carda-Broch, S. 2012. Is it really necessary to validate an analytical method or not? That is the question. *Journal of Chromatography A*, 1232:101-109.

Randviir, E.P., Metters, J.P., Stainton, J. & Banks, C.E. 2013. Electrochemical impedance spectroscopy versus cyclic voltammetry for the electroanalytical sensing of capsaicin utilising screen printed carbon nanotube electrodes. *Analyst*, 138(10):2970-2981.

Rangari, N.T. & Puranik, P.K. 2015. Review on recent and novel approaches to colon targeted drug delivery systems. *International Journal of Pharmacy & Pharmaceutical Research*, 3(1):169-186.

Ratnaparkhi, M.P., Somvanshi, F.U., Pawar, S.A., Chaudhari, S.P., Gupta, J.P. & Budhavant, K.A. 2013. Colon targeted drug delivery system. *International Journal of Pharma Research & Review*, 2(8):33-42.

Reddy, R.D., Malleswari, K., Prasad, G. & Pavani, G. 2013. Colon targeted drug delivery system: a review. *International Journal of Pharmaceutical Sciences & Research*, 4(1):42-54.

Renukuntla, J., Vadlapudi, A.D., Patel, A., Boddu, S.H. & Mitra, A.K. 2013. Approaches for enhancing oral bioavailability of peptides and proteins. *International Journal of Pharmaceutics*, 447(1):75-93.

Reyes-Escogido, M.d.L., Gonzalez-Mondragon, E.G. & Vazquez-Tzompantzi, E. 2011. Chemical and pharmacological aspects of capsaicin. *Molecules*, 16(2):1253-1270.

Roberts, M., Bentley, M. & Harris, J. 2012. Chemistry for peptide and protein PEGylation. *Advanced Drug Delivery Reviews*, 64:116-127.

Roger, E., Lagarce, F., Garcion, E. & Benoit, J.-P. 2010. Biopharmaceutical parameters to consider in order to alter the fate of nanocarriers after oral delivery. *Nanomedicine*, 5(2):287-306.

Rosa, A., Deiana, M., Casu, V., Paccagnini, S., Appendino, G., Ballero, M. & Dessí, M.A. 2002. Antioxidant activity of capsinoids. *Journal of Agricultural and Food Chemistry*, 50(25):7396-7401.

Sadeghi, A., Avadi, M., Ejtemaimehr, S., Abashzadeh, S., Partoazar, A., Dorkoosh, F., Faghihi, M., Rafiee-Tehrani, M. & Junginger, H. 2009. Development of a gas empowered drug delivery system for peptide delivery in the small intestine. *Journal of Controlled Release*, 134(1):11-17.

Sawyer, T.K. 2007. 2.15 - Peptidomimetic and nonpeptide drug discovery: Receptor, protease, and signal transduction therapeutic targets A2 - Taylor, John B. *(In* Triggle, D.J., *ed.* Comprehensive Medicinal Chemistry II. Oxford: Elsevier. p. 603-647).

Servier-Medical-Art. 2018. SMART: Servier Medical Art Cellular Biology. https://smart.servier.com/page/7/?s=Cellular+Biology Date of access: 13 Aug. 2018.

Shabir, G.A. 2003. Validation of high-performance liquid chromatography methods for pharmaceutical analysis: Understanding the differences and similarities between validation requirements of the US Food and Drug Administration, the US Pharmacopeia and the International Conference on Harmonization. *Journal of Chromatography A*, 987(1–2):57-66.

Shamkuwar, P.B., Shahi, S.R. & Jadhav, S.T. 2012. Evaluation of antidiarrhoeal effect of Black pepper (Piper nigrum L.). *Asian Journal of Plant Science and Research*, 2(1):48-53.

Sharma, P., Varma, M.V., Chawla, H.P. & Panchagnula, R. 2005. Absorption enhancement, mechanistic and toxicity studies of medium chain fatty acids, cyclodextrins and bile salts as peroral absorption enhancers. *Il Farmaco*, 60(11):884-893.

Sharma, S., Kalia, N.P., Suden, P., Chauhan, P.S., Kumar, M., Ram, A.B., Khajuria, A., Bani, S. & Khan, I.A. 2014. Protective efficacy of piperine against Mycobacterium tuberculosis. *Tuberculosis*, 94(4):389-396.

Shikanga, E.A., Hamman, J.H., Chen, W., Combrinck, S., Gericke, N. & Viljoen, A.M. 2012. In vitro permeation of mesembrine alkaloids from *Sceletium tortuosum* across porcine buccal, sublingual, and intestinal mucosa. *Planta Medica*, 78(03):260-268.

Shrivastava, A. & Gupta, V.B. 2011. Methods for the determination of limit of detection and limit of quantitation of the analytical methods. *Chronicles of Young Scientists*, 2(1):21-25.

Singh, C.K., Saxena, S., Yadav, M. & Samson, A.L. 2018. A review on novel approaches for colon targeted drug delivery systems. *PharmaTutor*, 6(7):11-22.

Singh, V., Singh, P., Mishra, A., Patel, A. & Yadav, K. 2014. Piperine: delightful surprise to the biological world, made by plant “pepper” and a great bioavailability enhancer for our drugs and great bioavailability enhancer for our drugs and supplements. *World Journal of Pharmaceutical Reseach*, 3(6):2084-2098.

Singletary, K. 2011. Red pepper: Overview of potential health benefits. *Nutrition Today*, 46(1):33-47.

Sjögren, E., Abrahamsson, B., Augustijns, P., Becker, D., Bolger, M.B., Brewster, M., Brouwers, J., Flanagan, T., Harwood, M., Heinen, C., Holm, R., Juretschke, H.-P., Kubbinga, M., Lindahl, A., Lukacova, V., Münster, U., Neuhoff, S., Nguyen, M.A., Peer, A.v., Reppas, C., Hodjegan, A.R., Tannergren, C., Weitschies, W., Wilson, C., Zane, P., Lennernäs, H. & Langguth, P. 2014. *In vivo* methods for drug absorption – Comparative physiologies, model selection, correlations with *in vitro* methods (IVIVC), and applications for formulation/API/excipient characterization including food effects. *European Journal of Pharmaceutical Sciences*, 57:99-151.

Sjögren, E., Thorn, H. & Tannergren, C. 2016. In silico modeling of gastrointestinal drug absorption: predictive performance of three physiologically based absorption models. *Molecular Pharmaceutics*, 13(6):1763-1778.

Srinivasan, B., Kolli, A.R., Esch, M.B., Abaci, H.E., Shuler, M.L. & Hickman, J.J. 2015. TEER measurement techniques for *in vitro* barrier model systems. *Journal of laboratory automation*, 20(2):107-126.

Srinivasan, K. 2007. Black pepper and its pungent principle-piperine: A Review of diverse physiological effects. *Critical Reviews in Food Science and Nutrition*, 47(8):735-748.

Srinivasan, K. 2016. Biological activities of red pepper (*Capsicum annuum*) and its pungent principle capsaicin: A review. *Critical Reviews in Food Science and Nutrition*, 56(9):1488-1500.

Srivastava, A.K. & Singh, V.K. 2017. Biological action of *Piper nigrum*-the king of spices. *European Journal of Biological Research*, 7(3):223-233.

Stappaerts, J., Brouwers, J., Annaert, P. & Augustijns, P. 2015. *In situ* perfusion in rodents to explore intestinal drug absorption: Challenges and opportunities. *International Journal of Pharmaceutics*, 478(2):665-681.

Stoica, R.-M., Moscovici, M., Tomulescu, C. & Băbeanu, N. 2016. Extraction and analytical method of capsaicinoids- A review. *Scientific Bulletin. Series F. Biotechnologies*, 20:93-98.

Sugano, K., Kansy, M., Artursson, P., Avdeef, A., Bendels, S., Di, L., Ecker, G.F., Faller, B., Fischer, H. & Gerebtzoff, G. 2010. Coexistence of passive and carrier-mediated processes in drug transport. *Nature reviews. Drug discovery*, 9(8):597.

Suresh, D., Manjunatha, H. & Srinivasan, K. 2007. Effect of heat processing of spices on the concentrations of their bioactive principles: Turmeric (Curcuma longa), red pepper (Capsicum annuum) and black pepper (Piper nigrum). *Journal of Food Composition and Analysis*, 20(3):346-351.

Swaan, P.W. 1998. Recent advances in intestinal macromolecular drug delivery *via* receptor-mediated transport pathways. *Pharmaceutical Research*, 15(6):826-834.

Takano, M., Yumoto, R. & Murakami, T. 2006. Expression and function of efflux drug transporters in the intestine. *Pharmacology & Therapeutics*, 109(1):137-161.

Tanaka, Y., Kitamura, Y., Maeda, K. & Sugiyama, Y. 2016. Explication of definitional description and empirical use of fraction of orally administered drugs absorbed from the intestine (Fa) and intestinal availability (Fg): Effect of P-glycoprotein and CYP3A on Fa and Fg. *Journal of Pharmaceutical Sciences*, 105(2):431-442.

Tatiraju, D.V., Bagade, V.B., Karambelkar, P.J., Jadhav, V.M. & Kadam, V. 2013a. Natural bioenhancers: An overview. *Journal of Pharmacognosy and Phytochemistry*, 2(3).

Tatiraju, D.V., Bagade, V.B., Karambelkar, P.J., Jadhav, V.M. & Kadam, V. 2013b. Natural bioenhancers: An overview. *Journal of Pharmacognosy and Phytochemistry*, 2(3):55-60.

Testa, B. 2009. Prodrugs: bridging pharmacodynamic/pharmacokinetic gaps. *Current Opinion in Chemical Biology*, 13(3):338-344.

Troutman, M.D. & Thakker, D.R. 2003. Efflux ratio cannot assess P-Glycoprotein-mediated attenuation of absorptive transport: Asymmetric Effect of P-Glycoprotein on absorptive and secretory transport across Caco-2 cell monolayers. *Pharmaceutical Research*, 20(8):1200-1209.

Umadevi, P., Deepti, K. & Venugopal, D.V.R. 2013. Synthesis, anticancer and antibacterial activities of piperine analogs. *Medicinal Chemistry Research*, 22(11):5466-5471.

Upadhyay, V., Sharma, N., Joshi, H.M., Malik, A., Mishra, M., Singh, B. & Tripathi, S. 2013. Development and validation of rapid RPHPLC, method for estimation of piperine in *Piper nigrum* L. *International Journal of Herbal Medicine*, 1:6-9.

USP. 2018a. Validation of compendial procedures. http://app.uspnf.com/uspnf/pub/index?usp=41&nf=36&s=1&officialOn=August%201,%202018 Date of access: 16 Aug. 2018.

USP. 2018b. Fluorescence spectroscopy http://app.uspnf.com/uspnf/pub/index?usp=41&nf=36&s=1&officialOn=August%201,%202018 Date of access: 15 Aug. 2018.

Vadlapudi, A.D., Vadlapatla, R.K., Kwatra, D., Earla, R., Samanta, S.K., Pal, D. & Mitra, A.K. 2012. Targeted lipid based drug conjugates: A novel strategy for drug delivery. *International Journal of Pharmaceutics*, 434(1):315-324.

Vagner, J., Qu, H. & Hruby, V.J. 2008. Peptidomimetics, a synthetic tool of drug discovery. *Current Opinion in Chemical Biology*, 12(3):292-296.

Veda, S. & Srinivasan, K. 2011. Influence of dietary spices on the in vivo absorption of ingested β-carotene in experimental rats. *British Journal of Nutrition*, 105(10):1429-1438.

Vlieghe, P., Lisowski, V., Martinez, J. & Khrestchatisky, M. 2010. Synthetic therapeutic peptides: science and market. *Drug Discovery Today*, 15(1-2):40-56.

Volpe, D.A. 2010. Application of method suitability for drug permeability classification. *The American Association of Pharmaceutical Scientists Journal*, 12(4):670-678.

Wagner, H. & Ulrich-Merzenich, G. 2009. Synergy research: Approaching a new generation of phytopharmaceuticals. *Phytomedicine*, 16(2–3):97-110.

Wahlang, B., Pawar, Y.B. & Bansal, A.K. 2011. Identification of permeability-related hurdles in oral delivery of curcumin using the Caco-2 cell model. *European Journal of Pharmaceutics and Biopharmaceutics*, 77(2):275-282.

Wang, Y.-H., Morris-Natschke, S.L., Yang, J., Niu, H.-M., Long, C.-L. & Lee, K.-H. 2014. Anticancer principles from medicinal Piper (胡椒 Hú Jiāo) plants. *Journal of Traditional and Complementary Medicine*, 4(1):8-16.

Wikipedia. 2018. *Capsicum anuum*. https://en.wikipedia.org/wiki/Capsicum_annuum Date of access: 21 Mar. 2018.

Woitiski, C.B., Carvalho, R.A., Ribeiro, A.J., Neufeld, R.J. & Veiga, F. 2008. Strategies toward the improved oral delivery of insulin nanoparticles *via* gastrointestinal uptake and translocation. *BioDrugs*, 22(4):223-237.

Wong, C.Y., Martinez, J. & Dass, C.R. 2016. Oral delivery of insulin for treatment of diabetes: status quo, challenges and opportunities. *Journal of Pharmacy and Pharmacology*, 68(9):1093-1108.

Woting, A. & Blaut, M. 2018. Small intestinal permeability and gut-transit time determined with low and high molecular weight fluorescein isothiocyanate-dextrans in C3H mice. *Nutrients*, 10(6):685-692.

Wu, X., Ma, J., Ye, Y. & Lin, G. 2016. Transporter modulation by Chinese herbal medicines and its mediated pharmacokinetic herb–drug interactions. *Journal of Chromatography B*, 1026:236-253.

Yu, H., Wang, Q., Sun, Y., Shen, M., Li, H. & Duan, Y. 2015. A new PAMPA model proposed on the basis of a synthetic phospholipid membrane. *PLOS One*, 10(2):e0116502.

Yun, Y., Cho, Y.W. & Park, K. 2013. Nanoparticles for oral delivery: Targeted nanoparticles with peptidic ligands for oral protein delivery. *Advanced Drug Delivery Reviews*, 65(6):822-832.

Zhang, D., Luo, G., Ding, X. & Lu, C. 2012. Preclinical experimental models of drug metabolism and disposition in drug discovery and development. *Acta Pharmaceutica Sinica B*, 2(6):549-561.

Zhang, Y., Huang, Z., Omari-Siaw, E., Lu, S., Zhu, Y., Jiang, D., Wang, M., Yu, J., Xu, X. & Zhang, W. 2016. Preparation and *in vitro–in vivo* evaluation of sustained-release matrix pellets of capsaicin to enhance the oral bioavailability. *American Association of Pharmaceutical Scientists PharmSciTech*, 17(2):339-349.

Zhao, W., Uehera, S., Tanaka, K., Tadokoro, S., Kusamori, K., Katsumi, H., Sakane, T. & Yamamoto, A. 2016. Effects of polyoxyethylene alkyl ethers on the intestinal transport and absorption of rhodamine 123: A P-glycoprotein substrate by *in vitro* and *in vivo* studies. *Journal of Pharmaceutical Sciences*, 105(4):1526-1534.